

AN INVESTIGATION OF INSTABILITIES  
ENCOUNTERED DURING HEAT TRANSFER  
TO A SUPERCRITICAL FLUID

By

ARCHIE JUNIOR CORNELIUS

Bachelor of Science  
Kansas State University  
Manhattan, Kansas  
1958

Master of Science  
Oklahoma State University  
Stillwater, Oklahoma  
1963


Submitted to the Faculty of the Graduate School  
of the Oklahoma State University  
in partial fulfillment of the requirements  
for the degree of  
DOCTOR OF PHILOSOPHY  
May, 1965

OKLAHOMA  
STATE UNIVERSITY  
LIBRARY

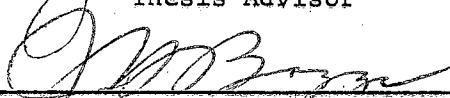
SEP 20 1965

AN INVESTIGATION OF INSTABILITIES  
ENCOUNTERED DURING HEAT TRANSFER  
TO A SUPERCRITICAL FLUID

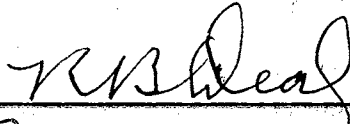
Thesis Approved:

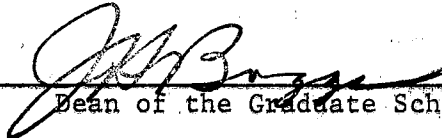


Thesis Advisor









Dean of the Graduate School

587470

## PREFACE

The literature of the last few decades contains reports of severe pressure and flow oscillations occurring spontaneously during heat transfer to a fluid at both subcritical and supercritical pressures. Although the oscillatory behavior has been studied rather extensively due to its technological significance, a satisfactory understanding of the phenomenon has not been obtained.

The purpose of this study is to investigate the unstable behavior of a heat transfer loop operating at a supercritical pressure. The oscillatory behavior is shown to be analogous to two types of more commonly encountered systems. The mechanism which triggers and maintains the oscillations is postulated. The results contribute an insight into the physical nature of the instabilities, which can be used to explain many of the oscillations which have been reported without explanation, and to dispel some of the apparently erroneous theories which have appeared.

The author is grateful for the inspiration and guidance furnished by his major advisor, Dr. Jerald D. Parker, who gave freely of his time and knowledge in directing the research. Thanks are also due to the other members of the advisory committee, Dr. James H. Boggs, Dr. Roy B. Deal, Jr., and Dr. Donald R. Haworth for their assistance. The contributions of the various professors and professionals who have advanced the author's professional development are warmly acknowledged

as are the fellowships granted by the National Science Foundation and by Jersey Production Research Company, which supported the author in his graduate study.

The research was carried out with the financial support of the U. S. Atomic Energy Commission and Associated Midwest Universities at the Argonne National Laboratory, Argonne, Illinois. It is a pleasure to acknowledge the financial support and the assistance of the Argonne technical and professional staff, particularly: Dr. Michael Petrick for technical suggestions and encouragements, Leonard M. Indykiewicz for assistance in building and operating the loop, Mrs. Marjorie A. Luebs for typing the thesis, and the entire D-11 Heat Engineering Section including fellow AMU students for their generous support.

In addition, the cooperation and understanding of the author's wife and children was a major factor in the successful completion of this program.

## TABLE OF CONTENTS

Chapter	Page
I. INTRODUCTION. . . . .	1
Definition and Properties. . . . .	3
II. LITERATURE SURVEY . . . . .	14
Single Phase Supercritical Results . . . . .	14
Boiling Instability. . . . .	26
Summary. . . . .	32
III. EXPERIMENTAL APPARATUS. . . . .	34
Component Description. . . . .	36
IV. EXPERIMENTAL PROCEDURE. . . . .	51
V. EXPERIMENTAL RESULTS. . . . .	56
Acoustic Oscillations. . . . .	56
Slow Oscillations. . . . .	70
Anomalous Behavior . . . . .	81
VI. ANALYSIS OF SLOW OSCILLATIONS . . . . .	84
Conservation Equations . . . . .	85
Numerical Computational Procedure. . . . .	92
Steady-State Calculations. . . . .	98
Results of Numerical Calculations. . . . .	100
VII. SUMMARY AND CONCLUSIONS . . . . .	111
Nomenclature . . . . .	116
Bibliography . . . . .	118
APPENDICES. . . . .	
A. Calculating Pressure Difference Between Two Pressure Taps due to Their Absolute Pressure Phase Varia- tion During Acoustic Oscillations. . . . .	124
B. Undamped Natural Frequency of a Closed Heat Transfer Loop . . . . .	126
C. Digital Computer Program . . . . .	131
Program Nomenclature . . . . .	138

LIST OF TABLES

Table	Page
I. Critical Data of Various Substances . . . . .	3
II. Vertical Height of Loop Components. . . . .	36
III. Wall Thermocouple Location. . . . .	46
IV. Lower Limit of Acoustic Oscillation Range . . . . .	58

## LIST OF FIGURES

Figure	Page
1. Specific Heat of Freon 114 at 500 psia . . . . .	4
2. Phase Regions for Freon 114. . . . .	6
3. Density of Freon 114 at 500 psia . . . . .	7
4. Enthalpy of Freon 114 at 500 psia. . . . .	7
5. Sonic Velocity of Freon 114 at 500 psia. . . . .	9
6. Qualitative Variation of Viscosity and Thermal Conductivity at a Supercritical Pressure. . . . .	11
7. Schematic Diagram of Heat Transfer Loop. . . . .	35
8. Sinusoidal Pressure Variation During Acoustic Oscillations	57
9. Experimental Record of Acoustic Oscillations . . . . .	59
10. Pressure "Beats" during Acoustic Oscillations. . . . .	61
11. Variation of Acoustic Frequency with Temperature for Various Loop Lengths . . . . .	63
12. Initiation of "Boiling-like Behavior" without Accompany- ing Acoustic Oscillations; Forced Convection Operation .	67
13. Experimental Record of Slow Oscillations; Wall Temperature Drop in Phase with Flow Oscillations . . . . .	72
14. Experimental Record of Slow Oscillations; Time Between Heat Transfer Improvements Longer than Flow Period . . .	74
15. Experimental Record of Slow Oscillations; Time Between Heat Transfer Improvements Shorter than Flow Period. . .	75
16. Simultaneous Occurrence of Acoustic and Slow Oscillations.	77
17. Experimental Record of Slow Oscillations; Flow Rate at Flowmeter and Venturi Difference . . . . .	78

LIST OF FIGURES (Contd.)

Figure	Page
18. Irregular Instability at Low Forced Convection Flow Rate. . . . .	79
19. Experimental Record of Slow Oscillations; Operation with Upper Horizontal Cooler. . . . .	81
20. Empirical Friction Pressure Drop Correlation. . . . .	90
21. Idealized Model of Flow Loop for Numerical Calculations. . . . .	93
22. Calculated Response Following Doubling of Electrical Heating Power . . . . .	102
23. Calculated Flow Response Following Doubling of Electrical Heating Power for Various Inlet Temperatures. . . . .	104
24. Calculated Flow Response Following Doubling of Electrical Heating Power for Various Inlet Temperatures. . . . .	105
25. Calculated Response Following Doubling of Electrical Heating Power; Upper Horizontal Cooler. . . . .	106
26. Calculated Behavior of Slow Oscillations; Triggered and Maintained by Changes of Heat Transfer Coefficient . . . . .	107
27. Calculated Behavior of Slow Oscillations; Higher Inlet Temperatures. . . . .	108
28. Calculated Behavior of Slow Oscillations; Lower Inlet Temperatures. . . . .	109
29. Idealized Model of Heat Transfer Loop . . . . .	126
30. Schematic of Minnesota Heat Transfer Loop . . . . .	129



## CHAPTER I

### INTRODUCTION

For several decades an aura of mystery has surrounded the behavior of a substance near its thermodynamic critical point. Early attempts to measure thermodynamic properties in this region yielded results which varied with experimental method due to the large variation of properties which occur and to the difficulty of achieving an equilibrium state within the sample. These early results led to the development of contradictory concepts regarding the behavior of a substance near the critical point. As more sophisticated experimental techniques were developed, many of the discrepancies were explained and a generally accepted pattern of thermodynamic behavior emerged. A similar situation exists today regarding the measurement of reliable transport properties near the critical point.

In recent years, studies of heat transfer to fluids near their critical point have revealed another anomaly. Reports of severe pressure and flow oscillations spontaneously accompanying the transfer of heat in this region have accumulated, although a plausible explanation of the phenomena has not been advanced. The purpose of this study is to investigate this unstable behavior, which occurs in connection with the transfer of heat to a fluid near its thermodynamic critical point.

A better understanding of such instabilities is required in several fields. A fluid near its critical point possesses the desirable properties of a large specific heat, which favors the transport of energy, and a large coefficient of thermal expansion, which may be regarded as the driving force of free convection. Hence a fluid's properties near the critical state make it an efficient heat transfer medium under the proper conditions. This capability has been used, with favorable results, for the cooling of gas turbine blades. The demand for increased efficiency of power generation plants has generated interest in employing supercritical water as a coolant, in order to increase the thermal efficiency of the plant. Several conventional steam power plants have been designed and built for operation at supercritical pressures. The design of a supercritical nuclear reactor power system has been considered. Another example of heat transfer to a supercritical fluid is in the modern rocket motor. The chamber pressures frequently exceed the critical pressure of the fuel, particularly when such fuels as liquid hydrogen are employed. Hence, a knowledge of instabilities which are associated with heat transfer to a fluid near its critical point is essential to present day technology.

In order to gain a better basic knowledge of the instabilities, a heat transfer loop was assembled which could operate by either natural or forced convection. The loop was instrumented so that an adequate record of the transient behavior was obtained. It was hoped that a better understanding of the microscopic behavior of a substance near the critical state might be gained by an examination of the

macroscopic experimental results, utilizing the knowledge and techniques which have evolved from the study of more conventional and familiar systems. The results of such an examination are presented in succeeding chapters. Analogies between the transient behavior and more conventional systems are drawn which may aid in the understanding of the phenomenon.

#### Definition and Properties

In order to understand what is happening during heat transfer to a supercritical fluid, it is necessary to consider the change of properties which is occurring in the neighborhood of the critical point and above. The critical pressure of a fluid is, by definition, the upper limiting pressure at which the liquid and vapor phase may co-exist in equilibrium. Therefore, at critical pressures or above only a single-phase is present at equilibrium conditions. The critical temperature is similarly defined. The critical point is at the intersection of the critical temperature and critical pressure. Values of representative critical point data for various substances are shown in Table I.

TABLE I  
CRITICAL DATA OF VARIOUS SUBSTANCES

	Temperature (°F)	Pressure (psia)	Specific Volume <sub>m</sub> <sup>3</sup> (lb <sub>m</sub> /ft <sup>3</sup> )
Alcohol	469.6	926	0.0576
Ammonia	270.3	1640	0.068
Carbon Dioxide	87.8	1071	0.0344
Freon 114	294.3	473	0.0275
Hydrogen	- 399.8	188	0.517
Nitrogen	- 232.8	492	0.053
Oxygen	- 181.8	730	0.0376
Pentane	387.0	485	0.069
Water	705.4	3204	0.051

Several interesting property variations occur at the critical point. Theoretically, the specific heat at constant pressure and the coefficient of thermal expansion approach infinity. This behavior may be considered to be a consequence of the fact that the critical point is the upper limit in which boiling occurs. The latent heat of vaporization approaches zero at the critical point, and the specific volume of the saturated liquid and gaseous phases converge. At a pressure infinitesimally smaller than the critical, it is possible to increase the enthalpy by an infinitesimal amount equal to the latent heat while the temperature remains constant. Simultaneously an infinitesimal volume increase occurs. Consequently, the specific heat and coefficient of thermal expansion assume infinite values below the critical pressure. A sharp finite maximum in the specific heat and coefficient of thermal expansion exists at pressures greater than the critical. See Fig. 1. There is no good experimental evidence

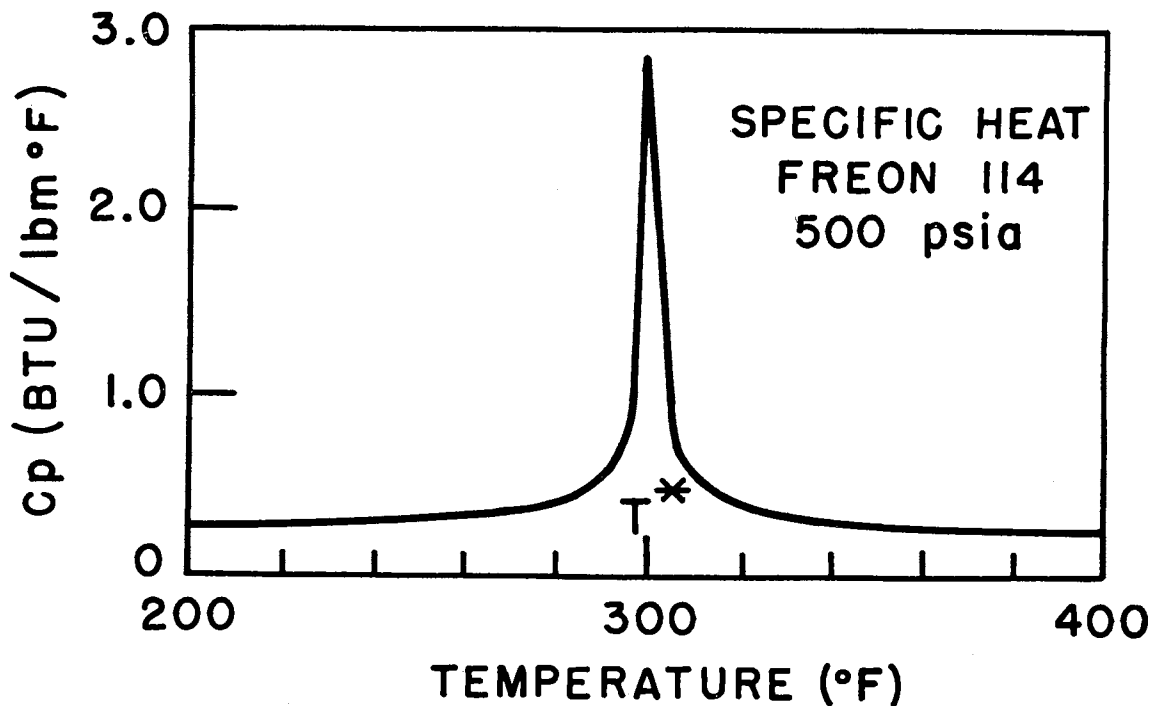


Fig. 1. Specific Heat of Freon 114 at 500 psia

that either property has an infinite value in a supercritical state. The supercritical temperature at which the maximum specific heat occurs is designated the pseudocritical temperature, following the terminology of Goldman (1). The pseudocritical temperature increases with pressure while the magnitude of the maximum specific heat decreases as in Fig. 2.

Consider the changes of properties which occur as heat is added to a unit mass of a substance whose initial temperature is below the pseudocritical temperature at a constant supercritical pressure as shown in Figs. 1 through 4. Initially the properties resemble those of a liquid; the density decreases slightly with the addition of heat, the specific heat is almost constant, and both the viscosity and thermal conductivity decrease with temperature. Such a state will be designated pseudoliquid, as shown in Fig. 2. Such a designation is purely arbitrary. Actually, a pseudoliquid cannot be distinguished from a subcooled liquid by any means other than the reference to the critical point. As the fluid is heated through the pseudocritical temperature, the density of the fluid decreases most rapidly with a small change of temperature. At a temperature above the pseudocritical, the density variation resembles a gas-like behavior and the viscosity and thermal conductivity reach a minimum and then begin to increase with temperature as is characteristic of most gases. Such a state will be designated pseudovapor as shown in Fig. 2. It is seen that a distinct analogy exists between passing through the pseudocritical temperature at a supercritical pressure and boiling at subcritical pressures. The difference is that at supercritical pressures

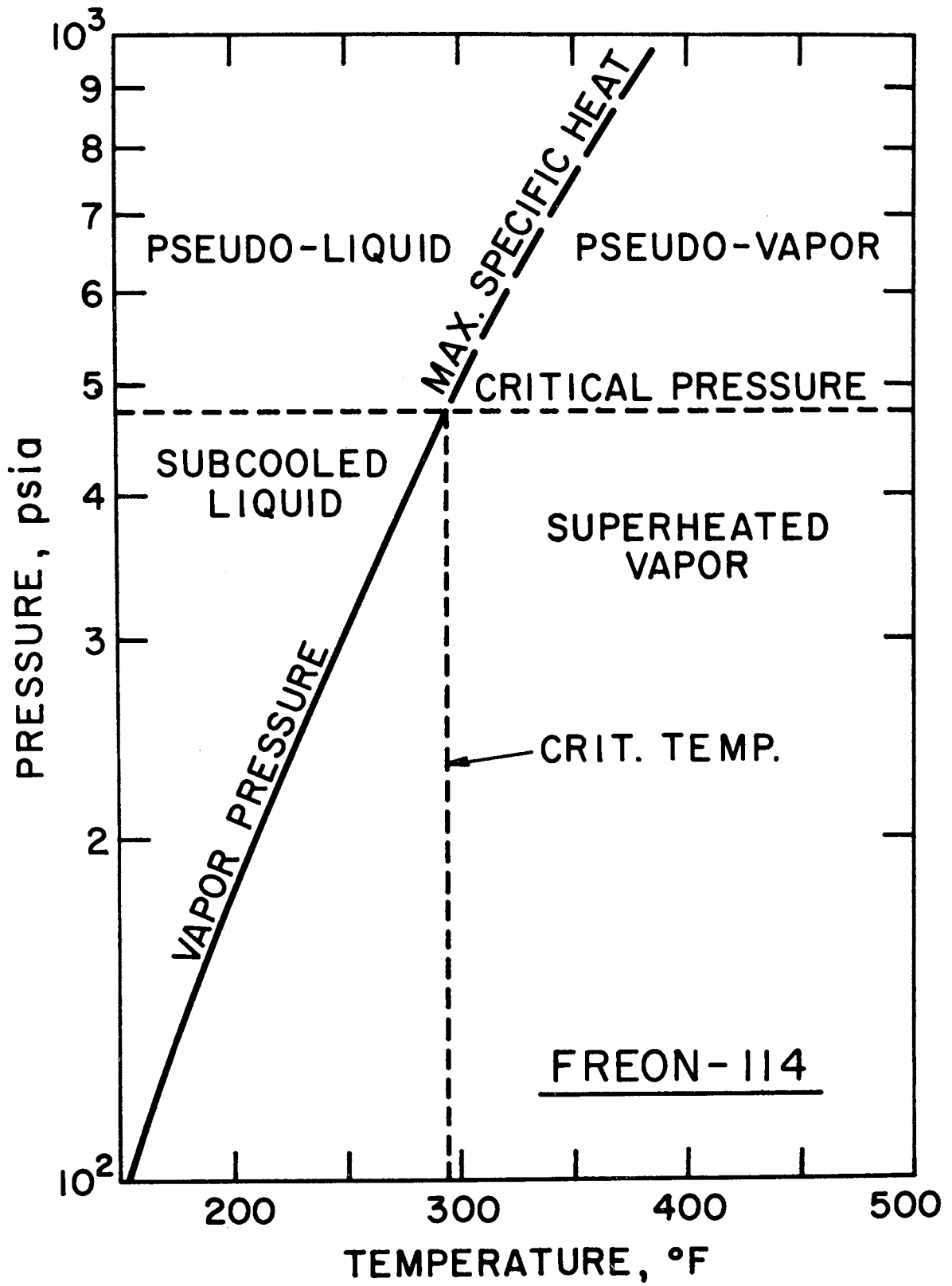


Fig. 2. Phase Regions for Freon 114

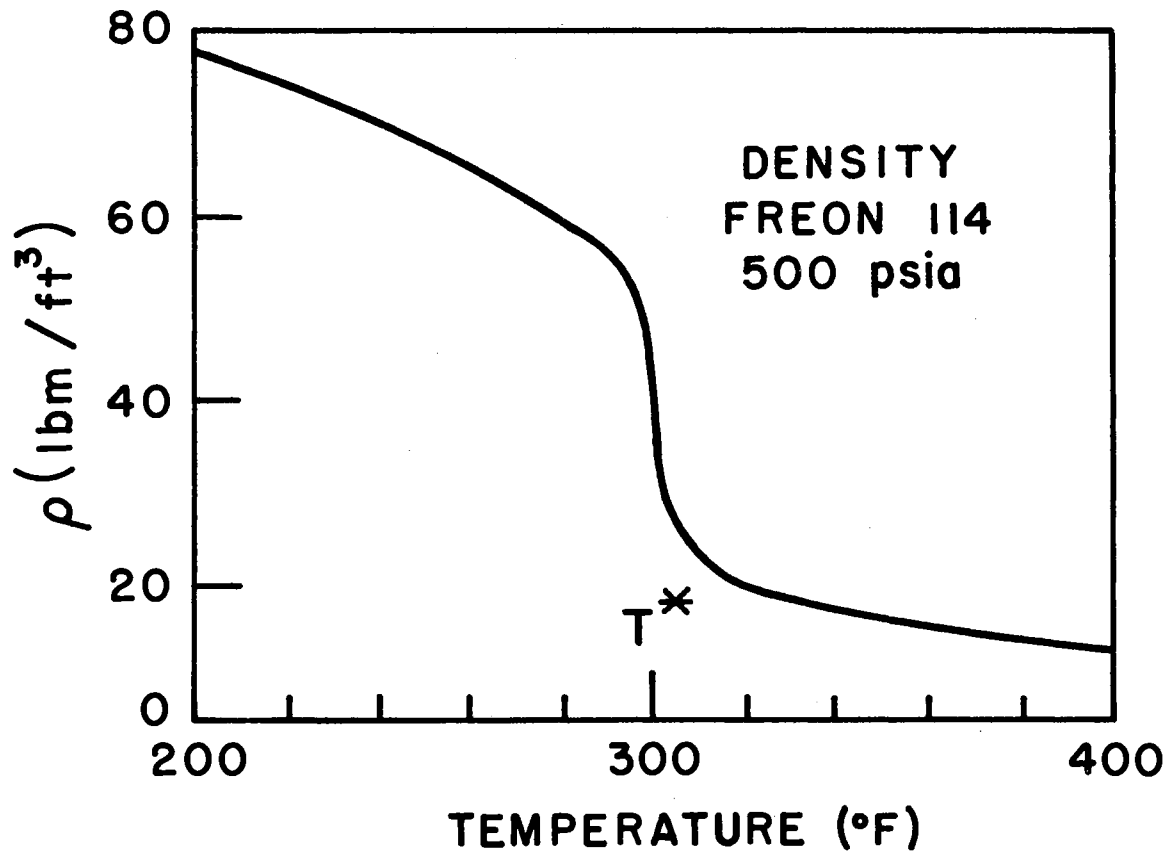


Fig. 3. Density of Freon 114 at 500 psia

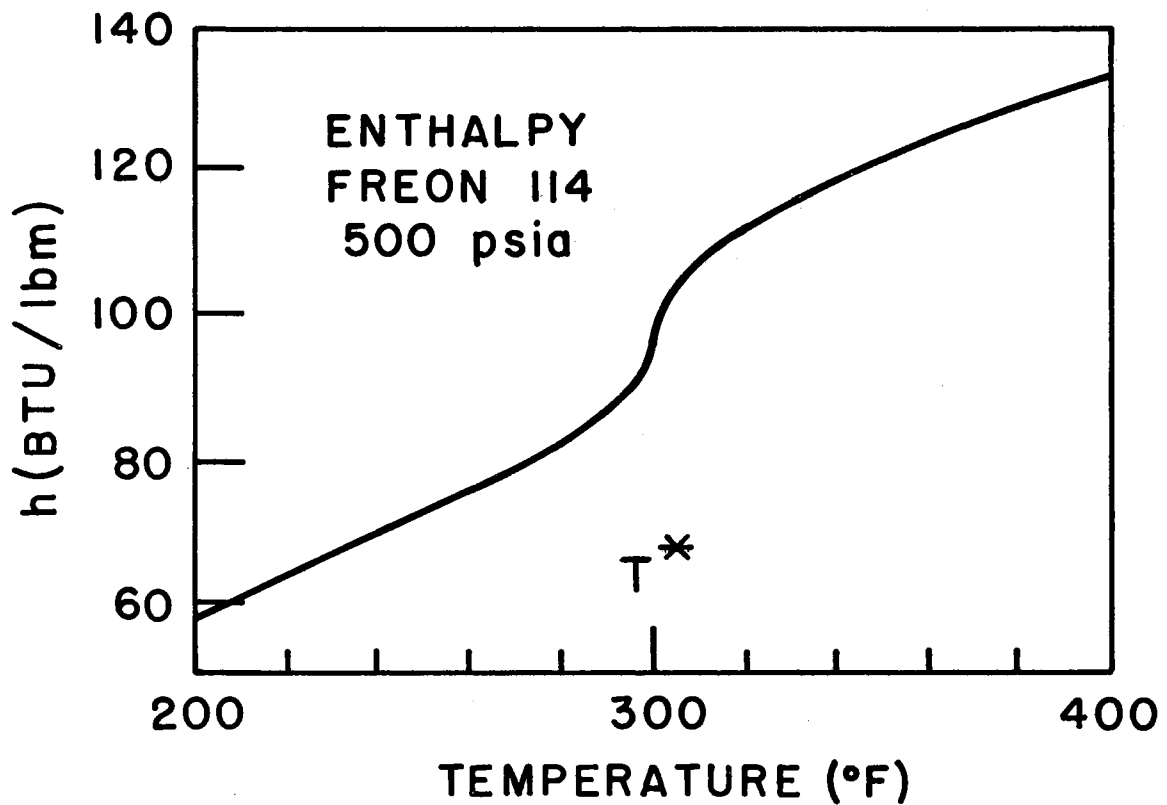


Fig. 4. Enthalpy of Freon 114 at 500 psia

the substance does not separate into two phases in equilibrium, and the relatively smaller volume and enthalpy increase requires a finite temperature change.

Another property which is of interest in compressible flow problems is the sonic velocity. The sonic velocity decreases from a rather high value in the pseudoliquid region to a minimum at the pseudocritical temperature, and then increases to an intermediate value in the pseudovapor region. (Fig. 5). The values of the sonic velocity in the pseudovapor region were calculated for the Freon 114 from the property data of Van Wie and Ebel (2) by Eq. (1.1).

$$c = \sqrt{\left(\frac{\partial p}{\partial \rho}\right)_s} \sim \sqrt{\frac{144 g_c (p_2 - p_1)_s}{(\rho_2 - \rho_1)_s}} \quad (1.1)$$

Since similar data for the pseudoliquid region were available only at temperatures close to the pseudocritical, the values shown in the pseudoliquid region were partially obtained from the experimental data by a method which is discussed in Chapter V. The sonic velocity varies approximately with the cube of the density in the compressed liquid region; a fact which furnishes a reasonable check of the experimental values. It has also been found that carbon dioxide exhibits results similar to those shown in Fig. 5 (.3).

The variation of the thermal conductivity and viscosity near the pseudocritical temperature has not been definitely established. Many correlations show both transport properties decreasing smoothly through the pseudocritical temperature to a minimum at a temperature greater than the pseudocritical (4). However, recent references (5,6) reporting results for carbon dioxide made with a high degree of



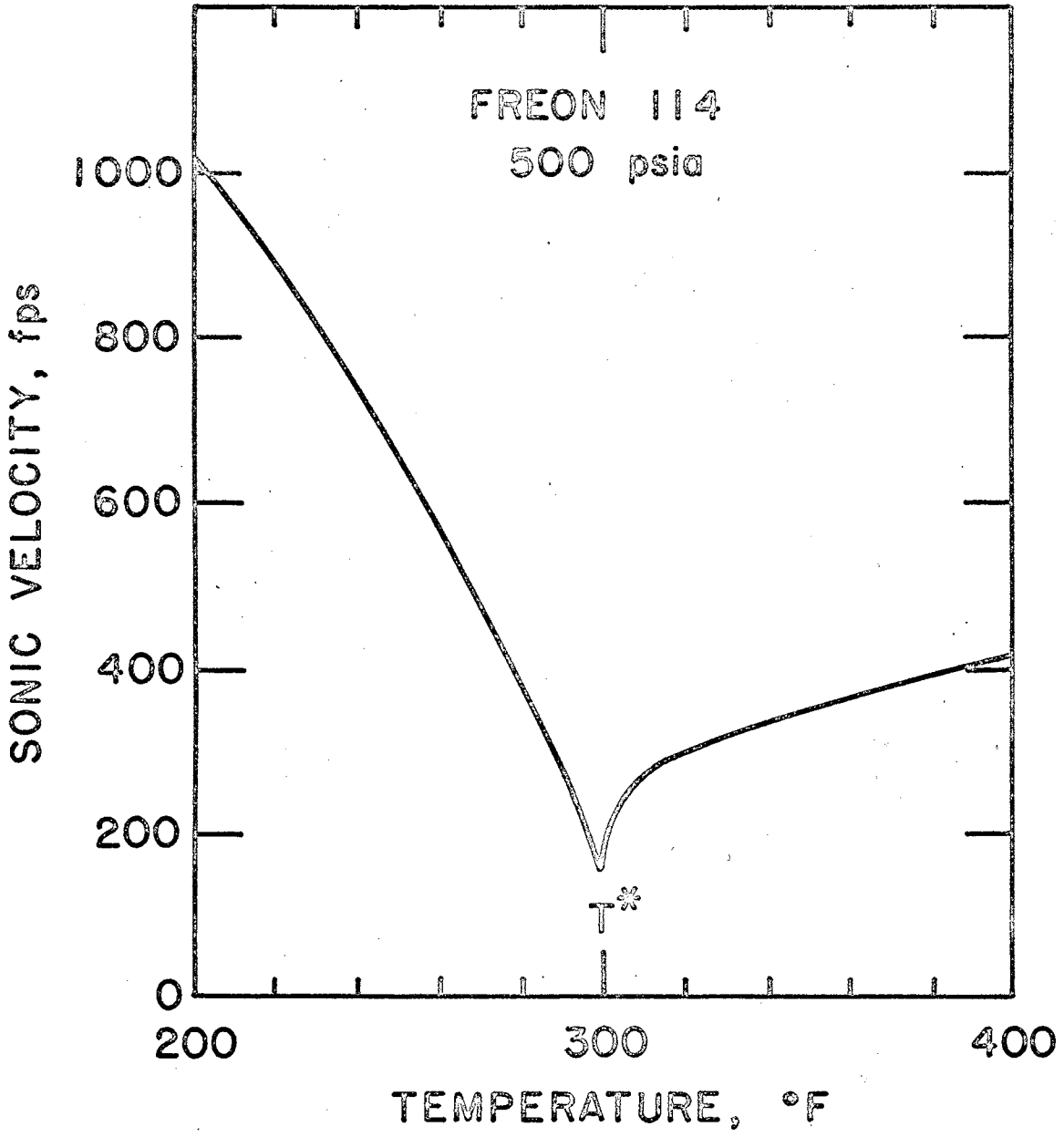


Fig. 5. Sonic Velocity of Freon 114 at 500 psia

precision, show a cusplike maximum in both properties near the pseudo-critical temperature as shown qualitatively in Fig. 6. The results depend, to some extent, upon experimental method and upon the heating rates involved. Simon and Eckert's results (5) for example, show the cusplike maximum vanishing as the heat rate is extrapolated to zero. The results of Sengers and Michels (6) exhibit a maximum which is independent of heat rate at similarly small temperature differentials. Since both tests were reportedly conducted under conditions such that convection effects were negligible, it is difficult to explain the phenomenon. Obviously, this contradiction must be resolved before a completely satisfactory understanding of near-critical transport processes can be attained.

Considerable insight into the liquid-like and gas-like behavior of supercritical fluids may be gained by considering the molecular theory of fluids. In the gaseous region, the molecules are generally considered as having a freedom of motion over distances very large compared with their size, being affected by neighboring molecules only during momentary collisions. When the density of the gas is increased, a point is reached when the mean free path of the molecules is so small that the molecules are affected by their neighbors for an appreciable length of time causing deviation from a "perfect gas" behavior. The close approach of the molecules causes a transitional approach to the liquid-like state, i.e., the molecules become grouped into clusters of pairs, triplets, etc., until the clusters are of microscopic size. The size of the clusters decreases with temperature and increases with density. A dense gas or vapor is considered to be

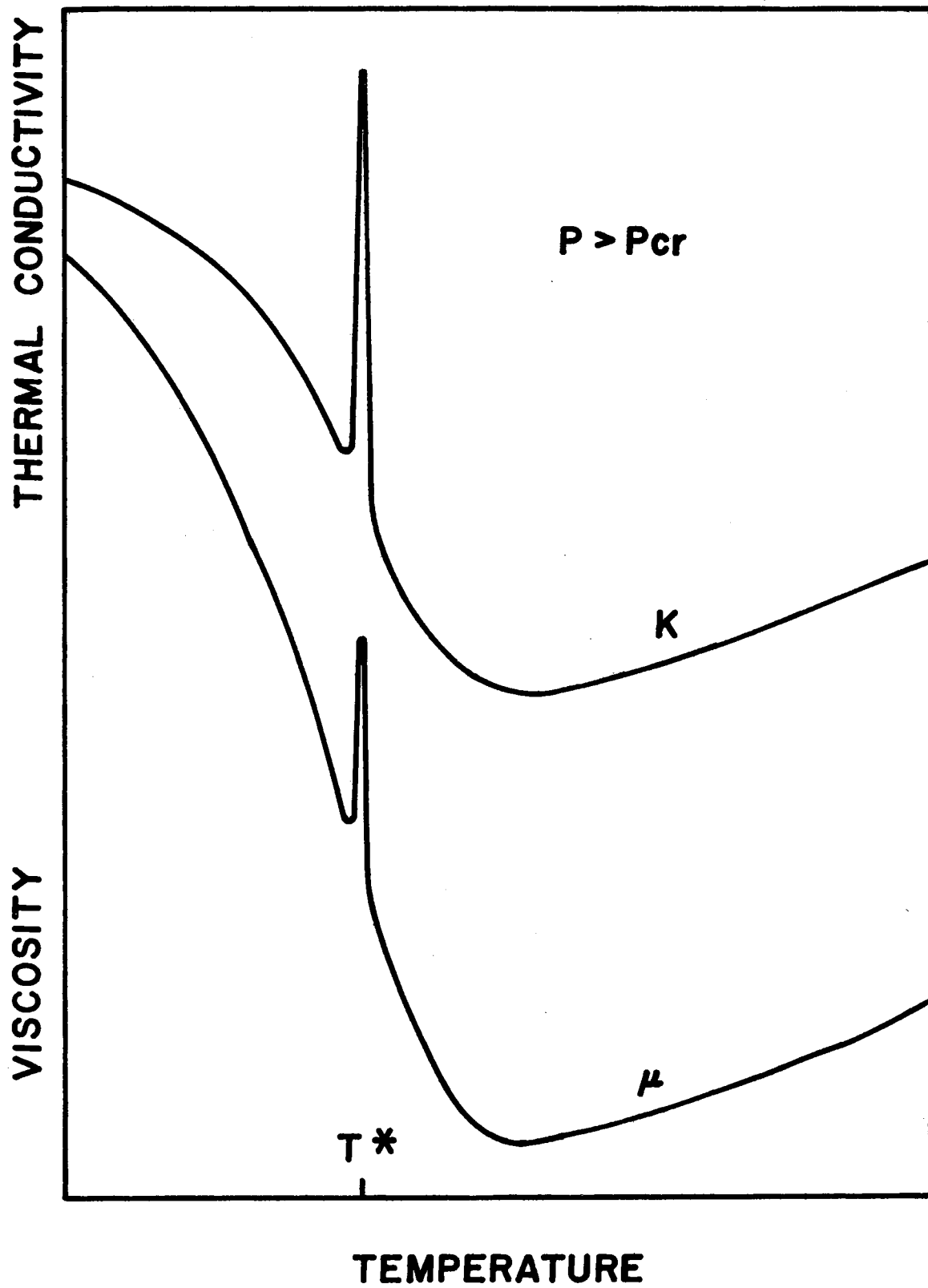


Fig. 6. Qualitative Variation of Viscosity and Thermal Conductivity at a Supercritical Pressure

composed of temporary clusters of molecules, dynamically in equilibrium with molecules which move independently. In the liquid-like region the molecules are considered to be grouped in cybotactic clusters, i.e., a regularly oriented group of molecules resembling a crystal structure.

When energy is added to a liquid-like fluid, the kinetic energy of the molecules is increased. The clusters tend to become smaller in size and spaced further apart. Below the critical pressure, a transition from the liquid to vapor state occurs at constant temperature as energy is added. The cybotactic clusters break up allowing individual molecules to escape. The latent heat is a measure of the energy required to effect this transition. During this subcritical phase transition the fluid can separate into distinct phases with the cybotactic clusters remaining in equilibrium with the individual molecules. It is interesting to note that frequently an excess amount of energy or "superheat" is required to initiate the phase transition, particularly if the fluid is contained in an especially smooth walled vessel. This indicates that nonequilibrium conditions can exist at subcritical pressures.

At pressures greater than the critical, a similar transition occurs. The high specific heat near the pseudocritical temperature is a macroscopic manifestation of the amount of energy required to cause the cybotactic clusters to break up, allowing the molecules to behave as a dense gas. The large coefficient of thermal expansion is a measure of the density change during this transition. During the supercritical transition, the fluid does not separate into two phases

in equilibrium. Rather, the fluid approaches equilibrium as a homogeneous mixture of the molecular groups. Judging from reports of property measurements, several hours or days may be required for this equilibrium to be achieved. The large time required to reach equilibrium is possibly the cause for discrepancies in property measurements, and also may result in various types of anomalous behavior.

## CHAPTER II

### LITERATURE SURVEY

A survey of the literature covering spontaneous oscillatory heat transfer phenomena is presented. It was found that such oscillations have been frequently encountered, are of general interest, but are not well understood, due to the lack of a satisfactory analytical model or physical explanation. Of particular significance to the present investigation are the infrequent references to two different modes of oscillations. The first is of an acoustic nature, with frequencies determined by the geometry of a resonating element and the average sonic speed within the resonator. The second is an oscillation whose frequency is comparable with the natural frequency of the system considered as a vibrating solid body.

#### Single-Phase Supercritical Results

The earliest reference describing oscillations during heat transfer to a supercritical fluid appears in the 1939 German publication by Schmidt, Eckert, and Grigull (7). They were studying the heat transfer characteristics of ammonia at supercritical pressures in an experimental natural circulation loop. "Near the critical pressure both pressure and temperature fluctuated very much in time, so that measurement in this region was made very difficult and in part impossible.

These fluctuations appeared not only during heating but persisted hours afterwards. In passing through the critical state during heating, the pressure and temperature increase was retarded greatly because of the increase of  $\beta$  and  $c_p$ . At about the critical pressure, the manometer pointer rose almost suddenly by about 5 atm." The authors did not attempt to study the oscillation in detail or to venture an opinion about its cause. It was concluded that there was a strong increase of heat transfer near the critical state characterized by an increase of the "apparent heat conductivity coefficient." However, the "apparent heat conductivity coefficient" was defined by the difference in inlet and outlet bulk temperatures, so care must be taken not to confuse the author's coefficient with one based on the temperature difference between the wall and fluid.

Similar pressure fluctuations were encountered during natural circulation heat transfer to Freon 12 close to the critical state by Holman and Boggs (8). Pressure fluctuations on the order of 20 to 30 psi were accompanied by an intense vibration of the test apparatus. The instability of operation was attributed to the rapid change of properties. The test results did not show an appreciable increase in the heat transfer coefficient in the critical region, which was believed to be a logical consequence of the fact that the fluid flow rate is dependent on the heat transfer rate in a natural circulation loop. No mention was made of the behavior of the heat transfer coefficient during the vibrations. This type of behavior was also observed during heat transfer to supercritical water by Van Putte and Grosh (9).

Goldmann (1) studied heat transfer to supercritical water at 5000 psi flowing at high mass flow rates through small diameter (0.075-in. ID) tubes. The experimental work was carried out on a classified project in 1952-1954 (10). Of special interest are observations of two distinctly different modes of heat transfer. For the "normal" mode, the experimental data compared quantitatively with analyses. The second mode was characterized by unexplainably high heat transfer coefficients and the presence of audible noises described as a whistle. The "whistle" occurred only at high heat fluxes and with bulk temperatures lower than the pseudocritical temperature. During the "whistle," the temperature of the last three inches of an eight inch test section remained almost constant. Strain gauge measurements indicated a pressure variation in the test section of up to 1000 psi. The frequency of the sound varied from 1400 cps to 2200 cps. Inlet temperature appeared to have the greatest effect on the frequency. A boiling-like mechanism in the supercritical fluid was postulated as the cause of the behavior.

Goldmann (11) has considered several interesting mechanisms which could possibly account for the audible noises:

- a. breakdown of boundary layer by the buildup of ripples similar to the breaking of ocean waves;
- b. sounds generated by Leidenfrost effect;
- c. sounds generated by the quenching of a hot solid in liquid;
- d. implosion of bubbles;
- e. rubbing surfaces.

Apparently he did not consider that the noise could be due to acoustic resonance in the small diameter tubing, possibly because the whistle



could be produced in various test sections whose length varied between two inches and eight inches. The reports do not mention whether the distance between the mixing chambers was varied substantially when the test section was changed. If not, then the "whistling" phenomena appears to be an excellent example of pressure oscillations due to acoustic resonance in the small diameter tubing.

The supercritical boiling-like phenomena was postulated to explain the increased heat transfer coefficients which were observed. Further substantiation of the supercritical boiling theory was provided when it was learned that similar sounds had been heard during boiling experiments (12,13). A visit by Goldmann and coworkers to various boiling study locations revealed that audible sounds had been heard at certain times but that no reasonable explanations had been found. The visits also revealed that some of the investigators were unaware of the sounds heard at other installations. It was concluded that high intensity sounds can be generated at pressures both above and below the critical. For water at subcritical pressures, high intensity sounds were noted under the following conditions:

- a. small diameter tubes (order of magnitude 1/8 in.);
- b. heat fluxes approaching burnout;
- c. large subcooling;
- d. no boiling at entrance of tube with nucleate or bulk boiling towards the end of tube.

Increasing the heat flux or decreasing the flow could cause the sounds to commence. The audible frequencies were either estimated or measured to be between 1000 and 2000 cps. These conditions described for the occurrence of sound during subcritical boiling were similar to the

conditions at which sounds were noted during the heat transfer experiments with supercritical water (10).

Visual verification that a supercritical boiling-like mechanism can exist was provided by two photographic studies. Griffith and Sabersky (14) observed and photographed bubble-like activity in supercritical R-114A (C Cl<sub>2</sub> F-C F<sub>3</sub>) near a heated surface. The behavior was similar to that observed during nucleate boiling at subcritical pressures. The bubble-like activity that was observed in the pool heating apparatus did not result in an increased heat transfer coefficient such as was observed during subcritical nucleate boiling. Nevertheless the observations support the view that bubble-like activity can exist in a supercritical fluid.

Pool heating of hydrogen at subcritical and supercritical pressures was investigated under varying accelerations by Graham, Hendrick, and Ehlers (15). High speed photographs revealed that a phenomenon resembling columnar boiling existed at supercritical pressures. Bubbles were not present, but sizable agglomerations of low density fluids were observed rising through a denser and colder fluid. This gave a boiling-like appearance to the supercritical heating process. At higher temperature differences the heat transfer coefficients in the supercritical region were similar to those measured during film boiling at subcritical pressures, leading to the conclusion that the heat transfer mechanism is similar for these conditions.

In a study of forced convection heat transfer to supercritical water, Dickinson and Welch (16) measured values of heat transfer coefficients which were twice as large as those predicted by extrapolation of data or by a theoretical analysis. This difference occurred

at fluid temperatures near the pseudocritical. The unexplainably high heat transfer coefficients were attributed to the boiling-like behavior which Goldmann had postulated. No mention was made of any oscillations or unusual noises in the high velocity forced convection runs. Possibly the loop geometry accounted for the lack of oscillations, an idea which will be developed further.

Similarly high heat transfer coefficients were observed by Doughty and Drake (17) during pool heating of supercritical Freon 12. Near the pseudocritical temperature the experimental heat transfer coefficients increased ten-fold over typical values in the pseudovapor region and were three times as large as typical pseudoliquid values. Although the increase was appreciable, the effect depended upon the heating rate and was limited to a narrow region of state conditions. During several experimental runs it was noted that a larger heat transfer coefficient was measured when the heat rate was increasing rather than decreasing. This effect was not always repeatable.

Bonilla and Sigel (18) studied natural convection from a horizontal flat plate to pentane in the vicinity of the critical point. Large temperature differences between wall and bulk temperatures were employed. It was found that the usual natural convection correlations were applicable except at very high Rayleigh numbers where a limiting Nusselt number of about 1300 was reached despite increased values of the Rayleigh number. Minor ( $2^{\circ}\text{F}$ ) temperature oscillations were noted.

In studies of forced convection heat transfer to liquid hydrogen and helium in an open loop McCarthy and Wolf (19) observed that under certain conditions the heat transfer was accompanied by spontaneous

pressure oscillations of 2 to 4 psi amplitude. The frequencies were on the order of 500 cps, approximately the fundamental acoustic frequency of the test section between two mixing chambers. The presence of the acoustic resonance was found to increase the heat transfer coefficient by as much as a factor of two. The conditions which caused the oscillations were not studied.

Thurston (20) examined the hydrogen oscillation in more detail in an open blowdown type of apparatus. Heating was provided by cooling the test section from ambient to liquid hydrogen temperatures during each run. Acoustic oscillations, which were identified as open pipe and Helmholtz resonance, were observed. A slower pressure oscillation, described as a sawtooth or negative pressure pulse, was accompanied by large variations in flow rate. None of the oscillations occurred when the inlet fluid was in a pseudovapor state. From this, it was concluded that the mechanism for driving the oscillations occurred only when a pseudoliquid was present in some part of the test section. No speculation was presented as to the nature of the mechanism.

Severe oscillations were encountered by Hines and Wolf (21) during heat transfer to supercritical hydrocarbon rocket fuels. Pressure fluctuations of 380 psi amplitude peak-to-peak at frequencies of 600 to 10,000 cps are reported. The vibrations caused many of the thin-walled test sections to fail during a thirty minute test period. The vibrations also occurred in thicker test sections which withstood the stresses. The oscillations were accompanied by sharply increased heat transfer coefficients and an audible noise, described as a high pitched scream which could be heard for 200 yards. An analysis of the frequency

spectrum showed that the dominant frequency varied from 1200 to 7500 cps. Minor frequencies were always present, ranging from 600 to 15,000 cps. From this, it was concluded that the pressure oscillations were not simple resonant acoustic oscillations such as had been reported by McCarthy and Wolf. However, it is interesting to note that the reported frequencies for a given experiment, tend to appear as multiples of a common factor. From this, one concludes that the pressure oscillations could be caused by an acoustic resonance in which the higher harmonic frequencies dominate the fundamental frequencies. This idea will be discussed further in a later chapter.

A hypothesis of a viscosity dependent mechanism which could cause the oscillations to be sustained was presented by the above authors. It was noted that very small changes in temperature near the critical point result in large changes in viscosity. A sudden increase in wall temperature could cause a thinning of the laminar boundary layer due to the viscosity variation. Thinning of the boundary layer would result in a drop in wall temperature, and a corresponding rise in viscosity. This would cause a thicker boundary layer and produce another rise in wall temperature. In this manner the process could perpetuate itself, leading to sustained oscillations. While the postulated viscosity dependent mechanism may contribute to certain types of oscillatory behavior, such a mechanism would not account for sustained oscillations which are acoustic in nature. In order for an acoustic pressure wave to be maintained, it is necessary that a pressure increase, rather than a temperature increase, triggers the mechanism. Since the viscosity normally increases with pressure, an increase of pressure at a point would result in a thicker boundary

layer, a reduced heat transfer rate, and would cause acoustic oscillations to be damped, rather than sustained.

Guevara, McInteer, and Potter (22) have observed temperature-flow instabilities in a system in which helium flows through a uniformly heated channel with an increase in the absolute gas temperature by a factor of 3.6 or more. This instability occurred in the region of negative slope on a steady-state pressure drop versus flow diagram. When a plenum preceded the channel the oscillation was sustained and spontaneous. Addition of an introductory impedance resulted in eliminating the region of negative pressure drop gradient and in stabilizing the system. According to the authors no satisfactory theoretical analysis was developed. Observations consisted largely of pressure drops across the test section and simultaneous flow and power measurements. The experimental periods were on the order of one thousand seconds which may have been caused by the large time required for temperature equilibrium to be established in the equipment rather than by hydrodynamic considerations.

A surprising result was obtained during heat transfer to oxygen near its critical temperature by Powell (23). It was found that a sharp minimum heat transfer coefficient existed at bulk temperatures near the critical which would tend to limit the use of this gas as a heat transfer fluid. Additional experiments with hydrogen and nitrogen were undertaken with similar results but details were not reported. No mention was made of any oscillatory phenomena. The tests with oxygen were made with high wall to bulk temperature ratios. The minimum heat transfer coefficient resulted in extreme axial temperature profiles at critical bulk temperatures, in which the wall temperature

increased from 400°R to 2000°R in only ten inches and then rapidly declined as the bulk temperature increased above the critical. Only one other report of a decreased heat transfer coefficient near the critical temperature has been found and is described below. A somewhat similar result was observed during the current test program.

A number of references are available covering heat transfer to supercritical carbon dioxide which describe forced convection, closed loop experiments. When the bulk temperature of the carbon dioxide was below the pseudocritical Koppel and Smith (24) reported unusual axial variations in the heat transfer coefficient. This behavior was most pronounced near the pseudocritical temperature where the wall temperature also was observed to fluctuate randomly with a period of about one second. These fluctuations were not studied extensively. At higher heat fluxes, results similar to Powell's were obtained, i.e., the wall temperature increased from 330°F to 680°F in six inches and then declined. Wood and Smith (25) measured the radial variation of velocity and temperature. The results indicated a flattening of the radial temperature profile, a maximum in the velocity profile between the wall and the tube axis, and a maximum heat transfer coefficient when the bulk temperature passed through the pseudocritical temperature. When measurements were taken within 1°F of the pseudocritical temperature, temperature fluctuations were observed with magnitudes of up to 2°F. Similar pressure fluctuations were not observed. Bringer and Smith (26) presented a generalized correlation for estimating heat transfer coefficients. No mention was made of unusual heat transfer coefficients or oscillatory behavior. Similar results were obtained by Petrukhov, Krasnoschekov and Protopopav (27).

In the carbon dioxide tests reported in the above paragraph, no flow or pressure oscillations were noted. Perhaps the reason is the low critical temperature of carbon dioxide (87.8°F). In all of the CO<sub>2</sub> closed loop tests, the cooling was controlled by tap water. Consequently, it was impossible to operate at high differential temperatures with bulk temperatures substantially below the pseudocritical; the operating conditions which generally cause the instabilities to occur.

A visual investigation of laminar free convection from a heated vertical plate immersed in carbon dioxide near its critical point was described by Simon and Eckert (5). The refractive index distribution was employed to calculate the heat transfer coefficient and the thermal conductivity of the fluid. Both properties showed a maximum near the critical point which depended upon the heat transfer rate despite extremely low heating rates and less than 0.01°C temperature differences across the heated boundary layer. This rate dependence suggests that a natural convective mechanism may have aided the conduction process, although the authors were unable to discern any circulation with their high resolution equipment. Near the critical point it was difficult to maintain equilibrium for over a few minutes, circulation in the fluid could not be avoided. At low heating rates a slow pulsating instability was evident in the boundary layer and at high heating rates transition to turbulence occurred.

Harden (28) studied the oscillations in a Freon 114 natural circulation loop. Although he did not recognize them as such, the pressure and flow oscillations may be considered to be of two types. The first was characterized by a dominant frequency of 10 to 20 cps, which



was two orders of magnitude greater than the second type of oscillation. Since all of the oscillations were encountered at bulk temperatures below the critical, Harden concluded that "the phenomena could not be attributed to the thermodynamic critical point but rather to a critical region." This conclusion was reached due to a consideration of only a one-dimensional model in which all effects were assumed to be caused by variation of bulk properties, rather than local properties. In neglecting the two-dimensional aspects of the problem, he failed to recognize that even though the bulk temperature was below the pseudocritical during the experimental instabilities, the fluid in the heated boundary layer could be, and in fact was, in a pseudovapor state. Consequently, the temperature passed through the pseudocritical in the heated boundary layer during the instabilities.

Harden further concluded that the instabilities occurred only when the product of the bulk density and enthalpy went through a maximum. He reached this conclusion from the fact that his plot of this product vs. temperature exhibited a maximum below the pseudocritical temperature in the general region where experimental instabilities were encountered. According to this criterion the instability occurs when the heater outlet bulk temperature is  $10^{\circ}\text{F}$  to  $15^{\circ}\text{F}$  below the pseudocritical temperature. Consequently, the instability would appear to be unrelated to the large variation of properties that takes place at the critical point. This conclusion is believed to be untenable for the following reasons. The location of the density-enthalpy maximum depends upon the arbitrary enthalpy reference point. If the enthalpy is assigned a value of zero at a state different than the one used (saturated liquid at  $-40^{\circ}\text{F}$ ), the maximum shifts up or

down in a readily predictable manner.<sup>1</sup> Hence, no especial significance can be attached to the shifting location. Further, the unstable behavior was observed outside the region defined by the density-enthalpy maximum criterion, both in the present test program and in several instances listed in Appendix E of Harden's report.

### Boiling Instability

The striking similarity between instabilities observed during subcritical boiling and supercritical heat transfer studies suggests a common mechanism. Since boiling instabilities have already received a good deal of attention, due to their importance in reactor design, the literature in this field was examined.

Over seventy references on two-phase flow oscillations or instabilities were listed by Gouse (29). He concluded that one cannot satisfactorily predict the onset, magnitude, frequency, or disappearance of flow oscillations in various situations. Further, he concluded that no satisfactory analytical model or satisfactory physical explanation of the various types of oscillatory phenomena existed (30). A similar conclusion was reached by others (31,32).

The uncertainty as to the cause of the instabilities limits the use of the analytical models which have been developed. The analytical models are useful only in predicting trends which can be compared with experimental data and in approximate extrapolation of the performance of existing reactors. They do not give a consistent theoretical

---

<sup>1</sup>This fact was first brought to attention by Howard Creveling of Purdue University.

understanding of the instabilities' basic nature sufficient to ensure that the instabilities can be avoided. This necessitates employing a large factor of safety in the reactor design which results in the overdesign of reactors which are inherently limited by stability considerations. This overdesign is emphasized since the instabilities have been believed to promote burnout in some instances (31).

The analysis of the boiling instabilities has proceeded along several lines. In one case, it has been assumed that extremum in the pressure drop vs. flow rate curve are responsible for unstable behavior. The analysis has consisted of determining where the inverse plot of flow rate vs. pressure drop is multiple valued, i.e., a given pressure drop occurs for more than one flow rate. This criterion was first used by Ledinegg (33) to analyze boiler tube instabilities. In several other instances it was reported that instabilities had occurred in the region defined by the criterion (22,34). However, unstable behavior has also been observed outside of this region, indicating that another mechanism exists (30,31,35,36).

The most general approach to the problem involves the solution of the mass, momentum, and energy conservation equations subject to the boundary conditions imposed by the loop geometry (36-43). The equations are nonlinear and the complexity of the problem requires simplifying assumptions whose validity is difficult to assess. Fortunately, the situation is improving in this respect, as a better understanding of the two-phase hydrodynamics is slowly acquired. The development of numerical techniques is also progressing rapidly in this field.

Possibly the chief stumbling block to an adequate solution is the

inability to properly describe the transient microscopic behavior during nonisothermal two-phase flow by empirical correlations of steady-state macroscopic observations. These empirical correlations, which relate such quantities as friction losses, heat transfer coefficients, flow regimes, and slip to such quantities as average fluid properties and flow rates, are of necessity an integral part of every analysis. In single-phase problems, separate correlations are commonly given for each of only two flow regimes; laminar and turbulent. The transition region between these regimes is not well defined and correlations therein are rarely attempted. The problem is compounded in two-phase problems where many regimes are recognized: mist flow, slug flow, annular flow, film boiling, nucleate boiling, etc. In order to properly solve the boiling instability problem by existing techniques, the usual correlations are required, not only for the separate regimes, but also for the transition region between the regimes. For example, the experimentally observed boiling instabilities have one feature in common. The boiling instabilities invariably occur only when the fluid at the heater inlet is subcooled and at least some nucleate boiling occurs in the heated section. Consequently, an adequate solution and understanding of the problem requires, as a minimum, that the behavior during the transition to nucleate boiling be thoroughly understood, not only for steady-state conditions, but during transient conditions as nucleate boiling starts and stops. While this conclusion seems elementary, and vitally important, no discussion of its effect has been found in the literature.

Pressure oscillations during boiling water reactor operation have

been observed to fall into two frequency ranges (44). Several reporters have speculated that the more rapid oscillations were due to acoustic resonance. The variation of the velocity of sound in a two-phase mixture is comparable to that in a supercritical fluid, (Fig. 5). The sonic velocity decreases from a high value in the compressed liquid state to a minimum at an extremely low quality. The sonic velocity then increases rapidly, assuming a value characteristic of superheated vapor at higher qualities (45). Fleck (46) pointed out that the small sonic velocity of low quality steam could result in acoustic resonance with fairly high periods on the order of three to four seconds. Most of the alleged acoustic oscillations have exhibited periods considerably smaller than this value, ranging downward to the order of milliseconds.

Christensen (47) described several instances in which acoustic resonance was suspected to be significant in reactor operations. He also reviewed the analogy between electric transmission lines and acoustic transmission systems. He concluded that a simple "lumped parameter" model was sufficient to describe the acoustic system of the particular reactor which he considered. In this model the steam dome and condenser volumes were replaced by equivalent electrical capacitors. The pipe connecting these two volumes was replaced by an equivalent electrical resistance in series with an inductance. The small volume of the pipe justified neglecting its equivalent capacitance. The resonance of the equivalent electrical circuit was 2.4 cps, compared with the experimentally determined acoustical resonance of 3.2 cps. The difference was believed to be due to the neglecting of

the more complicated piping arrangement of the physical system.

The occurrence of vibration phenomena during boiling heat transfer which resulted in the generation of audible sounds has already been described (12,13). Although the pressure oscillations which produced the sounds were not recognized as such, at the time, many of these pressure oscillations were probably of an acoustic nature. In order to avoid confusion, it may be well to note that an acoustic pressure oscillation inside a pipe does not necessarily result in noises which are audible to an observer standing beside the pipe. For one reason, the frequency may be outside the audible range (20 to 20,000 cps). Even acoustic frequencies falling in the audible range may not be audible outside the pipe. In order for a sound to be heard, the disturbance must be propagated through the pipe walls to the ambient surroundings with sufficient intensity for the observer's ear to perceive. Thick pipe walls, or layers of insulation, may prevent such a propagation.

Acoustic oscillations of 10 cps frequency were observed during boiling heat transfer studies by Gouse and Andrysiak (30). The acoustic oscillations caused small bubbles to appear to "blink," i.e., rapidly collapse and then expand in high speed photographs. The "blinking" was too fast to observe visually but was also detected by pressure transducers.

In a study of film boiling of water-methanol mixtures, Hoglund (48) encountered an instability which he designated as "chugging." This resulted in a sound similar to a steam locomotive with frequencies from 1100 to 1400 cycles per minute. The bubbles in the tube were observed

to expand and collapse in unison. The frequency of the "chugging" was found to decrease as the water temperature increased and as the water level above the tube was decreased. Addition of methanol to the system caused smaller bubbles to form and also resulted in a more violent "chugging."

It has been noted, in several instances, that the observed frequencies were comparable to the calculated undamped natural frequency of the hydraulic loop considered as a vibrating solid body. The comparison was made for systems with free surfaces and equivalent U-tube flow paths. Such oscillations were referred to as gravity oscillations by Viskanta (49). Using LaGrange's equations of motion in terms of one degree of freedom, and assuming a constant density, he calculated a natural frequency for the two-phase Armadilla flow loop of 0.598 cps. This frequency compares closely to the value of 0.67 cps which was observed at the "chugging" threshold. The method does not consider the fundamental cause of the instability but it was postulated that disturbances such as addition of makeup water or bubbling of steam through the boiling channel were sufficient to excite the gravitational oscillations. It was concluded that the fair agreement between the experimental and calculated value might be purely accidental.

Gouse and Andrysiak (30) also observed oscillations whose frequencies were on the order of the undamped natural frequencies of their loop considered as a U-tube manometer. Their test section consisted of parallel heated channels so that more than one natural frequency existed. In general, there are as many natural frequencies as

channels, but some may be identical due to symmetry. The natural frequencies were calculated by using LaGrange's equations of motion. The authors listed other experimental investigations where the flow oscillation frequencies were comparable to the natural frequencies of the respective systems considered as oscillating manometers (41, 50-52). This fact was not mentioned in the original references. The results of the Minnesota loop (43) were given as an example of a case where the observed frequencies were much lower than the calculated manometer frequencies. Experimental oscillation frequencies from this loop were lower by at least an order of magnitude than from most other loops. However, using the method described in Appendix B, it can be shown that the low natural frequency of this loop was due to its geometry, and the fact that a true free surface condition did not exist.

#### Summary

The oscillatory behavior encountered during heat transfer to a fluid appears to be similar, regardless of whether the fluid is at a subcritical or supercritical pressure. Although not too much attention has been given to this fact, the oscillatory behavior which has been reported for supercritical fluids is considered by the author to be mainly of a resonant acoustic nature. A similar behavior has often been observed for boiling subcritical fluids, but is generally treated sparingly in the literature. Conversely, the literature contains many reports of subcritical boiling instabilities which could be, although they have not usually been, considered as analogous to a



manometer type of oscillation. This type of oscillation also occurs in supercritical systems, but very few reports of such occurrences are available. The manometer type of oscillation is generally less symmetrical in nature, and is less rapid than the acoustic oscillation. It is of prime interest in boiling systems since it is believed to cause power fluctuations in nuclear reactor applications and contribute to premature burnout.

## CHAPTER III

### EXPERIMENTAL APPARATUS

A heat transfer loop, designed to operate by either natural or forced convection, was constructed to study the unstable behavior. The relative location of the essential features of the loop is shown schematically in Fig. 7. Refrigerant 114, symmetric dichlorotetrafluoroethane (critical pressure 473.18 psia, critical temperature (294.26 °F) was employed as the heat transfer medium in order to avoid operating at an excessive pressure and temperature. The results reported in the literature indicate that the behavior should be similar for most of the ordinarily employed coolants.

The entire loop and test section were fabricated from 1-in. OD, 0.93-in. ID, AISI Type 304 stainless steel tubing. The flow path was rectangular in shape, with the corners rounded to a 6 in. radius. The overall dimensions of the flow path were 18.09 ft high by 6.83 ft wide, measured along the tubing centers. This resulted in a length of 49.1 ft and a volume of 0.232 ft<sup>3</sup> for the loop. Heliarc welding was employed as much as possible in the loop construction, after it was found that the commercially available tubing connectors tended to buckle the thin tubing, resulting in leaks which were difficult to repair. Table II lists the vertical distance to the components shown in Fig. 7, measured from the bottom horizontal section.

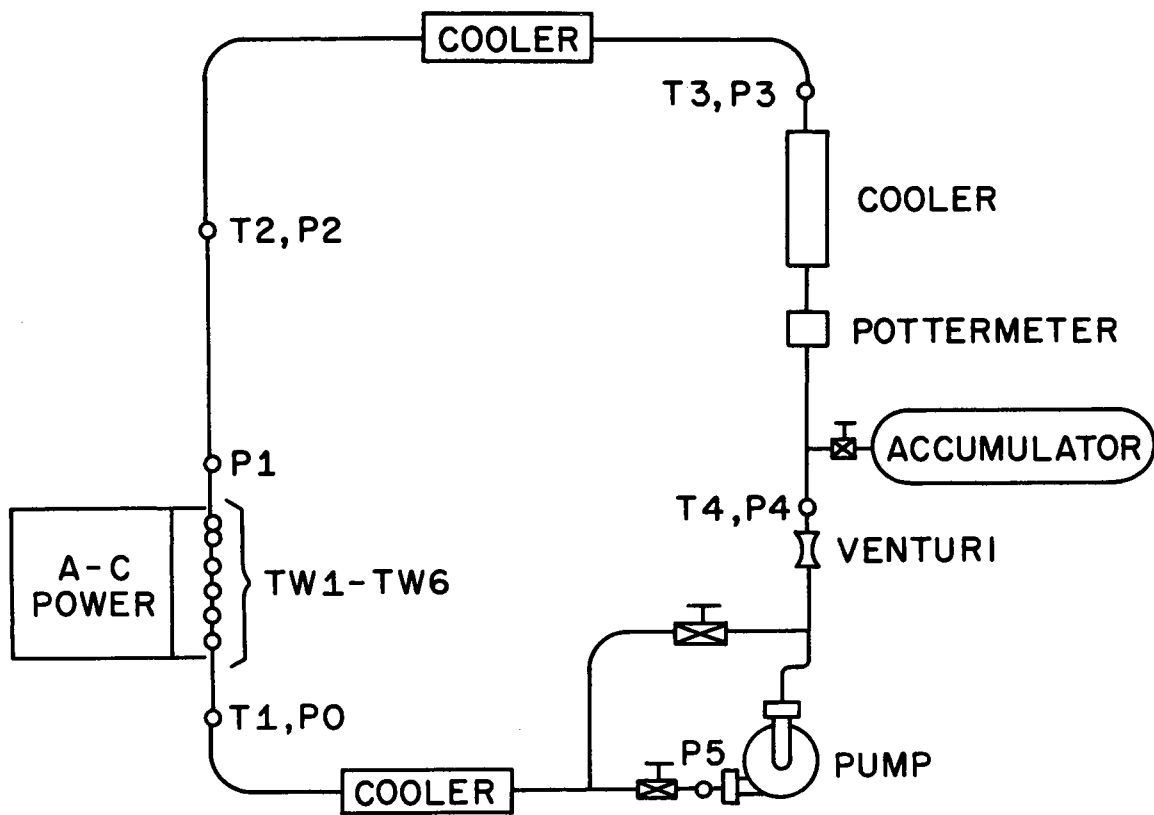


Fig. 7. Schematic Diagram of Heat Transfer Loop

TABLE II

## VERTICAL HEIGHT OF LOOP COMPONENTS

(REFER TO FIG. 7)

Component	Height * (ft)
Pump Exit, Pressure Tap (P5), and Bottom Horizontal Cooler	0
Bulk Temperature (T1) and Pressure Tap (P0)	1.58
Heater Inlet	2.07
Heater Outlet	5.07
Pressure Tap (P1)	5.50
Bulk Temperature (T2) and Pressure Tap (P2)	9.71
Upper Horizontal Cooler	18.09
Bulk Temperature (T3) and Pressure Tap (P3)	15.93
Top of Vertical Cooler	15.76
Bottom of Vertical Cooler	10.76
Pottermeter (Turbine Flowmeter)	10.19
Accumulator	5.31
Bulk Temperature (T4)	4.31
Pressure Tap (P4)	4.09
Venturi Throat Pressure Tap	3.88
Bypass	1.58

\*Measured to centers of tubing

## Component Description

Many of the loop components had been used in a previous study (28). Their availability dictated their use in the present tests, not only from the standpoint of conserving time and money by avoiding duplication of effort, but it also allowed a more meaningful comparison to be made of the effect of changing the loop geometry and operating techniques between the two experiments. A brief description of the loop components follows.

Test Section. The test section was fabricated from a three foot length of commercially available AISI 304 stainless steel tubing, with a 1-in. OD and a 0.035 in. wall thickness. The tubing is rated

for 500 psi pressure at 1000°F by ASA piping codes, with a safety factor of about four under these conditions. Copper bus-bars, (9x5x5/8 in.) were silver soldered to the ends of the test section. The test section was connected to the loop with one inch, 300 lb stainless steel pipe flanges. Durable gaskets were employed between the flanges and around the connecting bolts to electrically insulate the test section from the rest of the loop.

Power Supply and Measurement. The test section was electrically heated by AC power furnished by a portable ignitron controlled power supply. The power supply consisted of two independent transformers, each capable of stepping down the line voltage from 440 v to a selected value. The output voltage could be varied continuously from 0.75 to 7.5 v in the present tests. The ignitron circuits controlled the phase shift of the power cycle. The unit was rated to hold current fluctuations within  $\pm 0.25$  percent of full load current for line voltage variations of  $\pm 15$  percent. The power supply was capable of maintaining a constant rms power level to within less than  $\pm 1$  percent. No fluctuations in excess of this were noted with the instrumentation employed during the present tests, although occasionally a manual adjustment was necessary to compensate for a drift in the power level.

The electrical energy input to the test section was measured with a portable laboratory wattmeter, whose range was 0 to 500 w and whose accuracy was 0.25 percent full scale. As a check of the values obtained, the power was also determined by the product of the voltage drop across the test section and the heating current. The current was

reduced with a current transformer by a ratio of 2000:5 and read with a portable ammeter with a range of 0 to 10 amps and an accuracy of 0.25 percent full scale. The voltage across the test section was stepped up with a voltage transformer by a ratio of 10:1 and read on a portable voltmeter with a range of 0 to 30/60 v and an accuracy of 0.25 percent full scale.

Coolers. The fluid could be cooled at any or all of the three counterflow heat exchangers. Tap water from the laboratory water supply was used as a coolant. The coolant piping was manifolded to allow use of a single cooler, or several coolers in series. The coolant flow rate was measured with two calibrated rotameters, connected in parallel. The dual range of the rotameters, 0 to 10 gpm and 0 to 0.6 gpm, permitted a fine and coarse adjustment of the coolant flow rate by manual control. The coolant temperature was measured at each cooler inlet and outlet by chromel-alumel thermocouples immersed in the fluid stream.

The coolers consisted of a length of 2 in. schedule 40 stainless steel pipe, welded concentric to the 1 in. tubing. No allowance was made for the thermal expansion between the tubing and the shell, since previous operating experience (28) had shown this design to be satisfactory. The two upper coolers were each 5 ft long. The bottom horizontal cooler was of 45 in. length. For most of the tests only the cooler on the vertical leg was employed. When more cooling was desired, the vertical cooler was connected in series with the upper horizontal cooler. The bottom cooler was used mainly for cooling as the loop was being filled.

Pump. A canned-motor centrifugal pump was installed in the loop in order to compare results from natural and forced convection. All wetted surfaces were constructed of stainless steel and the 3/4 hp, 3500 rpm motor was lubricated and cooled by the test fluid, which minimized the chance of contamination. There was some question before the tests as to whether the supercritical fluid would provide sufficient lubrication so as to prevent bearing failure. The pump was operated at fluid temperature up to, and exceeding the pseudo-critical temperature with no apparent adverse effects. The pump operated satisfactorily at low flow rates, which were controlled by an air-operated throttling valve placed downstream of the pump exit. At higher flow rates, on the order of 8 to 10 gpm, an irregular pressure and flow disturbance occurred, which was attributed by the pump manufacturer to cavitation caused by the rather severe operating conditions.

Accumulator. The pressure and system mass were controlled with a gas bag hydraulic accumulator. The accumulator consisted of a 2-1/2 gallon commercially available stainless steel tank, in which a synthetic rubber bag, filled with nitrogen gas, absorbed pressure surges. A bank of three nitrogen bottles were connected in parallel with the gas bag to provide for a larger gas volume and minimize pressure variations. The accumulator provided a convenient means to automatically bleed off fluid due to volumetric expansion as the system was heated. Thus the system could be pressurized to a supercritical pressure before heating began, and the entire experiment could be conducted at this pressure by regulating the nitrogen pressure.

The accumulator was connected to the loop with 1/2 in. stainless steel tubing, which was run through a small water cooler to keep the temperature in the accumulator below 250°F.

Flow Measurement. The flow was measured during the early tests with a calibrated venturi. The venturi was constructed according to ASME recommendations with a throat diameter of 0.3963 in. and inlet and outlet diameters of 0.93 in. Details of the venturi construction and calibrations are given in Reference 28. Steady-state flow rates, as measured by the venturi, agreed with values calculated by making an energy balance across the test section to within two percent. The differential pressure across the venturi taps was measured during steady-state conditions and for calibration purposes with one of two parallel manometers, which contained respectively, a 2.95 specific gravity fluid and mercury. Transient measurements were made with a differential pressure transducer.

The rapid pressure oscillations which were encountered resulted in measuring differential pressure oscillations whose amplitude exceeded the average value, i.e., a flow reversal was indicated. Extreme examples of this type are reported in Reference 28. As soon as it was realized that the rapid oscillations were of an acoustic nature, it was suspected that the large venturi pressure drop amplitudes could be due to the phase relationship of the absolute pressure at the venturi pressure taps. This effect would be especially severe for acoustic oscillations of short wave length, since it can be shown to be inversely proportional to the wave length. (See Appendix A). However, subsequent analysis showed that the large pressure drop



amplitudes were not caused entirely by the absolute pressure phase effects for this type of acoustic oscillation.

It was noted that shaking or pounding on the supporting structure would cause the differential transducer signal to oscillate. The transducer and lines were remounted as solidly as possible, but the effect could not be entirely eliminated. It was concluded that it is possible for mechanical vibrations to cause large indicated pressure drop amplitudes, particularly if the differential transducer lines are not well secured. Since the loop tended to shake during the rapid oscillations, another means for measuring the transient flow was required.

A venturi does not give a true indication of flow rate during a rapidly recurring variation in velocity or pressure (53). Turbine-type flowmeters are available, whose accuracy is rated at better than 0.5 percent even when the flow is pulsating at the frequencies encountered (54). Therefore, the use of a turbine flowmeter was indicated; however, previous experience (28) had indicated that the turbine type of flowmeter (3/4 in. Pottermeter) tended to stick after a few hours operation for no observable reason. Shafer (55) has pointed out that there is some minimum rate, always above zero, where the electromagnetic and mechanical retarding forces cause the turbine rotor to cease rotating. The meter ceases to respond below such minimum rates and no indication of flow is generated. The minimum rate increases with the meter size, so the use of a smaller flowmeter was indicated to avoid the sticking difficulty at the relatively low natural circulation flow rates. The 3/4 in. Pottermeter used in the

previous study is rated for flows greater than 1.9 gpm; the 1/2 in. Pottermeter is rated for flows greater than 0.6 gpm and is linear for flow rates from 1.1 to 9.0 gpm.

A 1/2 in. Pottermeter was installed in the loop to help resolve the uncertainties concerning severe differential pressure oscillations measured across the venturi during the rapid oscillations. The time constant for this flowmeter was estimated to be on the order of one millisecond from theoretical considerations (56). Experimentally determined time constants for this type of meter were in the range of 2 to 4 milliseconds (55). Therefore, the meter should have been able to respond accurately to variations in flow rate of at least 100 cps which was adequate for the values of interest. The meter performed satisfactorily in its rated range, except that occasionally a sudden abrupt shift in its calibration factor occurred. This shift may have been caused by a slight temporary sticking of the turbine bearings, but is believed to have been caused by the erratic behavior of the electronic frequency converter which generated an electrical signal proportional to the turbine speed. This difficulty did not invalidate the results, but necessitated a frequent calibration check. The turbine flowmeter was calibrated in place daily, using the venturi as a standard.

Pressure Measurements. The pressure taps shown in Fig. 5 were connected by 1/4 in. stainless steel tubing, through a manifold arrangement, to a bourdon tube pressure gauge. The pressure gauge was located at a level parallel to the midpoint of the heated section, and was calibrated with a dead weight pressure tester. The static pressure

was also measured with high response pressure transducers, which were initially connected into the manifold arrangement. Subsequently the transducers were installed close to selected pressure taps by five inch lengths of tubing, in order to improve their response. The effect of such lines is discussed in the experimental results section. The calibrated pressure gauge was used as a reference to calibrate the pressure transducers.

Bulk Temperature Measurements. All bulk temperatures were measured with bare 30 gauge chromel-alumel thermocouple probes immersed in the fluid stream. The probes were positioned with their tips at the tube centerline, and were held in place by tubing connectors welded to the pipe walls.

All Freon 114 bulk thermocouples were preceded by a straight section to minimize asymmetrical effects. The inlet thermocouples for the heated section and cooler were located just upstream of these components. The outlet thermocouples were placed far enough downstream for turbulent mixing to result in a fairly constant radial temperature profile across the tube. Thermocouples were also welded to the pipe wall at the bulk thermocouple locations and connected to potentiometric type indicating instruments for control purposes. Their output was compared with those of the bulk thermocouples to verify that representative bulk temperatures were obtained. No significant difference was detected.

The bulk thermocouples were calibrated in a hypsometer over a temperature range from 200° to 500°F. No significant deviation of the thermocouples output from tabulated values was noted; hence the

tabulated values of emf versus temperature were used.

The time constant for such bare thermocouples was estimated to be on the order of 10 milliseconds (57). This should have been adequate to detect temperature variations at the frequencies encountered that were of sufficient amplitude to be discernible from the electrical noise. Unfortunately, this electrical noise level was fairly high and tended to mask any rapid ( $\sim 10$  cps) temperature fluctuations that may have occurred but which were less than about  $2^\circ\text{F}$  in amplitude.

Wall Temperature Measurements. Initially, the test section wall temperature was measured with 30 gauge chromel-alumel thermocouples, welded to the outside of the tube with a condenser discharge welder. The thermocouples were then wound around the tube for two turns to minimize thermal conduction errors, and taped in place with glass tape. It was found that this arrangement resulted in excess noise from electrical pickup. It was impossible to filter the signal sufficiently so that it could be recorded satisfactorily with the high response instrumentation, although potentiometric type instruments were sufficiently damped to do so.

Using potentiometric type indicating instruments, it was soon noted that large changes in wall temperature were occurring with the pressure and flow transients. Therefore, a record of the transient wall temperature behavior was required. Although it would have been possible to have employed a potentiometric type recording instrument to obtain such a record, the large amount of damping may have masked many features of interest.

Electrically insulated wall thermocouples were installed in order to reduce the IR electrical pickup. A 0.0007 in. sheet of mica was placed on the outside wall. A 30 gauge chromel-alumel thermocouple, with a small honed bead, was laid over the mica parallel to the tube axis. The thermocouple, including the bead, was securely taped in place with glass tape. The thermocouple was then bent out at a 90° angle so that it could be led away in a plane perpendicular to the tube axis. This arrangement was successful in reducing the electrical noise to a level comparable to that observed by the bulk thermocouples. One of the major sources of remaining noise originated in the DC amplifiers, which were part of the electronic recording circuit.

The time constant for the insulated thermocouple was estimated as follows. Using the electrical thermal analogy, the sheet of mica separating the wall and thermocouple is considered as an equivalent resistor and capacitor in series. The time constant for this circuit may be shown to equal the product of the equivalent resistance and capacitance. Using tabulated values (58) of mica properties, the time constant is calculated to be

$$RC = \frac{L^2 \rho c}{k} = 109 \text{ milliseconds} \quad . \quad (3.1)$$

This value appears reasonable upon comparison with experimentally determined values for insulated thermocouple probes (57). The actual value is probably somewhat higher due to neglecting contact resistance in the analysis. The electrical noise level was of sufficient amplitude such that it was impossible to detect any rapid ( $\sim 10$  cps) wall

temperature fluctuation of less than about 5°F amplitude. However, slower temperature fluctuations of this magnitude would have been detected.

The location of the wall thermocouples is shown in Table III, which lists their distance from the inlet of the heated section.

TABLE III

WALL THERMOCOUPLE LOCATION  
Distance from Heater Inlet

Thermocouple	Distance (inches)
TW 1	6
TW 2	12
TW 3	18
TW 4	24
TW 5	30
TW 6	33 1/4

Another thermocouple was welded diametrically opposite from thermocouple TW 5 and connected to a potentiometric type indicating instrument for control purposes.

The difference between the inside and outside wall temperature was estimated by using the constant property part of Clark's (59) solution, which was derived for an electrically heated tube. The part of his solution which accounts for the variable metal properties was found to be negligible. The temperature drop across the heater walls was estimated to be 5°F at 8 kw power input and was proportional to the electrical power input.

Recording Instrumentation. An essential feature of an instability study is that a suitable record of the time-dependent behavior of the pertinent variables must be obtained. Such a record was obtained,

in the present case, by recording the outputs of the thermocouples, absolute and differential pressure transducers, and turbine flowmeter with a recording oscillograph.

Briefly, the recorder consisted of banks of galvanometers, each of which deflected a small mirror proportional to the electrical signal. The mirrors reflected a light beam proportional to the deflection onto moving photosensitive paper whose linear speed was closely controlled at selected values. The galvanometers were the heart of the instrument and were selected so that their frequency response and sensitivity met the test requirements. All of the galvanometers used were rated to follow the signal to within  $\pm 5$  percent at frequencies less than 24 cps. Some of the fluid damped galvanometers which were used were similarly rated for frequencies up to 1000 cps. However, the sensitivity of the fluid damped galvanometers was so low that an amplifier was also required, which introduced additional electrical noise. Hence, the choice of a proper galvanometer required a compromise depending upon the test requirement.

One wire of all thermocouples was connected in series with an ice junction and a precisely calibrated bucking voltage of 0 to 10/20 mv range. The bucking voltages were required to limit the amplifier outputs to a desired range, so as not to overload the galvanometers. They also provided a convenient means of adjusting a signal's position on a record chart. The bucking voltages consisted of a potential dividing circuit connected to a 1.35 v mercury cell. The potential dividing circuit was sized so that the effect of loading would not cause the bucking voltage to vary by more than 1/2 percent.

Following the bucking voltage, the thermocouple leads were connected to a DC amplifier.

An amplifier was required in the thermocouple circuit, otherwise the galvanometer current would have caused a substantial IR voltage drop along the thermocouple leads. A high input impedance DC amplifier draws a negligible input current and its inclusion in the thermocouple circuit prevented this effect. The power to deflect the oscillograph galvanometer was then furnished by the amplifier power supply, rather than by the thermocouple. The high quality amplifiers, which were used, had 100 megohm input impedance and a gain of 1 to 1000 which could be varied continuously.

In order to reduce the electrical noise in the thermocouple circuits to a tolerable level, it was necessary to connect a 100  $\mu\text{f}$  capacitor across the thermocouple leads at the amplifier input. This method was successful in reducing the electrical noise, but the noise may have masked temperature variations less than the order of  $2^{\circ}\text{F}$  for bulk temperatures and  $5^{\circ}\text{F}$  for wall temperature at the higher test frequencies.

All of the pressure transducers produced a signal which did not require further amplification. The transducers required a constant voltage input, which was furnished by power supply units, rated to vary less than 0.002 v for a line voltage variation of 15 v. The noise level of the power supplies was rated at less than 100  $\mu\text{v}$  rms. The transducer output signals were fed directly to the recording oscillograph.

The turbine flowmeter signal consisted of a periodic voltage



whose frequency was proportional to the turbine speed and fluid volumetric flow rate. This signal was converted by a commercially available electronic frequency converter to a DC voltage proportional to the flow rate. The noise level of the frequency converter output required a filter to suppress the high frequency noise. The filtered signal from the frequency converter was recorded by the oscillograph.

Safety Features. The heated section was surrounded with a 1/4 in. aluminum plate shield, designed to protect personnel from a test section failure. A 1000 psi rupture disc located at the accumulator connection protected the loop from being accidentally overpressured. The laboratory water piping system was isolated from a pressure surge in the event of a cooler failure by a 600 psi check valve installed upstream of the coolers. In addition, a safety interlock shut off the electrical heating power if: the pressure exceeded a set value, which could be varied at a pressure limit switch; the temperature near the heater exit exceeded a preset value; or the flow rate fell below a selected value.

Thermal Insulation. After the loop and instrumentation assembly was complete, the entire loop was thermally insulated. The loop had been insulated during assembly at all points of contact with the supporting framework with several layers of 85 percent magnesia insulation before being loosely clamped in place. This type of assembly was chosen to allow the loop to "grow" during thermal expansion. The test section was covered with a 2 in. layer of molded 85 percent magnesia insulation. The balance of the loop was covered with two layers of 1-1/2 in. thick spun fiberglass bats, with aluminum foil

on the outside. Temperature drops of only 1 to 2°F were measured between the heater and vertical cooler, during operation, attesting to the efficiency of the insulation.

## CHAPTER IV

### EXPERIMENTAL PROCEDURE

The loop was hydrostatically tested with nitrogen gas at 800 psi after the loop was assembled. A large amount of effort was required to seal all the leaks at the tubing connectors which tended to buckle the thin tubing. In all subsequent modifications, heliarc welding was employed as much as possible to avoid this trouble. When the leaks were stopped so that the hydrostatic pressure could be held overnight a similar check was made with a vacuum pump which evacuated the loop to an absolute pressure of 50 microns Hg.

When the system was satisfactorily sealed, the evacuated loop was filled with fluid by heating the Refrigerant 114 supply cylinder, which was connected to the P5 pressure tap, with heating tapes so that the saturation pressure in the supply tank was about 20 psi greater than the saturation pressure corresponding to the temperature in the loop. The temperature in the loop was lowered by circulating tap water through the bottom horizontal cooler so that a pressure of 40 psig in the supply tank was sufficient for the filling operation. When the loop was full of liquid R-114, the pressure in the loop rose to the pressure level in the supply cylinder. The accumulator valve was then opened and a small additional amount of R-114 was added to ensure that there was sufficient fluid in the system to permit

pressurization with the accumulator. All manometer and pressure lines were then bled to remove any air which may have remained in the system.

At the start of an experimental run, the system was pressurized to a supercritical pressure by regulating the nitrogen pressure on the gas side of the accumulator. This supercritical pressure was maintained throughout the experiment, ensuring that subcritical boiling would not be encountered.

During the initial pressurization the calibration of the absolute pressure transducers and their electronic circuits was checked by comparing their output at the oscillograph with the bourdon tube pressure gauge. When the system was pressurized, the turbine flowmeter was checked by starting the pump and comparing the flowmeter output at the oscillograph with the venturi pressure drop at the manometer. To check the thermocouple circuit, a calibrated signal was fed to each amplifier in turn and its gain was adjusted so that the proper oscillograph response was obtained. The calibration could also be checked during a test by comparing the recorded values with values read from a potentiometer connected to the thermocouples through a selector switch.

As soon as the daily check of the instrumentation was complete, the cooling water was turned on to maximum capacity, the pump was started and the flow rate was set if a forced circulation run was planned, and then the electrical heating power was slowly increased to a selected value where it was maintained. After the system reached thermal equilibrium the cooling water was slowly decreased, causing

the bulk temperature to increase. In this manner the bulk temperature was varied slowly from ambient temperatures to temperatures exceeding the pseudocritical. Several runs were made to ensure that the behavior of the system was similar when the system was slowly cooled over the same range. During the run, a complete record of the transient behavior was obtained by recording the outputs of selected wall and bulk thermocouples, pressure transducers, and flowmeter with the recording oscillograph. A close visual check of these quantities was maintained as they were recorded by the oscillograph and with the indicating instrumentation.

As the system was heated, the thermal expansion of the fluid would tend to increase the pressure of the system. The pressure was kept at a constant level by regulating the nitrogen pressure on the gas side of the accumulator, allowing the fluid to expand into the accumulator. The accumulator also tended to absorb any pressure surges which were encountered during the oscillations.

It was found that the accumulator did not affect the rapid type of oscillations to an appreciable extent. This was determined by closing the accumulator valve while the rapid oscillations were occurring, or were about to occur. This closing had no appreciable effect on the inception or maintenance of the rapid oscillations.

Closing of the accumulator valve had much more effect on the slower type of oscillations which were encountered with bulk temperatures slightly below the pseudocritical. These slow oscillations were accompanied by a sudden improvement of the heat transfer coefficient during each cycle, as will be explained in the next chapter,

which resulted in an accompanying increased heat transfer rate to the fluid. This resulted in an abrupt expansion of the fluid in the heated section. With the accumulator valve open, the resultant pressure surge was greatly absorbed, but a comparatively large mass interchange occurred between the loop and the accumulator during each pressure cycle which caused the heater inlet temperatures to vary substantially. This inlet temperature variation was a confusion factor in the interpretation of the results. With the accumulator valve closed, a large variation of pressure occurred which could not be tolerated. A compromise between these extremes was reached by operating with the accumulator valve barely cracked open. The pressure surge was absorbed to a great extent, and the inlet temperature still did not vary substantially.

In order to obtain consistent results, the wall temperatures could not be allowed to exceed 600 to 700°F. If this temperature limit was exceeded a chemical reaction apparently was started or accelerated on the wall. Eventually a deposit would build up so that the outside wall temperatures were up to 200°F higher than their former values. The deposit would cause the inception point of the oscillations to vary but otherwise did not affect the qualitative behavior of the loop, i.e., the same types of oscillations were observed with and without the deposit. The deposit tended to make the rapid oscillations occur at lower bulk temperatures, probably due to the higher wall temperatures. They also tended to make the transition to the "boiling-like" behavior, which triggered the slow oscillations, less abrupt, so that this type of oscillation was less severe after

the deposit had formed. When the test section was thoroughly cleaned with a wire brush and alcohol, the loop reverted to its original behavior. The reaction limited the electrical power to 9 kw.

The inclusion of the 1/2 in. turbine flowmeter in the loop caused a substantial damping of the rapid type of oscillations. Rapid pressure oscillations of up to 120 psi amplitude were observed before the flowmeter was installed. The amplitude did not exceed 30 psi for the same type of oscillation after the flowmeter was installed, and did not occur at all during subsequent forced convection runs, unless the pump bypass valve was partially open.

It was also found that certain sizes of pressure transducer lines caused spurious pressure oscillations. These oscillations were characterized by the fact that the frequency varied at various transducers, and with the length of line between the pressure tap and the transducer. In general they could be avoided by either increasing or decreasing the length of the line, to avoid a resonant condition.

## CHAPTER V

### EXPERIMENTAL RESULTS

Instabilities, which result in a periodic variation of flow and pressure during heat transfer to a fluid at a supercritical pressure, were studied in a heat transfer loop designed to operate by either natural or forced convection. The instabilities were strongly damped during forced convection operation at flow rates greater than would be attained by natural convection, so attention was concentrated on the instabilities observed during natural convection operation.

Two different types of oscillatory behavior were observed during the tests. The first was of an acoustic nature, exhibiting harmonic pressure and flow oscillations in the frequency range of 5 to 30 cps. The acoustic oscillations occurred over a range of bulk temperatures below the pseudocritical temperature. The second type of instability was characterized by a frequency which was two orders of magnitude less than for the sonic type. This type of oscillation occurred as the heater outlet bulk temperature approached the pseudocritical temperature, and is best described by considering the entire fluid mass as a rigid body vibrating about its equilibrium condition.

#### Acoustic Oscillations

As the system was heated, sinusoidal fluctuations in flow and pressure were encountered. See Fig. 8. The frequency of these



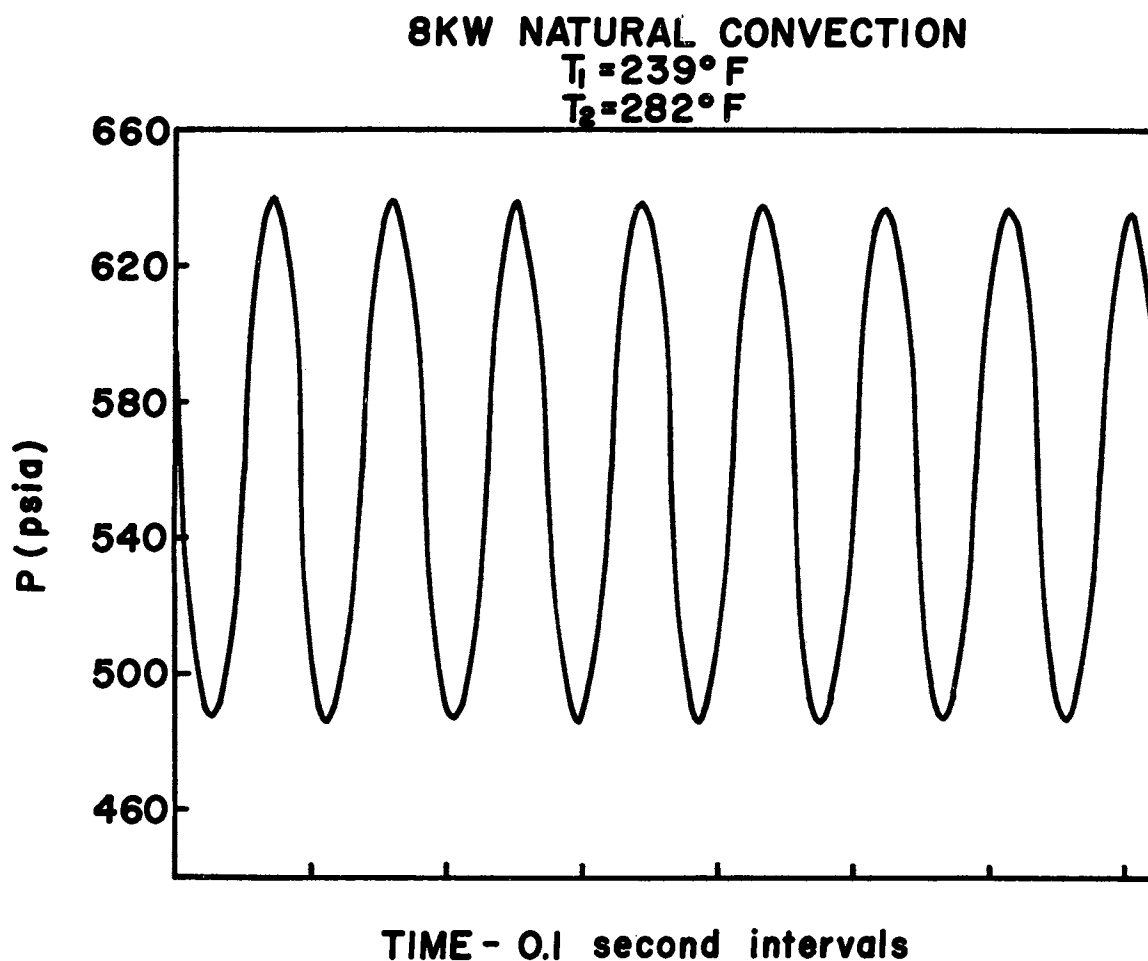


Fig. 8. Sinusoidal Pressure Variation During Acoustic Oscillations

oscillations varied from 5 to 30 cps, decreasing as the average temperature in the loop was raised up to the pseudocritical temperature. These oscillations occurred intermittently as the loop was slowly heated at constant electrical power from the ambient temperature to the pseudocritical temperature. The amplitude of the pressure oscillations varied intermittently as the test progressed, generally falling in the range of 0 to 40 psi, with a maximum recorded amplitude of 120 psi. The frequency did not depend upon, and the amplitude increased only slightly with, the heating rate.

The bulk temperature at which the oscillations first occurred decreased with the heating power. Representative conditions at which the oscillations first occurred are shown in Table IV.

TABLE IV

## LOWER LIMIT OF ACOUSTIC OSCILLATION RANGE

Power (kw)	Inlet Bulk Temperature °F	Outlet Bulk Temperature °F
2	205	246
4	140	195
6	130	211
8	120	203

The acoustic oscillations were observed over the temperature range from the lower limit shown in Table IV up to outlet bulk temperatures near the pseudocritical temperature.

In this range the oscillations occurred spontaneously as the loop was slowly heated or cooled. In some cases the oscillations were sustained for over thirty minutes. Varying the inlet temperature, pressure, power, or flow rate could also cause the oscillations to commence or subside. The frequency of the oscillations did not depend upon their amplitude or how they were initiated. Occasionally the oscillations would start, although generally at small amplitude, without any discernible change in any of the observed parameters.

Generally when large amplitude fluctuations commenced, the wall temperature dropped in part or all of the test section indicating an improvement of the heat transfer coefficient. A typical record of this occurrence is shown in Fig. 9, which illustrates the wall temperature drop as the large amplitude pressure oscillations commenced and

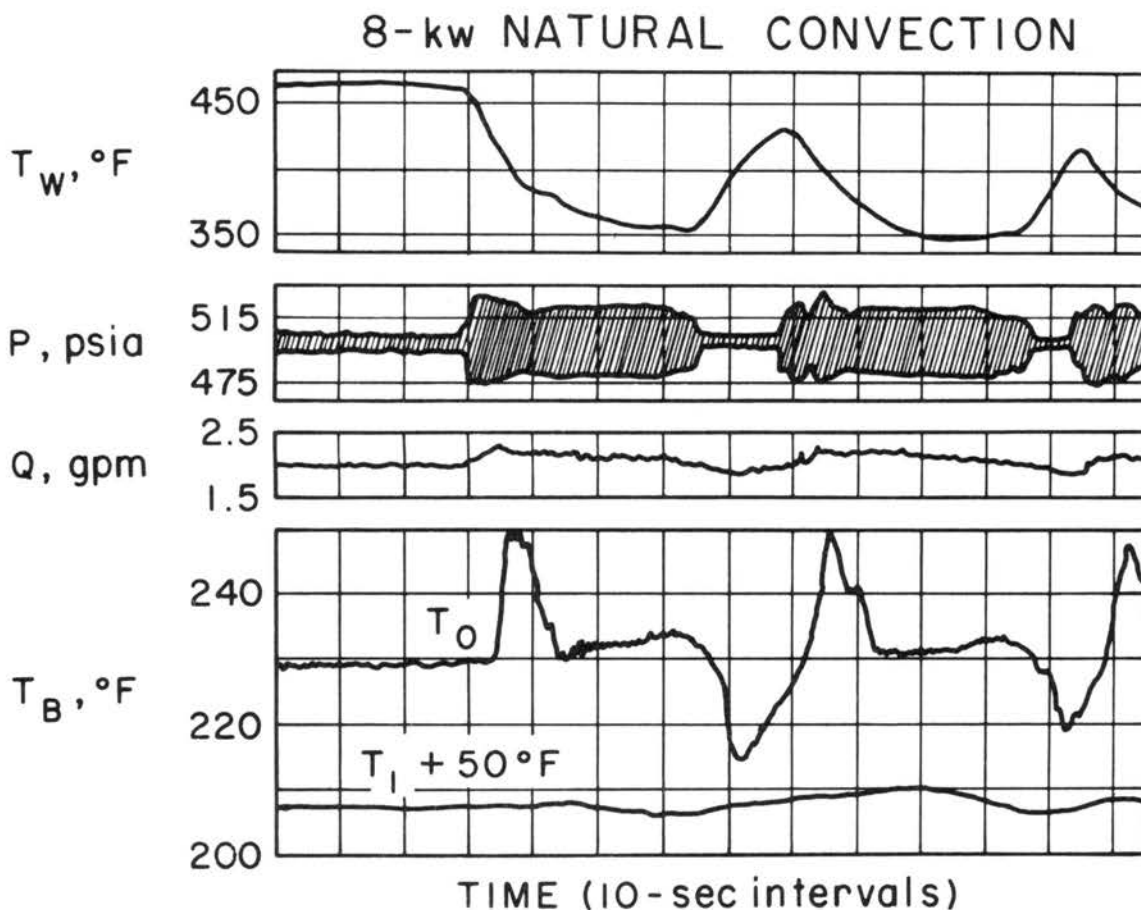


Fig. 9. Experimental Record of Acoustic Oscillations

the subsequent wall temperature increase as the large amplitude oscillations subsided. The pressure oscillations continued, but at a decreased amplitude, between these events. Only relatively minor flow oscillations were detected at these conditions but the high frequency flow oscillations became more pronounced at higher temperatures.

Figure 9 also illustrates the abrupt increase of the outlet bulk temperature as the heater wall was cooled. The abrupt change in  $T_o$  reflected the increased heat transfer rate to the fluid as the heater wall was cooled and the subsequent decreased heat transfer rate when part of the electrical energy was used for heating the heater wall. The outlet bulk temperature lagged behind the wall temperature because

of the downstream location of the outlet bulk thermocouple. Despite the relatively large bulk temperature change at these low temperatures, the flow rate and pressure were not greatly affected.

Frequently the rapid type of oscillations were sustained for much longer periods than shown in Fig. 9. At certain conditions the oscillations seemed to be capable of maintaining themselves indefinitely provided that the system parameters could be held constant. On several occasions, the oscillations were maintained for over thirty minutes before the inlet temperature or power was intentionally changed, causing the oscillations to subside. The envelope of the pressure oscillations in Fig. 9 is an example of the intermittent nature of the pressure amplitude.

A more regular variation of the pressure amplitude is illustrated in Fig. 10, which illustrates a type of "beating" phenomenon which was observed on several occasions. The beats are believed to have occurred due to the superposition of two different, but almost equal, frequencies. In such a case, a periodic rise and fall of intensity occurs at a frequency equal to the difference between the two component frequencies. For example, the pressure beats shown in Fig. 10 could have occurred due to the superposition of 13 cps and  $13 \pm 1$  cps pressure oscillations.

The experimental results suggested that the high frequency oscillations encountered at bulk temperatures substantially below the pseudocritical were an acoustical wave type of disturbance. In this region, a high response differential pressure transducer connected across the venturi indicated large oscillations in the venturi.

## 6KW NATURAL CONVECTION

$$T_1 = 230^\circ\text{F}$$

$$T_2 = 268^\circ\text{F}$$

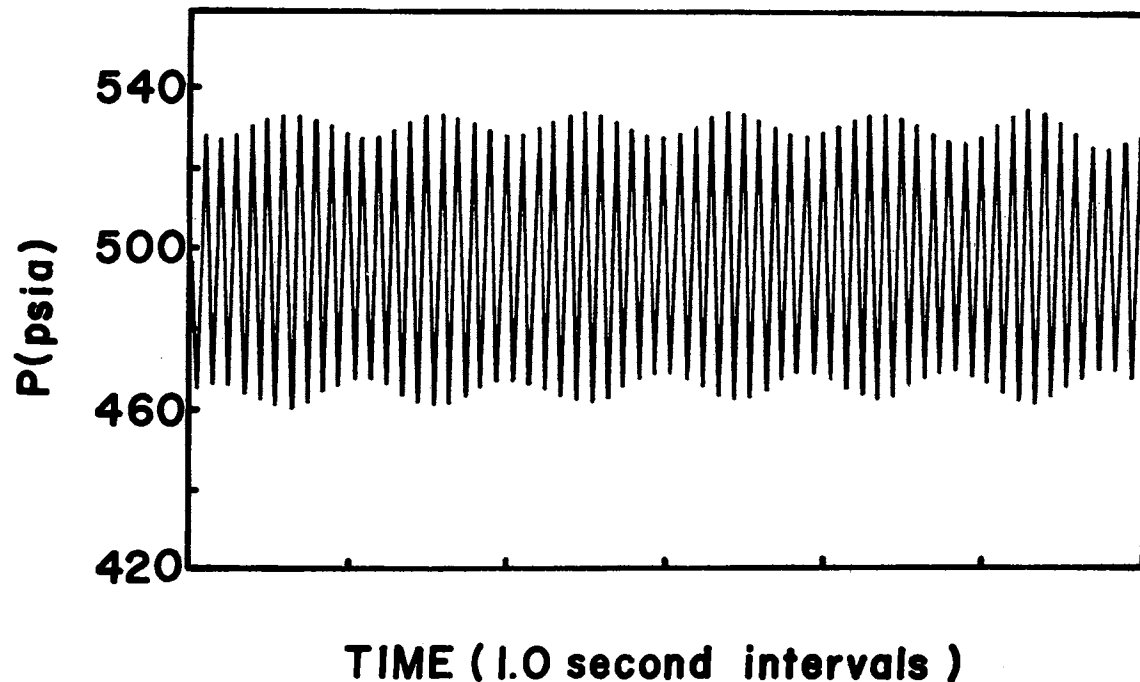


Fig. 10. Pressure "Beats" during Acoustic Oscillations

differential pressure drop. A high response turbine type flowmeter was installed in the loop to check if these oscillations were caused by variation in the flow. The turbine flowmeter did not indicate large fluctuations in flow that corresponded to the fluctuating pressure drop measured across the venturi. It was suspected that the large venturi pressure drop fluctuations were caused by acoustic type pressure waves crossing the venturi taps, with the pressure phase difference causing the large venturi pressure fluctuations. This theory could explain all of the excess venturi pressure drop which was observed if the acoustic wave length was sufficiently short. However, subsequent analysis (see Appendix A) revealed that the acoustic wave length was too long to

account for all of the excessive venturi pressure fluctuation. It is now believed that the large venturi pressure fluctuations were caused partly by a mechanical vibration of the loop and venturi pressure lines.

The sinusoidal behavior of the oscillations at such definite frequencies indicated that they were of an acoustic nature. If some element of the loop acted as an acoustic resonator, then the fundamental frequency of the oscillation would depend upon the sonic speed of the fluid in the resonating element and the characteristic wave length of the resonating element according to the equation,

$$f = c/\lambda \quad . \quad (5.1)$$

A plot of the experimentally determined frequencies versus average bulk temperature for the 49.1 ft loop used in the present tests is shown in Fig. 11. Also included are the results for two different lengths of loop from Reference 28. Two facts are evident. The frequency decreased with increasing temperature as would be surmised from Eq. (5.1) and the behavior of the sonic velocity which similarly decreases with temperature in the given region. The frequency was inversely proportional to the length of the loop for a given average temperature. Evidentially the rapid oscillations were acoustic in nature with a wave length proportional to the length of the loop. Calculation of the wave length from Eq. (5.1) and the property data of Van Wie and Ebel (2) showed that the wave length was equal to the length around the loop.

The sonic velocity was calculated from the experimentally determined frequencies using the above conclusions. The results are shown

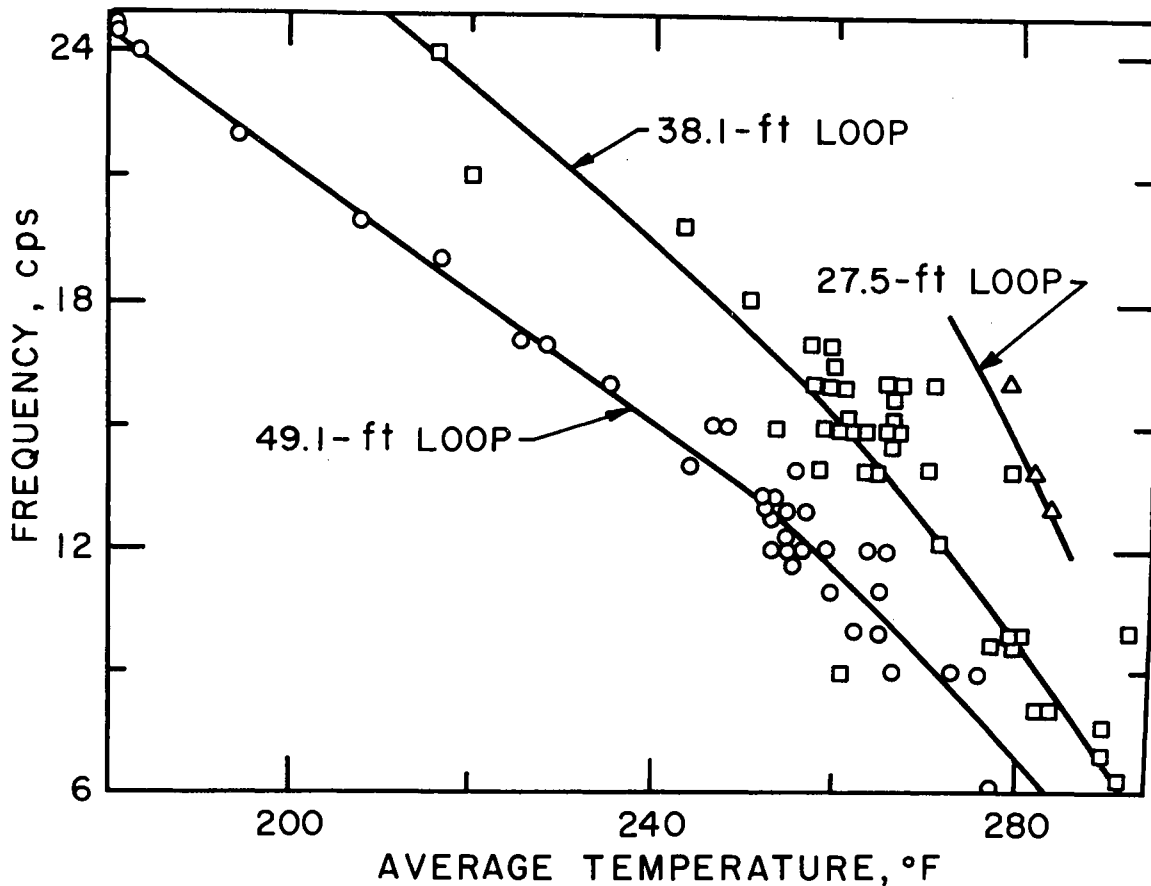


Fig. 11. Variation of Acoustic Frequency with Temperature for Various Loop Lengths

in Fig. 5. The calculated values agree reasonably well with the approximation that the sonic velocity varies with the cube of the density in the compressed liquid region, and with experimentally measured carbon dioxide sonic velocities (3).

In several isolated instances, when the power was suddenly increased, the frequency was twice as large as shown by the relationship in Fig. 11. Evidently, the loop was vibrating temporarily at the second harmonic frequency, with a wave length equal to half the loop length. These isolated instances resulted in more severe pressure oscillations across the venturi as would be expected.

These results offer convincing evidence that the rapid type of

pressure oscillation was an acoustic wave traveling around the loop with a wave length equal to the loop length. What remains to be explained is the mechanism which perpetuated the oscillation after it was initiated by some type of disturbance. In the absence of a periodic forcing function the oscillation would have quickly damped out due to the natural damping of the system. In order for the oscillation to have been maintained it is necessary that a mechanism existed such that the acoustic pressure wave was reinforced upon passing a given point in the system.

An analogous situation, in which a small gas flame introduced into a resonant chamber caused a musical note at the natural frequency of the resonator, was noticed as early as 1777. A detailed examination by Sondhauss (61) and Lord Rayleigh (62) proved that the vibration was caused by a varying supply of gas furnished to the flame. A resonant vibration was set up in the gas supply line, which resulted in a variable source of heat from the singing flame which could maintain the resonant oscillations if the supply line was the proper length. Frequently, some outside means were necessary to initiate the vibrations, but once started they could maintain themselves at the natural frequency of the resonator. The critical factor as to whether the vibrations were maintained or strongly damped was the length of the gas supply line. If conditions were such that the maximum heat transfer rate coincided with the instant of greatest condensation, i.e., the heat supply was in phase with the condensation, the vibrations were most strongly maintained. If the heat supply was in phase with the rarefactions the vibrations were strongly damped. It is



reasonable to conclude that this type of model could be used to explain the mechanism which causes acoustic oscillation to be maintained during heat transfer to a supercritical fluid.

Consider a heated surface in contact with a fluid, at a pressure exceeding the critical pressure of the fluid, and with a bulk temperature less than the pseudocritical temperature. Assume that the wall temperature exceeds the pseudocritical temperature. Then the bulk of the fluid is "liquid-like" but in the heated boundary layer the fluid properties tend to resemble those of a gas, i.e., the fluid in the boundary layer is highly compressible with a low density. The thermal conductivity of the boundary layer fluid increases with pressure. A pressure wave passing the heated surface tends to compress the fluid in the boundary layer, and improve the heat transfer rate to the fluid momentarily. As a rarefaction wave passes the surface, the boundary layer expands causing a decrease in the heat transfer rate. It is seen that conditions are ideal for maintaining the vibrations in a manner similar to that of the "singing flame."

Apparently it was necessary for the bulk of the fluid to be in a pseudoliquid state for the oscillations to occur, since the oscillations were not noted at bulk temperatures greater than the pseudocritical. The pressure increase may have compressed the gas-like boundary layer fluid so that it resembled a liquid in density, in which case the resulting "implosion" could have generated pressure waves which would have amplified the original pressure disturbance in addition to the heat transfer effect described in the preceding paragraph.

The wall temperature tended to decrease rapidly as the acoustic oscillations commenced. It was difficult to determine whether the wall temperature drop preceded the pressure oscillations, or vice-versa. Experimental evidence has shown that sound waves from an external source affect the boundary layers on heated surfaces, resulting in increased heat transfer coefficients (63). Consequently, one might suspect that the drop in wall temperature was caused by an improvement of the heat transfer coefficient due to the interaction of the acoustic field with the local flow field at the heated surface. This introduces the interesting possibility that an optimum frequency may exist for improving the heat transfer coefficient. The resonant frequency of the loop could be varied by changing the loop geometry so as to coincide with the optimum frequency, resulting in minimum wall temperatures. Possibly this acoustic effect can explain part of the increase in heat transfer coefficient which has been observed near the critical state and which has been attributed to "boiling-like" effects.

The experimental data indicate that the acoustic effect described above was not the only cause of the sudden drop in wall temperature. Installation of the turbine flowmeter in the loop introduced sufficient acoustic damping such that the acoustic oscillations never occurred thereafter in forced convection runs with the bypass valve closed, and the amplitude of the acoustic oscillations which occurred during subsequent natural convection operation was reduced by a factor of 2 to 4. The acoustic oscillations occurred at low forced convection flow rates in which the pump bypass valve was slightly opened; however,

this type of run was essentially a mixed convection type. At flow rates comparable to those observed during natural convection operation, the pump did not contribute materially to the process since the density head was sufficient to overcome the frictional head. Apparently the combination of the flowmeter and the pump in series was sufficient to prevent the acoustic wave from traversing the loop although neither would suffice by itself. Nevertheless, an improvement of heat transfer coefficient occurred as evidenced by rapidly decreasing wall temperatures and increasing bulk temperatures without any detectable acoustic oscillations. See Fig. 12. Evidently the

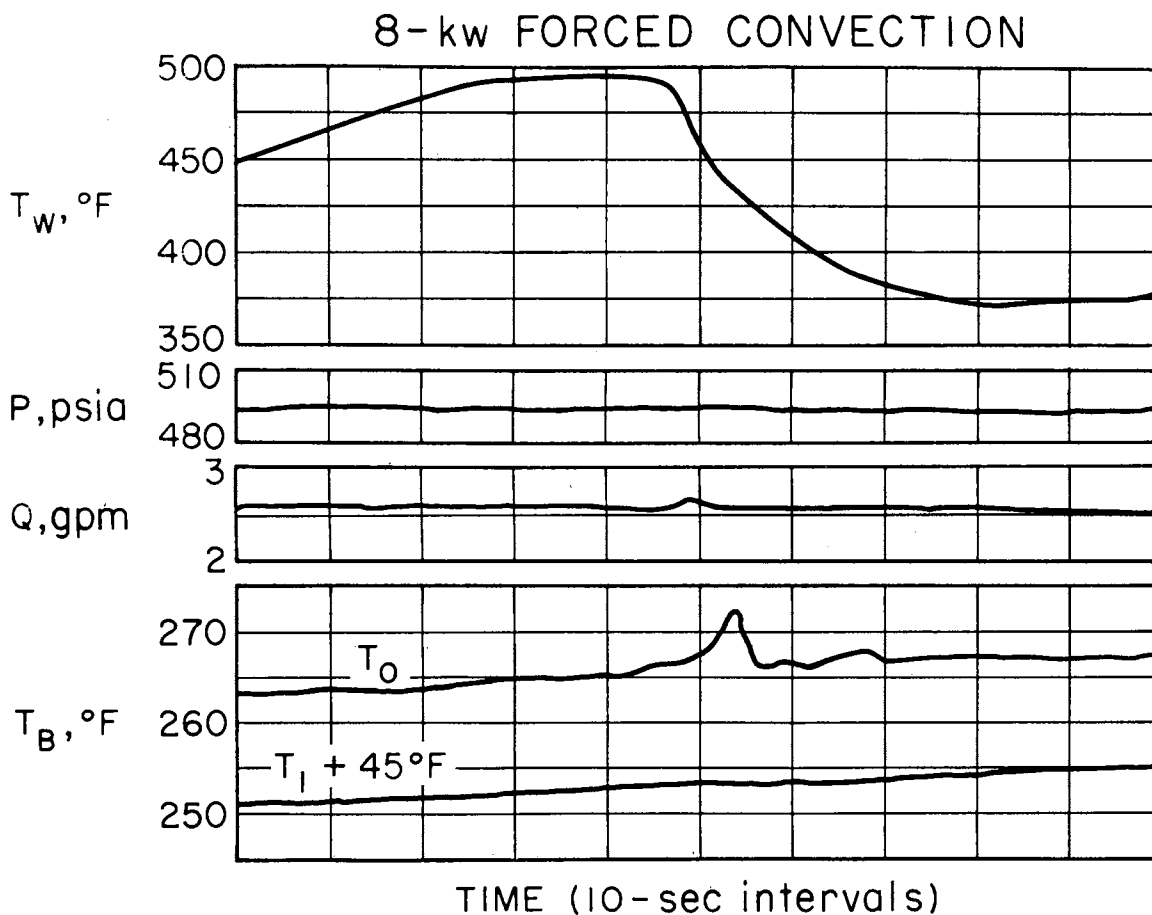


Fig. 12. Initiation of "Boiling-like Behavior" without Accompanying Acoustic Oscillations; Forced Convection Operation

"boiling-like" behavior occurred independently of the acoustic vibrations. This suddenly increased heat transfer coefficient will be referred to as "boiling-like" behavior in the balance of this thesis.

The abrupt transition to the "boiling-like" behavior momentarily more than doubled the heat transfer rate to the fluid as the heater wall was rapidly cooled. This caused the fluid to expand rapidly, sending out pressure waves at the speed of sound which triggered the oscillatory behavior only if conditions were such that the pressure wave was sufficiently undamped during its journey back to the heated surface. These results demonstrate that the acoustic oscillations can be avoided provided sufficient acoustic attenuation is incorporated into the heat transfer loop. This may explain the absence of this type of oscillation in the supercritical water tests reported by Dickinson and Welch (16). It seems that these results also offer further evidence of the supercritical "boiling-like" phenomenon which Goldmann (11) first postulated, and which has been used to explain high heat transfer coefficients measured near the pseudocritical temperature (16).

The initial pressure disturbance was propagated both upstream and downstream at the sonic speed superposed on the fluid velocity. Hence the pressure wave propagated downstream would arrive back at the point where the disturbance originated before the pressure wave propagated upstream. This difference should result in a "beating" phenomenon such as is shown in Fig. 10. At representative fluid velocities, the period of the beats would be at least ten times greater than shown in Fig. 10. The absence of beats with such periods

was interpreted to mean that only one of the propagated pressure waves was maintained. Comparison of the pressure phase difference at two adjacent pressure taps indicated that the pressure wave which was propagated downstream was maintained.

If the heated test section were a small diameter channel connected to the rest of the loop by large diameter mixing chambers or connections, the resonating element would not be the entire loop, but merely the small diameter channel. A pressure disturbance generated in the small diameter tubing would be reflected back at the connection and standing waves would develop, in contrast to the traveling waves generated in the constant diameter closed loop. Acoustic oscillations would occur in this type of system regardless of the damping (pump, orifice, etc.) which was included in the rest of the loop, and also whether the loop was a closed or open flow path. The small diameter section would behave as an open ended tube, with constant pressure at the ends and the maximum pressure variation at the midpoint of the resonator for the fundamental frequency. The fundamental wave length would be approximately twice the length of the small diameter section. When the heated section was not centered on the small diameter section, i.e., greater entrance length than exit length, it would be necessary for higher harmonic frequencies to develop if the maximum pressure variation were to occur at the heated section. A similar situation would exist if the heated section extended over most of the resonator. Systems of more complex geometry, multichannels, etc., could also act as acoustic resonators, but a more complex analysis would be required to determine the fundamental frequency.

Several examples of both types of resonating elements are available in the literature. The loops with small diameter heated sections have often exhibited high frequencies and audible screaming noises (1,12,19-21). The results of Reference 21 appear to be an excellent example of standing pressure waves in a short, small diameter tube with higher harmonics present. The loops consisting of essentially constant diameter tubing have exhibited a lower resonant frequency due to their longer fundamental wave length as characterized by the results of this study and those of References 7, 8, 28 and 64. Frequencies calculated using the acoustic resonator model agree quantitatively with the results which are available. This supports the conclusion that the high frequency oscillations are of a resonant acoustic nature. Attempts to duplicate this type of result with analytical models which neglect sonic effects have proved fruitless.

#### Slow Oscillations

A slower oscillation, distinctly different than the sonic type discussed previously, occurred as the outlet bulk temperature approached the pseudocritical temperature from the pseudoliquid state. The flow rate fluctuated at a much larger amplitude and at a frequency (0.05 to 0.1 cps) two orders of magnitude less than was observed during the sonic oscillations.

The slow oscillations which were encountered at less than 8 kw electrical power input were of a similar nature, but were less severe, spontaneous, or sustained, than at the higher power input. The slow oscillations encountered at 9 kw did not differ significantly from

those observed at 8 kw power. Operation at higher power inputs resulted in excessive heater wall temperatures as described at the end of this chapter.

Instead of acoustic pressure waves propagating around the loop, this type of oscillation is analogous to the fluid in the loop, considered as a solid body, performing a mechanical vibration about the equilibrium position. Such a vibration, similar to that performed by a U-tube manometer, would quickly damp out due to the natural damping forces if it were not periodically perturbed. The data indicate that the perturbing force, or forcing function occurred due to a sudden change in the heat transfer coefficient. The sudden improvement of the heat transfer coefficient is attributed to the occurrence of a "boiling-like" phenomenon in the supercritical fluid. The rapid change indicates that a nonequilibrium condition may be involved similar to the "superheat" required to initiate nucleate boiling.

A record of the experimentally observed behavior during the slow oscillations is shown in Fig. 13. When the heat transfer coefficient improvement or "boiling-like" phenomenon occurred the wall temperature dropped rapidly, as approximately indicated by the insulated thermocouple on the outside wall. Simultaneously the net heat transfer to the fluid increased rapidly due to the decreased energy stored in the heater walls even though the electrical power to the test section remained constant. Cooling the 0.035 in. thick heater wall 45°F in two seconds required a twofold increase in the heat transfer rate to the fluid at 8 kw electrical power input. The suddenly increased heat transfer rate caused a rapid expansion of the fluid in the test

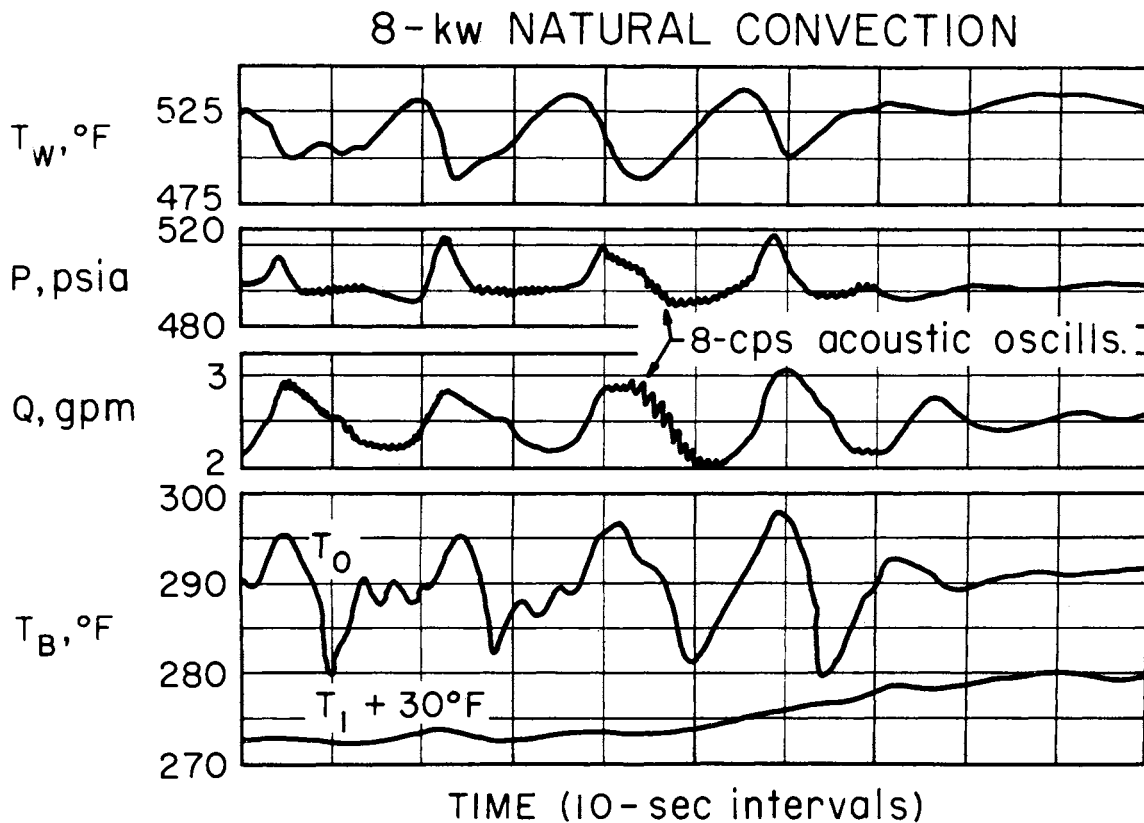


Fig. 13. Experimental Record of Slow Oscillations; Wall Temperature Drop in Phase with Flow Oscillations

section, resembling a mild flashing, and caused the pressure pulse that was observed. The expansion of the fluid in the heated section and riser, contributed to a greater density head, which is the driving force of free convection flow. This caused the flow rate to suddenly increase at a more rapid rate. The flow rate increased to a maximum and then decayed asymptotically. If the "boiling-like" phenomenon were not repeated, the oscillations would damp out after only a few cycles as is graphically illustrated at the end of the record.

The asymmetrical shape of the sustained flow oscillations is characteristic of the results of many other instability studies.



Such a shape indicates that a perturbing force was affecting the system, resulting in an increased time derivative of the flow rate while the perturbing force was effective.

Near the pseudocritical temperature, the enthalpy increase resulting from the increased heat transfer rate caused a relatively small bulk temperature increase and a large specific volume increase. The rapid expansion of the fluid, resembling a minor explosion, caused the pressure level of the loop to increase abruptly unless absorbed by the accumulator, while the resultant increased density head was sufficient to increase the natural circulation flow rate by nearly 20 percent. This increase may be compared to the smaller effect at lower temperatures which is shown in Fig. 9. The decreased effect at the lower temperature was due to the smaller rate of change of the density with enthalpy as the temperature decreased from the pseudocritical. However, the smaller specific heat at the lower temperatures, resulted in a more severe outlet bulk temperature variation.

The increased flow rate and rapidly changing conditions at the heated surface caused the "boiling-like" behavior to soon terminate as evidenced by the rising wall temperature. If conditions were such that the "boiling-like" behavior was repeated, a periodic transient developed. Figure 13 is an illustration of the heat transfer improvements occurring in phase with the flow oscillations, as frequently happened. When the conditions were held constant, this type of oscillations appeared capable of being maintained indefinitely.

Occasionally the heat transfer improvements occurred out of phase with the flow oscillations, and the resulting record provided

additional insight into the mechanism. When the time between improvements was longer than the flow period, the flow decayed asymptotically back to equilibrium following an impulse, as shown in Fig. 14. This record definitely shows that the improvements had to be repeated for the oscillations to be sustained and is a good illustration of the damped nature of the flow oscillations.

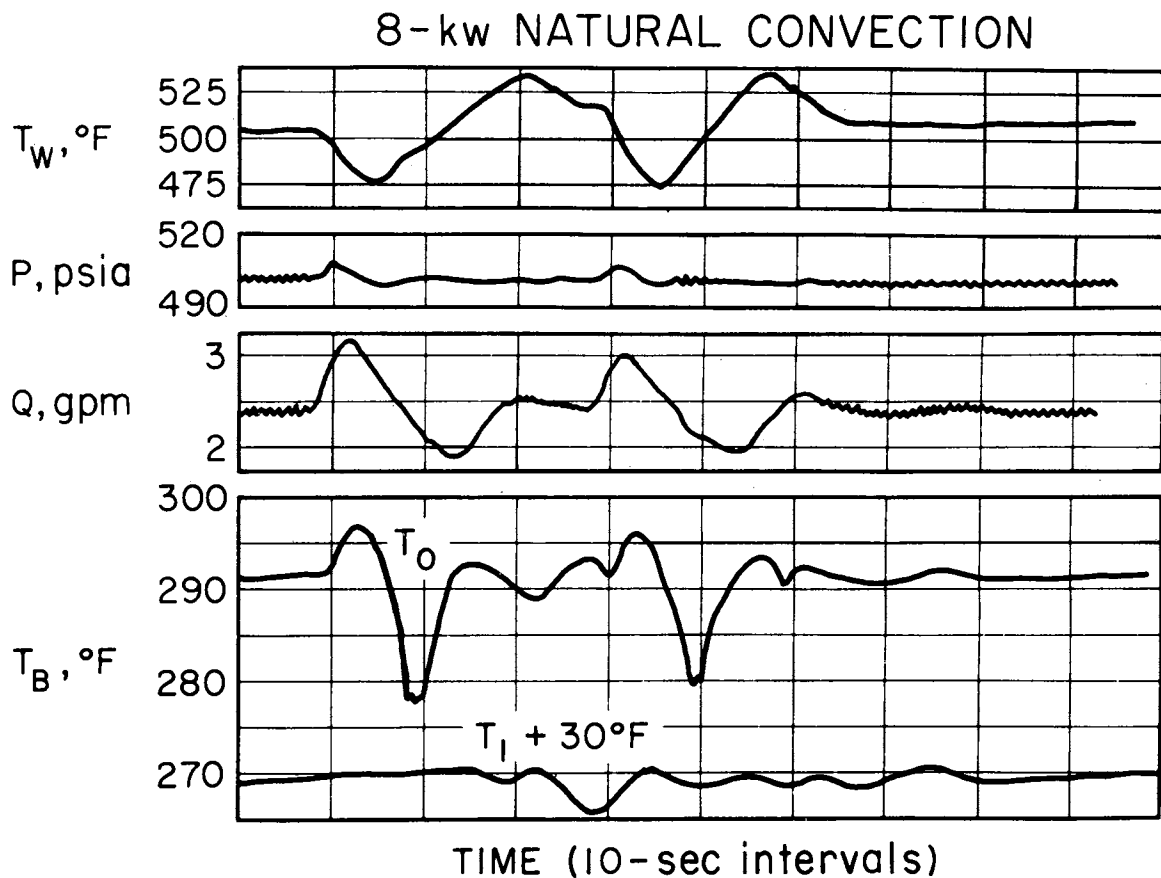


Fig. 14. Experimental Record of Slow Oscillations: Time Between Heat Transfer Improvements Longer than Flow Period

Figure 15 illustrates a shorter time between heat transfer improvements than the flow rate period. It is seen that the effect of a heat transfer improvement out of phase was to cause a pressure impulse, but to not greatly affect the flow rate. This behavior is

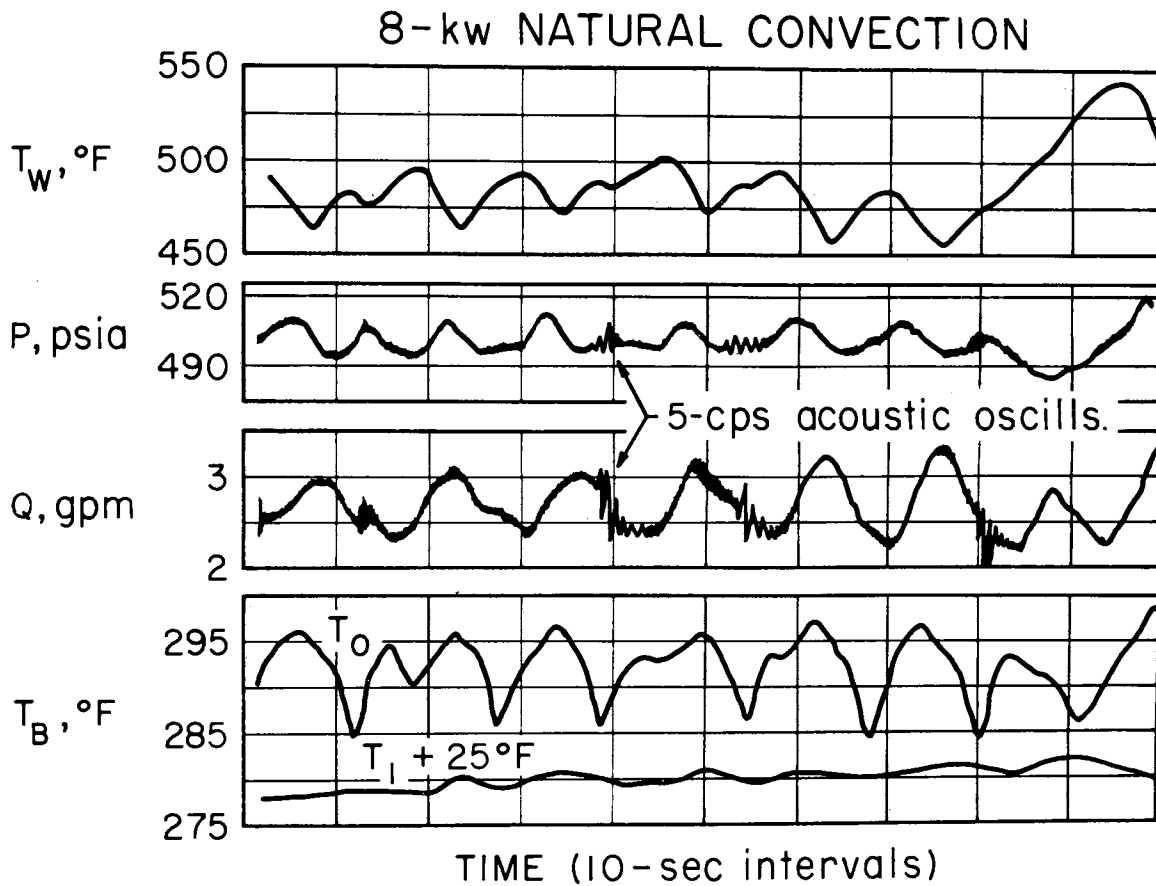


Fig. 15. Experimental Record of Slow Oscillations; Time Between Heat Transfer Improvements Shorter than Flow Period

similar to that observed when pushing a child in a swing. If the pushes coincide with the natural frequency of the swing, a large amplitude results with little effort. If the pushes are out of phase, the inertia of the child may be greater than the force applied and the swing's amplitude will be decreased but the swing will not be stopped. Similarly, the flow rate's amplitude was decreased, but the flow rate still tended to oscillate at its natural frequency.

Since forced convection heat transfer coefficients generally increase with the mass flow rate, it could be argued that the wall temperature drop was caused by the flow rate change, rather than vice

versa. However the results shown in Fig. 15 tend to refute this idea. Also it would seem that if an increased flow rate (which could be caused by a suddenly decreased frictional pressure drop) had initiated the transient, the pressure should have initially decreased, rather than increased as the data show.

The factors which caused the "boiling-like" behavior to be initiated must be better understood before an explanation of the non-periodic times between heat transfer improvements can be advanced. Nevertheless these results clearly illustrate the role of the heat transfer improvement in triggering and maintaining the slow oscillations. It is believed that a similar conclusion holds for subcritical boiling systems. The suddenly increased heat transfer coefficient as subcooled nucleate boiling is initiated may well be the primary forcing function which causes boiling instability to be initiated and sustained, rather than the hydrodynamic characteristics to which the boiling instability is often attributed.

The reason for the more severe pressure surges in Figs. 13 and 15 than in Fig. 14 is that the accumulator valve was barely cracked open in the two former runs. This also resulted in less variation of the inlet bulk temperature than is shown in Fig. 14, which was caused by the introduction of colder fluid from the accumulator. Completely closing the accumulator valve resulted in 60 psi pressure surges, but the oscillatory behavior was similar to that observed with the accumulator valve slightly open. Results of such tests indicated that the forcing mechanism did not depend primarily upon either the pressure surges or an inlet temperature feedback.

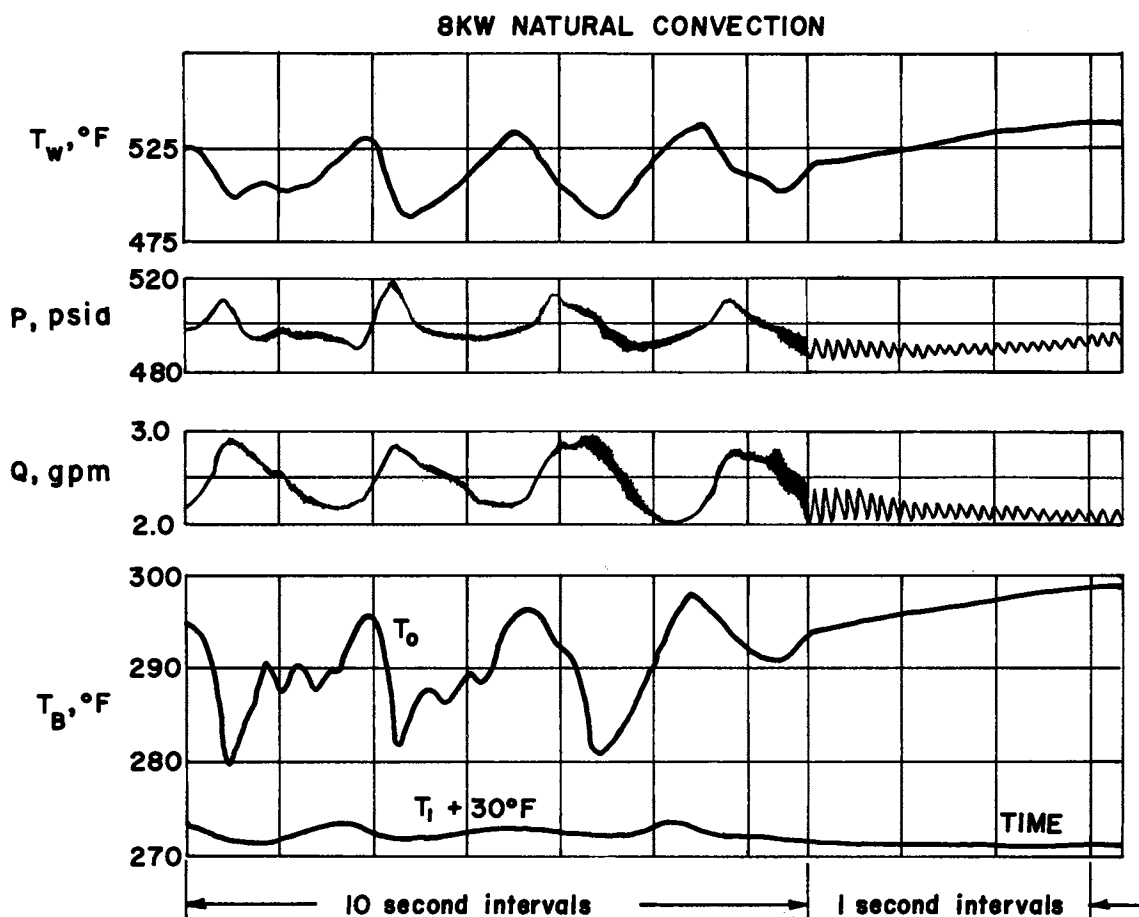


Fig. 16. Simultaneous Occurrence of Acoustic and Slow Oscillations

Frequently the acoustic type of oscillation occurred simultaneously with the slow oscillations, as is shown in Figs. 13 and 15 and on an expanded time scale in Fig. 16. These oscillations were the slowest acoustic oscillations measured during the test program due to the minimum sonic velocity at these conditions. It was noted that the flow rate amplitude increased for the slower sonic oscillations. The simultaneous occurrence of the two types of oscillations is further proof that they were of a distinct nature.

Another feature which distinguishes the two types of oscillations is that the frequency of the sonic oscillations decreased with temperature while the frequency of the slow oscillation increased with

temperature, as can be seen by comparing Figs. 13 and 14. The increase of the slow oscillations' frequency with temperature is predicted by the analytical model described in the next chapter.

The incorporation of the turbine flowmeter and venturi in the loop permitted flow measurement at two independent locations. Since the venturi was located between the accumulator and heater entrance and the turbine flowmeter was located between the heater exit and the accumulator, see Fig. 7, they could be used to compare the flow rate at the heater inlet and exit respectively. Such a comparison is shown in Fig. 17. It is seen that the heat transfer improvement

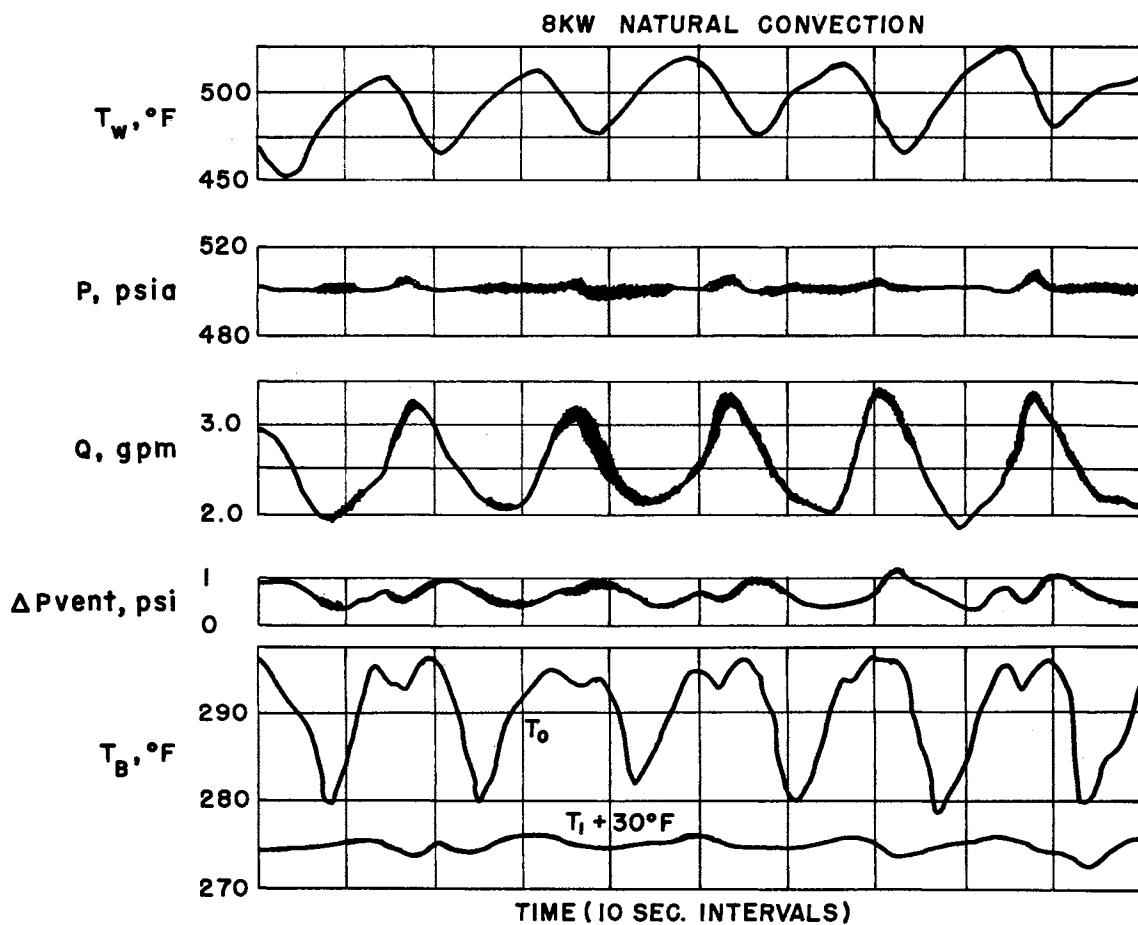


Fig. 17. Experimental Record of Slow Oscillations; Flow Rate at Flowmeter and Venturi Difference

caused the flow rate to increase from the heater exit, but to decrease at the heater inlet. This is the type of behavior which would be expected and has been described for a boiling system by Meyer (40). It is seen that, except for a short time after the impulse, the inlet velocity tended to follow the exit velocity. The analytical model presented in Chapter VI neglects this variation and should predict an average velocity between these two extremes.

The instabilities were strongly damped during forced convection operation at flow rates greater than the natural convection flow rate. This suggests that a means of avoiding the instabilities would be to operate by forced convection, although economic and practical considerations might make such a design undesirable. Figure 18 illustrates a type of instability which was observed during forced convection operation, with the bypass valve closed, at a flow rate

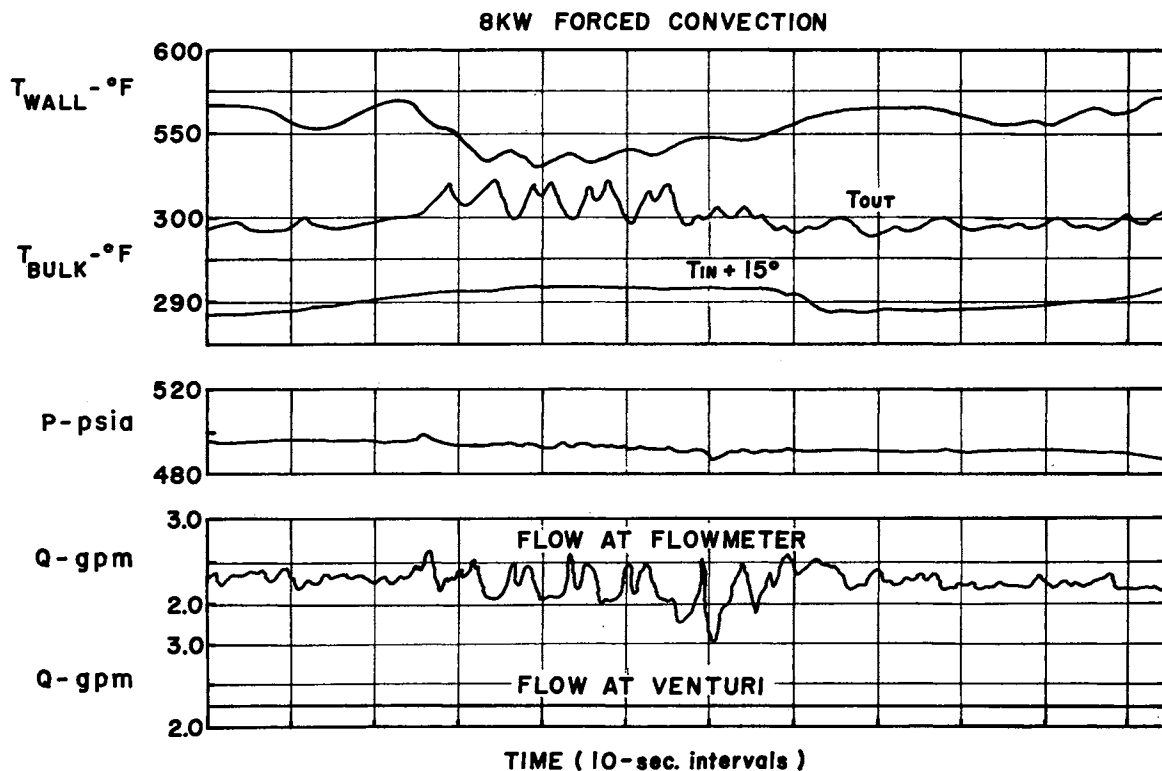


Fig. 18. Irregular Instability at Low Forced Convection Flow Rate

slightly lower than the natural convection flow rate. The wall temperature variation indicates a sporadic "boiling-like" occurrence caused the flow between the heater outlet and accumulator to vary in an irregular fashion as measured by the turbine flowmeter. The flow rate from the pump, as measured by the venturi, did not exhibit a similar variation. These results demonstrate that the sporadic nature of the supercritical "boiling-like" phenomenon does not depend entirely upon a large temperature or flow feedback. The more regular nature of the slow oscillations during natural convection operation was due to the freedom of the fluid to vibrate about the equilibrium conditions which the restraint imposed by the pump and throttling valve prevented.

All of the previous results were obtained when only the cooler on the vertical leg was employed. Operation with the upper horizontal cooler is illustrated in Fig. 19. It is seen that the greater height between the heater and cooler resulted in a larger flow rate as would be expected. The first part of the record shows the wall temperature varying out of phase with the flow oscillations. Although fairly high pressure surges resulted, the flow rate was not affected greatly. As the inlet temperature was raised, the heat transfer improvement began to vary at a frequency comparable to the natural flow frequency, which was larger than that observed at a similar temperature employing the vertical cooler. The flow amplitude increased, but not to the extent observed during operation with the vertical cooler. The pressure surges were more severe than during similar operation with the vertical cooler. The reasons for these differences are discussed in Chapter VI and Appendix B.



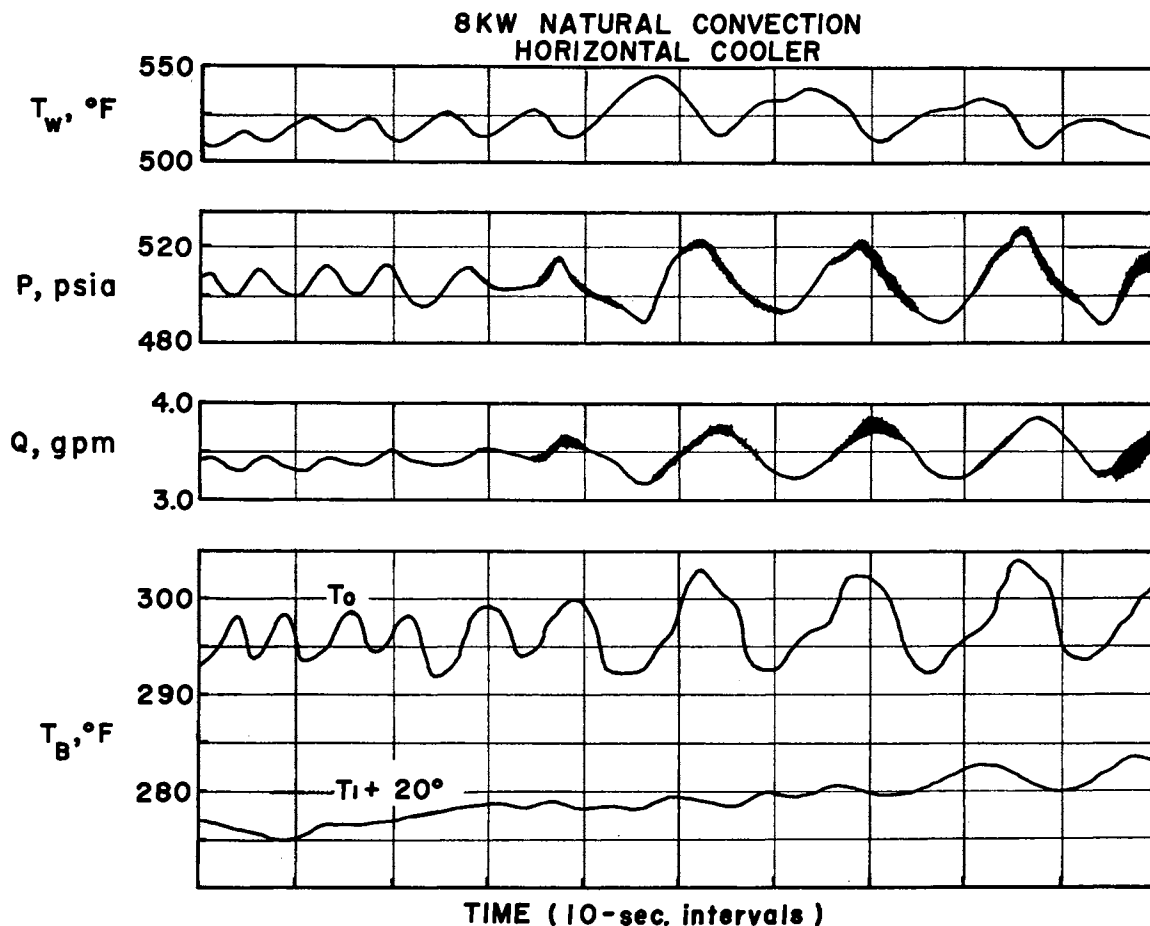


Fig. 19. Experimental Record of Slow Oscillations;  
Operation with Upper Horizontal Cooler

#### Anomalous Behavior

When transducers were connected to the loop at the  $P_0$  and  $P_1$  locations shown in Fig. 7 by three foot lengths of quarter inch tubing, it was found that extraneous  $\sim 100$  cps resonant oscillations were maintained in these connecting lines under certain conditions. These extraneous vibrations were characterized by the fact that the frequency was often different at the two transducers and tended to be superposed upon the other oscillations which have been reported in this chapter. Lengthening one of the lines to six feet cut the dominant

extraneous frequency of that transducer in half, which confirmed that the connecting tubing was responsible for the extraneous pressure oscillations. The length of connecting tubing was reduced to five inches, and all superfluous pressure lines were eliminated from the loop. This reduced the extraneous vibrations to a minimum.

When the wall temperature was allowed to exceed 600° to 700°F, a chemical reaction was started or accelerated at the wall. Eventually a deposit would build up on the heater wall so that the outside wall temperatures were up to 200°F higher than their former values. Another effect noted was that the "boiling-like" behavior was initiated more frequently and at correspondingly lower bulk temperatures, resulting in more acoustic oscillations, but less severe slow oscillations near the pseudocritical temperature. Otherwise, the deposit did not seem to affect the transient behavior of the loop. When the test section was thoroughly cleaned with a wire brush and alcohol, the loop reverted to its original behavior. The reaction limited the electrical power input to 9 kw.

An interesting result was obtained when this limit was exceeded briefly. A subsequent forced convection run at 8 kw power and 5 gpm flow rate was started. The higher flow rate should have resulted in a lower wall temperature than during a similar natural convection run. With bulk temperatures less than 200°F (94°F below the critical) and wall temperatures of about 400°F, a hot spot developed at the test section exit. The wall temperature increased to greater than 600°F at the top thermocouple. As the bulk temperature was raised slowly, the hot spot moved down the section, affecting one thermocouple at a

time. This particular experiment was repeated three times with similar results, although the wall temperature level gradually rose as the tests progressed, indicating that the deposit was building up in the test section. This indicated that a chemical reaction was responsible for the anomalous behavior. Similar results were observed for oxygen at supercritical pressures (23) where a wall temperature increase from 400°R to 2000°R occurred over a small axial distance in the heated section.

## CHAPTER VI

### ANALYSIS OF SLOW OSCILLATIONS

During certain transients, the fluid in a natural circulation loop can be considered analogous to a vibrating solid body such as the fluid in a U-tube manometer. The system possesses inertia, exchanges momentum with the confining walls which tends to damp any transient behavior which occurs, and has a density head which may be considered as the driving force of the natural convection flow. When disturbed from an equilibrium condition, the loop tends to return to equilibrium via a damped oscillation around the final equilibrium position. In the absence of a periodic forcing function the oscillation should decay rather quickly due to the natural damping forces. A sustained oscillation should develop only if an analogous forcing function exists which could result, for example, from a time varying energy input to the system or from a sporadic shift in either the frictional pressure drop or heat transfer coefficient correlation.

The experimental data indicated that a sudden and periodic improvement of the heat transfer coefficient, which was attributed to the initiation of a "boiling-like" behavior in the supercritical fluid acted as a forcing function and was responsible for the initiation and maintenance of the slower type of flow oscillations. The heat transfer coefficient improvement resulted in a sudden drop of the wall

temperature, less energy stored in the heater walls, and an increased heat transfer rate to the fluid from the walls, even though the electrical heating power remained constant. In order to demonstrate that this effect was of sufficient magnitude to account for the maintenance and magnitude of the flow oscillations observed experimentally, during natural circulation operation, the following analysis was made.

Basically, the solution consists of solving the energy, mass, and momentum conservation equations, subject to the boundary conditions imposed by the loop geometry. The equations are nonlinear partial differential equations and an analytical solution is impossible with available mathematical techniques. The solution of such space and time dependent equations by numerical techniques has received much attention in recent years, particularly for two-phase systems. Using suitable simplifying assumptions and empirical correlations, solutions to the equations may be obtained. The validity of the assumptions may be partially judged by comparing calculated and experimental results.

#### Conservation Equations

The derivation of the conservation equations has been covered in complete detail in thermal and fluid dynamics texts (65,66). In order to solve these equations for turbulent nonadiabatic flow in a constant area pipe the following assumptions are commonly made.

1. One dimensional geometry is assumed to adequately represent the system, i.e., radial variations of properties and velocity are neglected. Viscous stresses and heat transfer rates at the wall

are evaluated from empirical correlations rather than from calculated temperature and velocity gradients.

2. Heat conduction along the axial coordinate is neglected since it is much smaller than the convective energy transfer.

3. The velocity is assumed to equal zero at the wall but to assume a uniform value away from the wall, so there is no contribution to the energy equation from shear forces at the wall.

4. The kinetic and potential energy terms are assumed to contribute negligibly to convective energy transport in the energy equation.

5. The variation of pressure with time and distance is assumed to have a negligible effect on the energy balance.

6. All properties are considered to be evaluated at a mean pressure. With this assumption the properties may be evaluated as a function of the enthalpy in a single-phase system.

7. The effects of viscous dissipation are neglected in the energy equation.

With these assumptions the conservation equations for the fluid may be written as follows:

Conservation of Mass

$$\frac{\partial \rho}{\partial t} + \frac{\partial G}{\partial z} = 0 \quad , \quad (6.1)$$

Conservation of Momentum

$$\frac{1}{g_c} \frac{\partial G}{\partial t} + \frac{1}{g_c} \frac{\partial}{\partial z} \left( \frac{G^2}{\rho} \right) = - 144 \frac{\partial p}{\partial z} - \frac{\tau_w}{A} - \rho \frac{g}{g_c} \quad , \quad (6.2)$$

Conservation of Energy

$$\rho \frac{\partial h}{\partial t} + G \frac{\partial h}{\partial z} = q''' \quad , \quad (6.3)$$

where use has been made of the fact that for a constant pressure system

$$\frac{\partial(\rho u)}{\partial t} = \frac{\partial(\rho h)}{\partial t} \quad .$$

Neglecting the pressure effect (assumptions 5 and 6) eliminates sonic effects from the solution but considerably simplifies the calculations (40). Therefore, the solution of the above equations should not be expected to duplicate the experimentally observed acoustic type of oscillations.

For certain transients further simplification may be obtained when the amount of fluid does not change too rapidly in any increment of the loop. Therefore the time derivative of density in Eq. (6.1) may be neglected so that

$$\frac{\partial G}{\partial z} = 0 \quad , \quad (6.4)$$

or

$$G = G(t) \text{ only} \quad . \quad (6.5)$$

Equation (6.5) implies that since the mass flux is constant around the loop at a given time, any disturbance tends to accelerate the entire fluid system, i.e., local acceleration is neglected. This type of behavior is similar to that observed experimentally, except for a short time after the heat transfer improvement, so the simplified model should be expected to represent the average mass velocity reasonably well.

Using Eq. (6.5), Eq. (6.2) may be integrated around the loop to obtain:

$$\frac{L}{g_c} \frac{dG}{dt} = -\frac{1}{A} \int_0^L \tau_w dz - \frac{1}{g_c} \int_0^L \rho g dz \quad (6.6)$$

When multiplied on both sides by A, Eq. (6.6) is a form of Newton's second law of motion, equating the loop's inertia force to the algebraic sum of the friction and gravitation forces.

The first term on the right hand side of Eq. (6.6) is proportional to the total friction pressure drop around the loop. Daily and Deemer (60) found that steady-state friction factors were applicable to the transient flow of a fluid, i.e., the total pressure drop across a horizontal section equalled the algebraic sum of the acceleration head and the instantaneous frictional pressure drop except during periods of high initial impulse. Friction factors measured or extrapolated from steady-state experiments are now commonly used in transient analyses. The resistance term may be evaluated from a summation of calculated pressure drops across individual loop elements. If conventional friction factors (66) are used to calculate the friction pressure drop

$$\frac{1}{A} \int_0^L \tau_w dz = \sum \frac{2fLvG^2}{g_c D} \quad (6.7)$$

where L is the equivalent element length, accounting for bends, fittings, valves, etc. Using the Blasius formula (66) for f,  $f = 0.0791 (N_{RE})^{-0.25}$



$$\frac{1}{A} \int_0^L \tau_w dz = \sum \frac{0.158 L v \mu^{0.25} G^{1.75}}{g_c D^{1.25}} \quad (6.8)$$

$$\doteq 4.5 \frac{\bar{v}}{v} G^{1.75} \quad (6.9)$$

for the present tests.

The friction pressure drop may also be evaluated from steady-state experimental measurements by making use of Eq. (6.6), noting that the left hand side vanishes for steady-state conditions. For steady-state conditions only,

$$F \equiv \frac{1}{A} \int_0^L \tau_w dz = - \frac{1}{g_c} \int \rho g dz \quad (6.10)$$

Equation (6.9) suggests the form of the test data correlation which is shown in Fig. 20,

$$F \equiv \frac{1}{A} \int \tau_w dz = \frac{8.96 G^{1.59}}{\bar{\rho}} \quad (6.11)$$

and which is valid for temperatures up to the pseudocritical. This type of correlation eliminates uncertainties about the effects of variable properties, geometry, roughness, etc., and is particularly convenient for the numerical calculations. It agrees closely with the results of Alstad, et al., (68) for water in a natural circulation loop and with Eq. (6.9). The difference between the mass flow exponent in Eqs. (6.9) and (6.11) is partially due to the viscosity effect on the friction factor. However, experimental pressure drop correlations do not always agree exactly with the Blasius friction

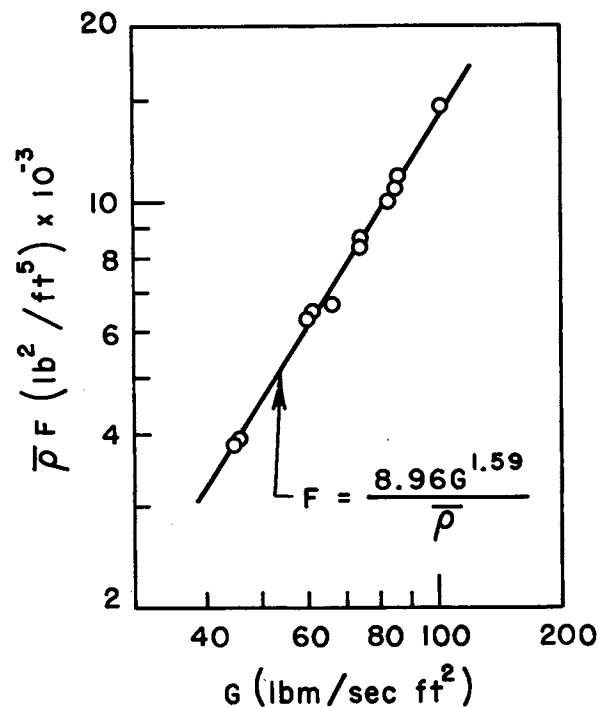


Fig. 20. Empirical Friction Pressure Drop Correlation

factor. The results of Reference 60 for R-11, trichloromonofluoromethane, indicate that the friction factor,  $f$ , varies inversely with the 0.32 power, rather than the 0.25 power, of the Reynolds number, which would account for nearly one-half of the variation in the mass flow exponent.

In order to account for the thermal response of the walls, an energy balance is made on an incremental element with the following simplifying assumptions:

1. At each axial position a single mean temperature is sufficient to represent the wall temperature.
2. Axial heat conduction is neglected.
3. The heat loss to the atmosphere through the insulation is considered negligible.

4. Variation of metal properties with temperature is neglected.

5. The heater walls are heated electrically and uniformly along the test section.

The resulting equation, which, when coupled to the fluid conservation equation, describes the wall temperature behavior is

$$\left( \rho c_p A \right)_w \frac{\partial T_w}{\partial t} = q'_e - \pi DH(T_w - T_b) \quad (6.12)$$

The rate at which heat is transferred to the fluid per unit fluid volume  $q'''$  Eq. (6.3) is given by

$$q''' = \frac{\pi DH(T_w - T_b)}{A} \quad (6.13)$$

Equations (6.3), (6.5), (6.6) and (6.12), may now be solved numerically with the aid of Eq. (6.11) provided that a proper correlation of the heat transfer coefficient,  $H$ , is available, and that the relationship between the fluid density, temperature, and enthalpy is known for the reference pressure level.

For the calculations which are reported, the relationship between the properties was obtained from the tables of Van Wie and Ebel (2). It was necessary to extrapolate the data in the pseudoliquid region from saturation values using the correlation of Lyderson, Greenkorn, and Hougen (69). The data used are illustrated in Figs. 3 and 4 and listed in Appendix C.

Several relationships between the heat transfer coefficient and the other variables were tried. The most satisfactory method was to use the suggestion of Dickinson and Welch (16) and assign a constant

value to the coefficient which depended only upon the mass velocity. The heat transfer coefficient was assumed to vary with the 0.8 power of the mass flow rate. At periodic time intervals, the ratio of the heat transfer coefficient to the mass flow term was given a step change sufficient to approximately duplicate the experimental wall temperature behavior during the "boiling-like" occurrence. The factors which caused the "boiling-like" behavior to be initiated must be better understood before a more realistic model, which would depend upon the conditions in the heated boundary layer, can be developed. Nevertheless, the simple model is adequate to demonstrate the importance of the varying heat transfer coefficient, which was observed experimentally, in triggering and maintaining the slow type of oscillation.

#### Numerical Calculational Procedure

The geometry of the idealized numerical model is shown schematically in Fig. 21. The system consists of the closed, rectangular flow path, constructed of constant diameter tubing, and the fluid contained therein.

The natural circulation flow is maintained by the gravity head due to the difference in density in the hot and cold vertical legs of the loop. It is assumed that a perfect surge tank exists, to accommodate changes of fluid volume, such that the pressure level remains constant with time. Further, it is assumed that sufficient heat is removed in the cooler to result in a constant temperature in the cold leg between the cooler and heater. It was observed experimentally

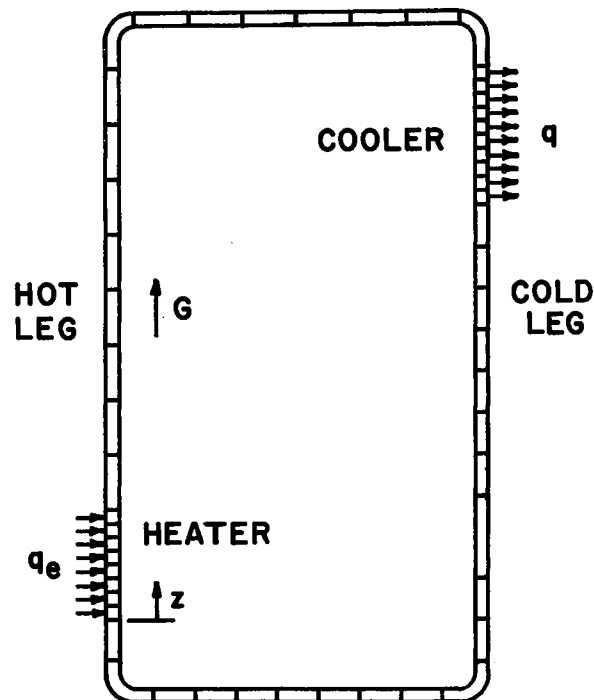


Fig. 21. Idealized Model of Flow Loop for Numerical Calculations

that neither the pressure surges nor the temperature feedback through the system contributed significantly to the mechanism which maintains the slow oscillations. Consequently, both the pressure surge and temperature feedback effect are eliminated from the numerical model, which also considerably reduces the calculation time. The electrical energy input to the heater walls is allowed to vary only with time, generally remaining constant throughout the solution except possibly for an initial step change. The fluid exchanges heat with the tube walls around the loop, except in the cold leg where thermal equilibrium is assumed. The heat transfer coefficient is assumed to vary with the 0.8 power of the mass flow rate. At selected intervals, the ratio of the heat transfer coefficient to the mass flow term may be changed stepwise in the heater, so that the experimentally observed

wall temperature behavior is approximately duplicated. This results in a time varying rate of energy transfer to the fluid, even though the heater electrical power is constant.

The loop is considered to be arbitrarily divided into  $n$  segments along the axial length and numbered consecutively with index  $j$ . A variable subscripted with  $j$ ,  $j+1$ ,  $j+1/2$ , refers to the value of that variable at the beginning of, end of, or midpoint of the  $j$ th axial segment. A variable subscripted with  $j+1$  also refers to the conditions at the beginning of the  $j+1$ th axial segment as well as at the end of the  $j$ th segment. Similarly the time is considered to be arbitrarily divided into increments. A variable superscripted with  $i$ ,  $i+1$ ,  $i+1/2$ , refers to the value of the variable at the beginning of, end of, or midpoint of the  $i$ th time interval.

#### Transient Calculations

The derivatives in Eqs. (6.3), (6.6) and (6.12) are replaced by finite difference approximations. Care must be taken when evaluating any type of problem by numerical methods, but particularly for instability studies, that a numerical instability does not introduce spurious variations in the solution. These numerical instability considerations impose certain restrictions on the selection of allowable time and space increments, which depend upon which, of the many available, differencing methods are employed. It has been found (70), for second order equations, that the solution is unconditionally stable, i.e., the solution does not depend upon the length of time step used, if the space derivatives are at least partially evaluated at the new

time step. This method, known as implicit differencing, was used in the present analysis whenever possible.

The energy Eq. (6.3) may be approximated by

$$\rho_{j-1/2}^i \left[ \frac{h_{j-1}^{i+1} - h_{j-1}^i + h_j^{i+1} - h_j^i}{2(\Delta t)^i} \right] + G^i \left[ \frac{h_j^{i+1} - h_{j-1}^{i+1} + h_j^i - h_{j-1}^i}{2(\Delta z)_{j-1}} \right] = (q''')_{j-1/2}^{i+1/2}, \quad (6.14)$$

where  $\rho_{j-1/2}^i$  is the density evaluated at  $1/2 (h_j^i + h_{j-1}^i)$

and  $(q''')_{j-1/2}^{i+1/2}$  is defined by Eq. (6.24). This differencing scheme, which is numerically stable for any size time step, is essentially the "box method" of Reference 71. It permits evaluation of the value of enthalpy at axial position,  $j$ , and time  $i+1$  in terms of known values, if the value of enthalpy at axial position  $j-1$  and time  $i+1$  is known and all values are known at time  $i$ ,

$$h_j^{i+1} = h_{j-1}^i + \left( h_j^i - h_{j-1}^{i+1} \right) \frac{(1-\alpha)}{(1+\alpha)} + \frac{2(q''')_{j-1/2}^{i+1/2} (\Delta t)^i}{\rho_{j-1/2}^i (1+\alpha)}, \quad (6.15)$$

where:

$$\alpha = \frac{G^i (\Delta t)^i}{\rho_{j-1/2}^i (\Delta z)_{j-1}}. \quad (6.16)$$

Analysis of the numerical results revealed an undesirable feature of this differencing method. When calculating  $h_j^{i+1}$  by Eq. (6.15), an increase of  $h_{j-1}^{i+1}$  contributed negatively to  $h_j^{i+1}$ , and a decrease of  $h_{j-1}^{i+1}$  caused  $h_j^{i+1}$  to increase. This was particularly noticeable and undesirable in the riser, where utilization of Eq. (6.15) resulted in

calculating that a step increase in power input resulted in a relatively hot mass of fluid flowing up the riser which was preceded by a relatively cold mass. In order to avoid this situation, another difference approximation to the energy equation was employed, in which the enthalpy space derivative was evaluated at time  $i+1$ , and the enthalpy time derivative was evaluated at position  $j$ ,

$$h_j^{i+1} = \frac{1}{1+\alpha} h_j^i + \frac{\alpha}{1+\alpha} h_{j-1}^{i+1} + \frac{(q''')_{j-1/2}^{i+1/2} (\Delta t)^i}{\rho_{j-1/2}^i (1+\alpha)}, \quad (6.17)$$

where  $\alpha$  is defined by Eq. (6.16).

The enthalpy distribution was calculated in the heater by Eq. (6.15) and in the riser by Eq. (6.17) which eliminated the previously mentioned "cold bank" effect. Results of this method did not vary over 1 percent from utilizing Eq. (6.17) in both sections, so the choice is somewhat arbitrary. Because of the experimentally determined boundary condition that the heater inlet temperature did not vary significantly during the slow oscillations, the enthalpy distribution around the loop at time  $i+1$  can be determined from Eq. (6.15) or (6.17) starting from the heater inlet. This eliminates one of the undesirable features of the implicit differencing method which ordinarily requires the solution of  $n$  simultaneous equations by one of the shortcut methods which have been developed.

When the enthalpy distribution around the loop is known at time  $i+1$ , from Eq. (6.15) or (6.17) the density distribution can be obtained from the tabulated property relationships. This permits Eq. (6.6) to be solved numerically for the average mass flow rate at



time  $i+1$ ,

$$G^{i+1} = G^i + \frac{g_c (\Delta t)^i}{L} \left[ -F^i - (\Delta P)^i \right] \quad , \quad (6.18)$$

where, from Eq. (6.11),

$$F^i = \frac{8.96 (G^i)^{1.59}}{\bar{\rho}^i} \quad , \quad (6.19)$$

$$\bar{\rho}^i = \frac{1}{L} \sum_{j=1}^n \rho_{j+1/2}^i (\Delta z)_j \quad , \quad (6.20)$$

and

$$(\Delta P)^i = \sum_{\text{hot leg}} \rho_{j+1/2}^i (\Delta z)_j - \sum_{\text{cold leg}} \rho_{j+1/2}^i (\Delta z)_j \quad . \quad (6.21)$$

A simple means to find allowable time steps for Eq. (6.18) has not been found. However, the use of this differencing method has not resulted in numerical instability for reasonably large time steps. The procedure used to check for stability was to compare solutions made with various time steps for convergence. If the solutions did not depend appreciably upon the time step used, they were assumed to be numerically stable.

Equation (6.12) is approximated by,

$$(T_w)_{j+1/2}^{i+1} = \frac{(\Delta t)^i (q_e')_{j+1/2}^{i+1/2}}{\left[ \begin{matrix} \rho & c_p & A \\ & & w \end{matrix} \right]_{j+1/2}} + \beta (T_b)_{j+1/2}^i + (1-\beta) (T_w)_{j+1/2}^i \quad , (6.22)$$

where:

$$\beta = \frac{\pi H_{j+1/2}^{i+1/2} D(\Delta t)}{\left[ \begin{matrix} \rho & c & A \\ & p & \\ & & w \end{matrix} \right]_{j+1/2}} \quad (6.23)$$

For numerical stability, it is necessary that  $\beta < 1$ , which only required that the time increments be less than about three seconds in the present case. The heat transfer rate to the fluid is calculated by Eq. (6.24),

$$(q''')_{j+1/2}^{i+1/2} = \frac{\pi H_{j+1/2}^{i+1/2} D \left[ (T_w)_{j+1/2}^{i+1} - (T_b)_{j+1/2}^i \right]}{A}, \quad (6.24)$$

for use in Eq. (6.15) or (6.17).

#### Steady-State Calculations

Besides a given inlet enthalpy and electrical heating power history, the transient calculations require an initial estimate of the mass flow rate  $G^1$  and enthalpy distribution  $h_j^1$ ,  $j = 1, 2, \dots, n$ . The choice of these initial values is arbitrary, and depends upon the physical nature of the problem being considered. Perhaps the most obvious, although impractical, choice would be to start with zero flow, zero power, and thermal equilibrium around the loop and study the resulting transient behavior as the power is slowly increased. The procedure followed was to assume that the loop was initially operating under steady-state conditions at a given power and inlet enthalpy. The steady-state flow rate and enthalpy distribution were calculated by an iterative procedure described below and used as initial values in the transient calculations.

The steady-state values could also have been obtained, but at the expense of computer time, from any initially assumed values by executing the transient calculations until the initial transients were dissipated. If the heating power and heat transfer coefficients were not changed, the loop would then continue to operate stably.

For steady-state operation, all time derivatives in the conservation equations vanish. Integrating Eq. (6.3) across the heater, with the aid of (6.12) and (6.13), results in

$$G(\Delta h)_h = q''' L_h = \frac{q_e}{A}, \text{ or}$$

$$(\Delta h)_h = \frac{q_e}{AG}, \quad (6.25)$$

giving the fluid enthalpy rise across the heater for a given power and flow rate. For space invariant electrical heating, the enthalpy increase is linear with axial distance,  $z$ , in the heater permitting the enthalpy distribution to be calculated. The enthalpy in the channels between the heater and cooler is constant for steady-state operation, and the fluid enthalpy decreases linearly in the cooler by the amount given by Eq. (6.25).

The steady-state iteration consists of assuming a value for the mass flow rate  $G$ ; calculating the enthalpy distribution by the procedure described in the preceding paragraph; evaluating the density distribution and the property relationships and then calculating an improved value for  $G$  from Eq. (6.10) and (6.11). The iteration proceeds until the improved value for  $G$  does not vary from the previously calculated value of  $G$  by more than a prescribed amount (usually 0.5 percent). Only 2 to 6 iterations are required for

reasonable initial values.

The wall temperatures do not affect the steady-state flow iterations, since for equilibrium conditions, the heat transfer rate to the fluid in the heater equals the electrical power to the heater walls, as can be deduced from Eq. (6.12) and Eq. (6.13). After the steady-state flow rate and enthalpy distribution has been determined, the bulk temperature distribution can be determined from the enthalpy distribution and the property relationships. The initial wall temperature distribution can then be calculated from Eq. (6.12),

$$(T_w)_j^{1/2} = \frac{(q_e')_j^{1/2}}{\pi D H_j^{1/2}} + (T_b)_j^{1/2} \quad (6.26)$$

The numerical solution consists of determining an initial steady-state condition by the iteration method just described, and then evaluating the loop response to a step change in electrical power input or in the heat transfer coefficient. The problem was programmed for solution on an IBM 3600 digital computer, using the program listed in Reference 28 as a guide for the programming techniques. The complete program is listed in Appendix C.

#### Results of Numerical Calculations

The general type of mathematical model which was described in the previous sections has been used, with fair success, to calculate transient behavior in parallel boiling channels (40) when the time rate of change in channel vapor content was not too large. It has also been used with good success by Alstad, et al., (68) in calculating

the transient behavior of a single-phase natural circulation loop.

Harden (28) used essentially the same mathematical model, but with different differencing techniques, and neglected the heat capacity of the heater walls which resulted in a constant heat transfer rate to the fluid when the electric power was constant. His solution exhibited sustained flow oscillations of small amplitude below the pseudocritical temperature at constant power input.

Since these results were contrary to those observed in the present tests and to what one would logically expect from the mathematical model, i.e., the flow oscillations should quickly damp out due to natural dissipative forces following a disturbance in heat input to the fluid, Harden's solution was carefully examined. It was found that the solution depended upon the time step employed, and that the calculated enthalpy distribution was extremely erratic, i.e., following a step increase in heat input, the enthalpy declined substantially at certain nodes even in the heater. This indicated that the sustained oscillations resulted from a numerical instability, and were not representative of the physical system. With the same initial conditions, geometry, property relationships, and frictional pressure drop correlation, but utilizing the implicit differencing technique shown in Eq. (6.15), the solution converged smoothly to a steady-state value following a disturbance. This example illustrates the caution which must be exercised when utilizing numerical methods in instability studies to ensure that the results are valid.

The calculated effect of increasing the electrical power stepwise from 4 kw to 8 kw is shown in Fig. 22. The flow rate approached

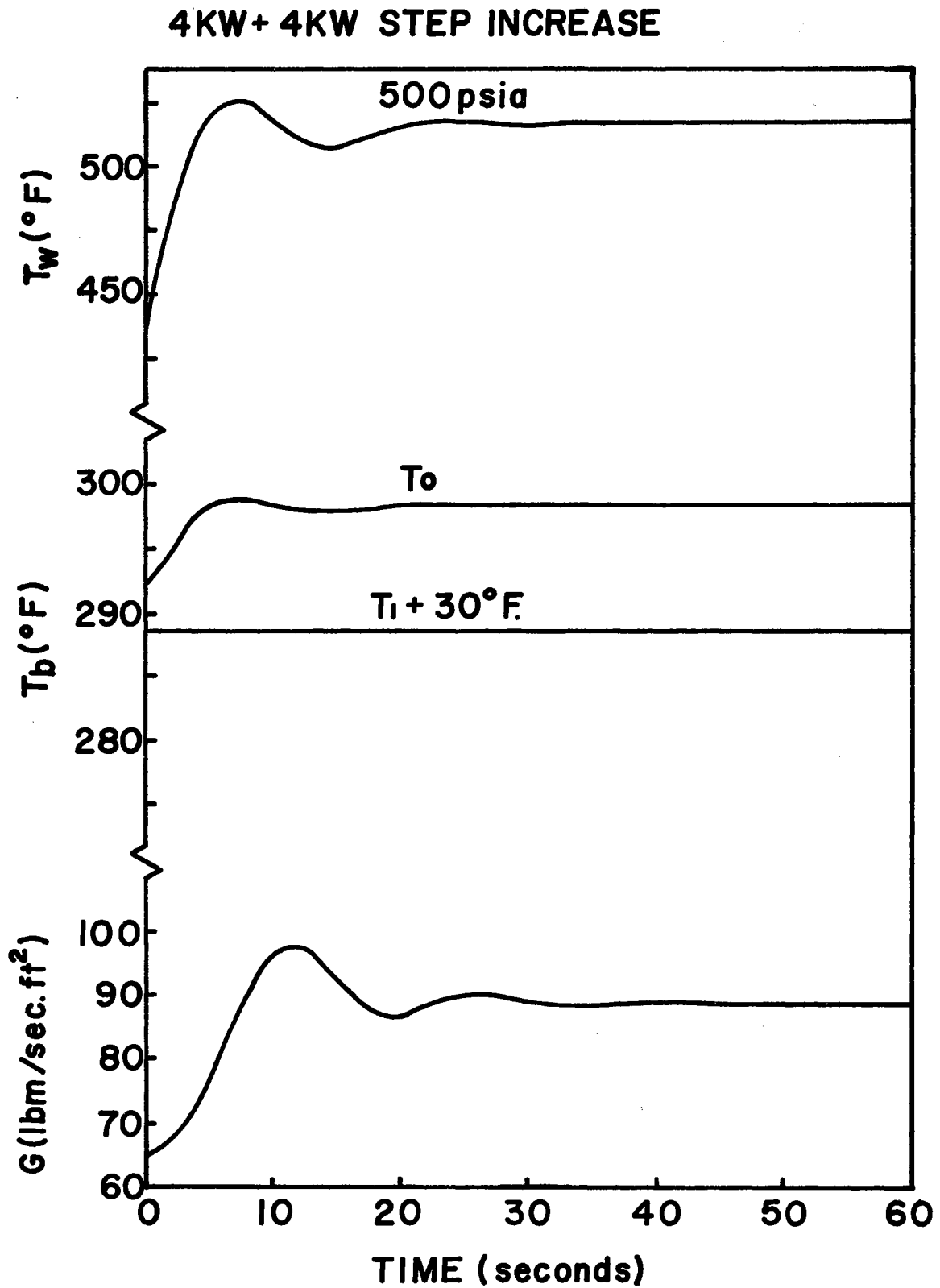


Fig. 22. Calculated Response Following Doubling of Electrical Heating Power

equilibrium after only a few damped oscillations about the final equilibrium position, as did the wall temperature and the outlet bulk temperature. Similar calculations were made for a range of inlet bulk temperatures up to the pseudocritical temperature. There was no tendency for sustained oscillations to develop at these conditions. The variation of the flow rates following the step electrical power increase is shown in Figs. 23 and 24 for inlet temperatures ranging from 200° to 300°F. It was found that the damped oscillation period compared quite closely with those observed experimentally at similar inlet temperatures. The period decreased with increasing inlet temperatures as was observed experimentally, and as predicted by the method described in Appendix B. As the pseudocritical temperature was approached, the mass flow rate decreased with increased inlet temperatures. At higher temperatures, the low undamped natural frequency (Appendix B) caused the system to become first critically, and then overdamped ( $T_i = 296.2$  and  $299.5$ ). In all of these respects, the agreement between the calculated results and the observed experimental behavior was quite good.

The results of the same type of calculation as described above, but for operation with the upper horizontal cooler, is illustrated in Fig. 25. The higher mass flow rate introduced sufficient additional damping so that the oscillatory behavior was much less extreme than for similar operation with the vertical cooler (Fig. 22). Also it is seen that the horizontal cooler caused a longer oscillation period as is predicted by the method of Appendix B. These results furnish an explanation for the relatively low flow amplitudes but relatively

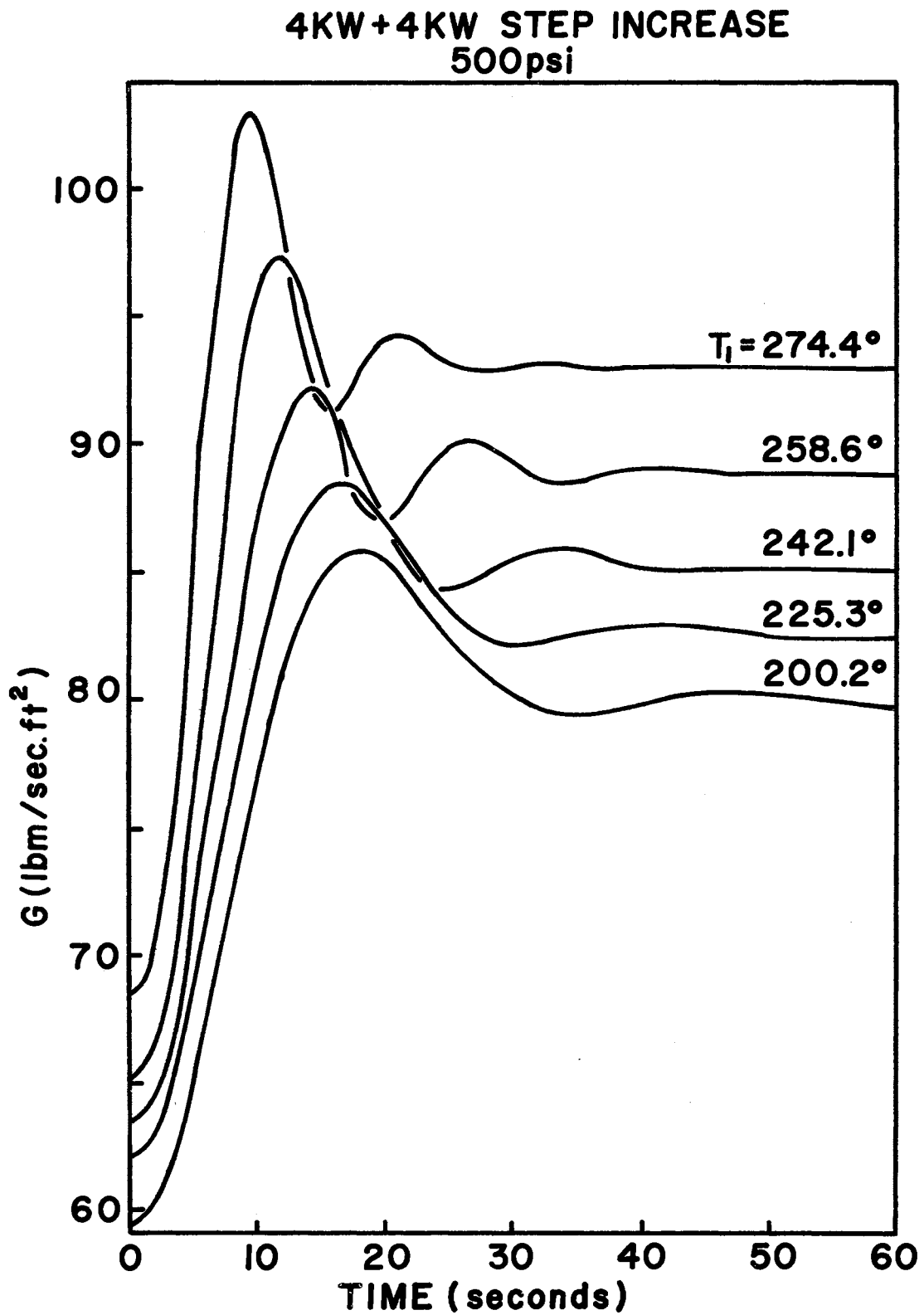


Fig. 23. Calculated Flow Response Following Doubling of Electrical Heating Power for Various Inlet Temperatures



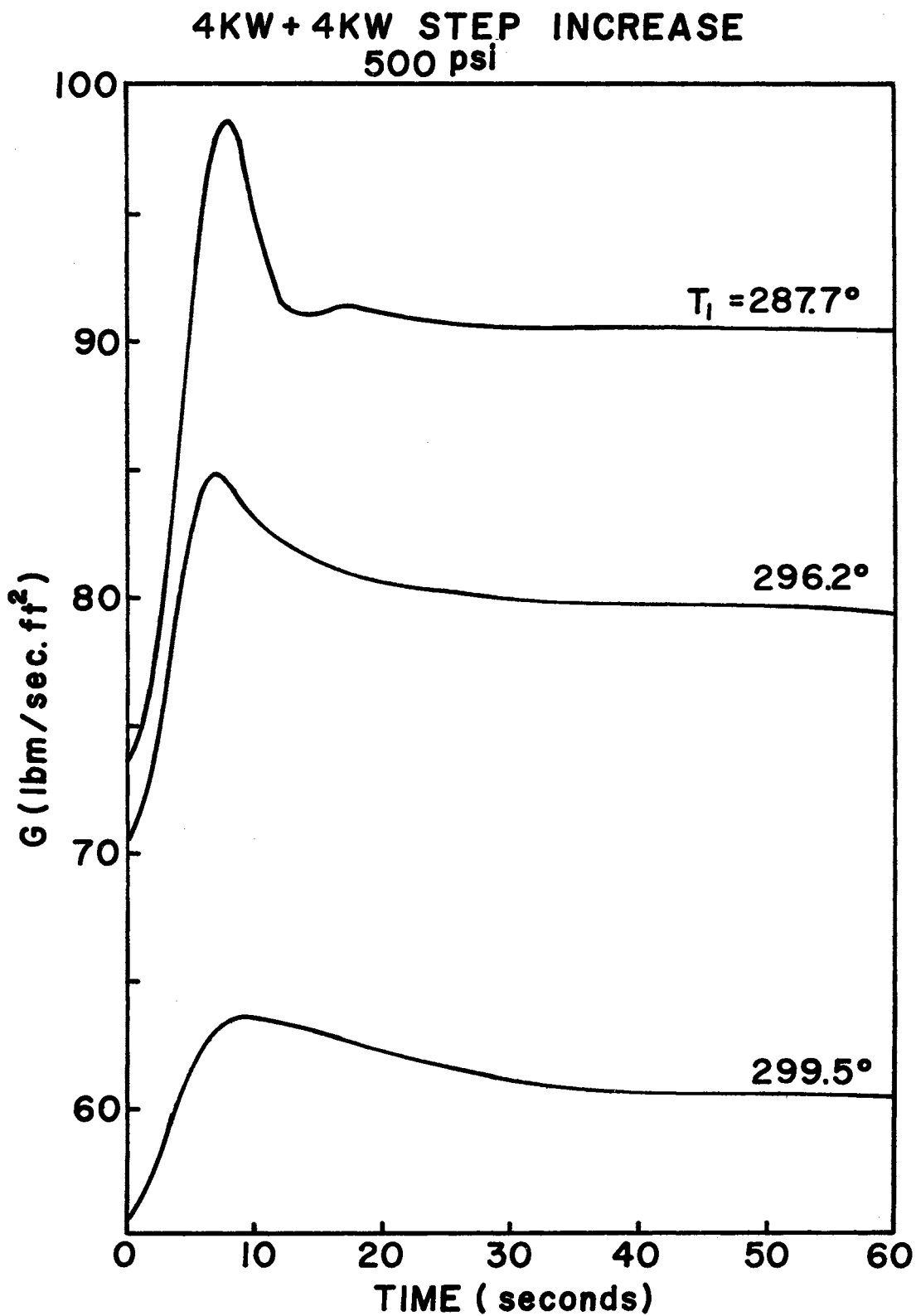


Fig. 24. Calculated Flow Response Following Doubling of Electrical Heating Power for Various Inlet Temperatures

**4KW + 4KW STEP INCREASE  
HORIZONTAL COOLER  
500 PSIA**

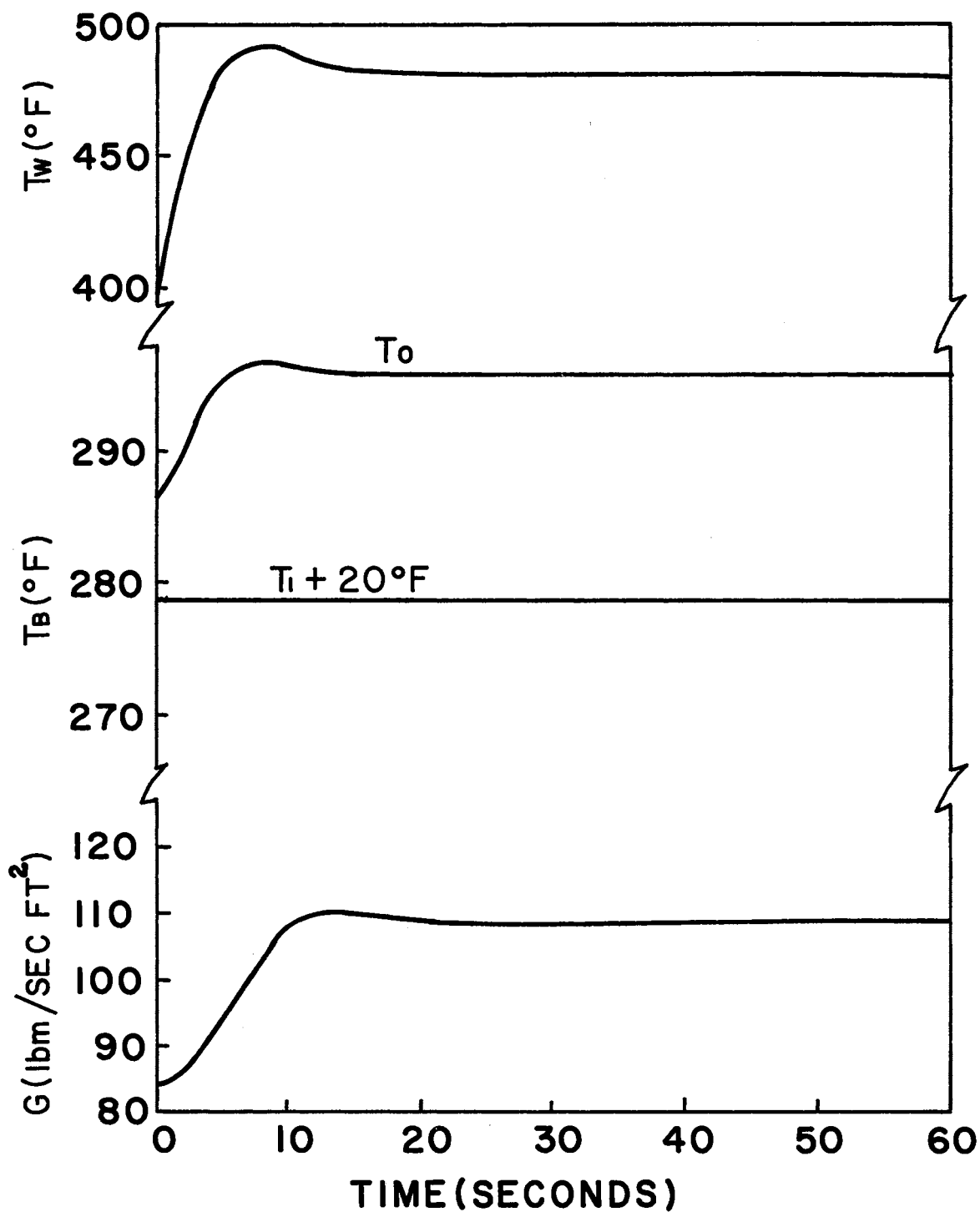


Fig. 25. Calculated Response Following Doubling of Electrical Heating Power; Upper Horizontal Cooler

large pressure surges illustrated in Fig. 19.

In order to simulate the experimentally observed "boiling-like" behavior, the ratio of the heat transfer coefficient to the mass flow term ( $H/G^{0.8}$ ) was given a step increase, sufficient to approximately duplicate the experimentally observed wall temperatures. After a given time the ratio was then changed stepwise back to its initial value. The results of increasing the ratio by 60 percent for two seconds is shown in Fig. 26. The "boiling-like" behavior was repeated four times in phase with the flow oscillations. It is seen that a periodic and sustained oscillation developed, in response to

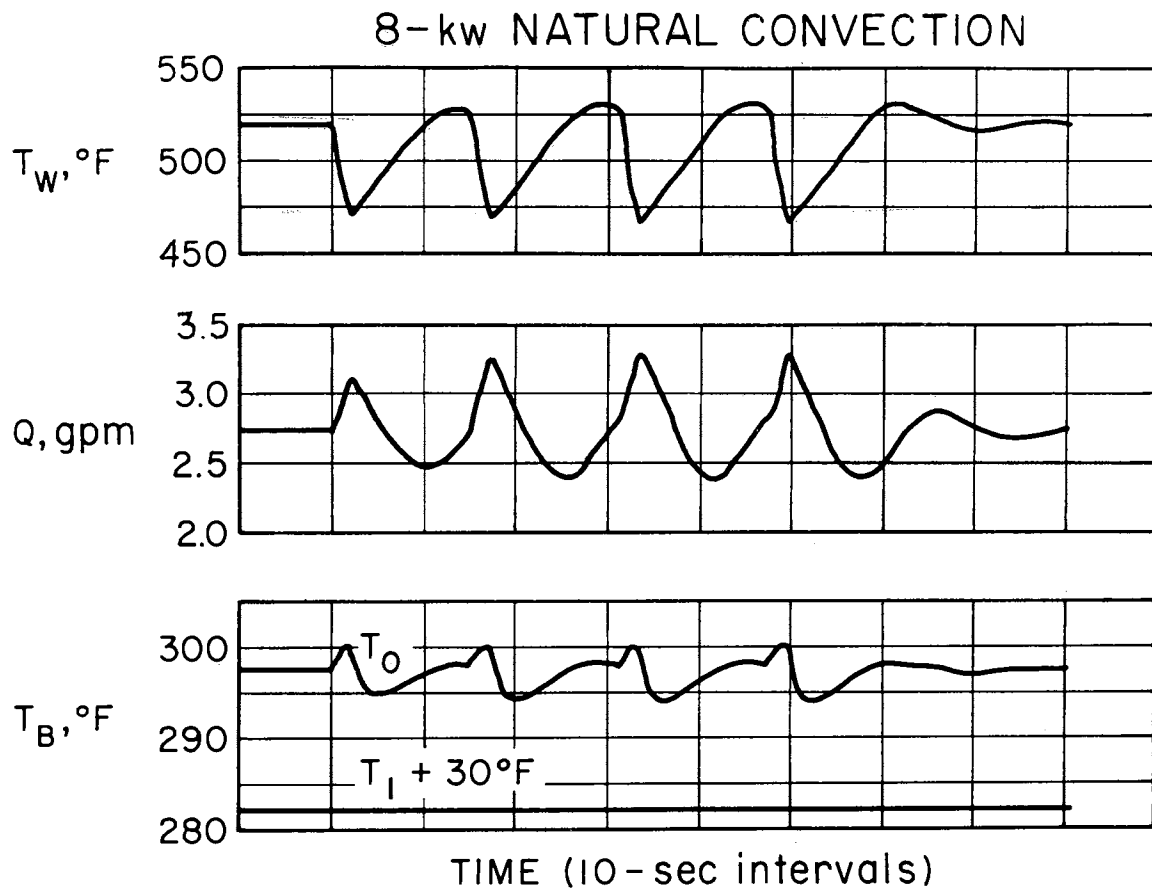


Fig. 26. Calculated Behavior of Slow Oscillations; Triggered and Maintained by Changes of Heat Transfer Coefficient

the imposed forcing function. These calculated results should be compared with the experimental results shown in Fig. 15, which are at a similar inlet temperature, and with Fig. 13, which are at a lower inlet temperature, but which illustrate the heat transfer improvements in phase with the flow oscillations, and the rapid decay of the oscillations when the heat transfer improvements terminated. The reasonably good agreement substantiates the hypothesis that the heat transfer improvement was a dominant factor in triggering and maintaining the slow oscillations.

At higher bulk temperatures up to the pseudocritical, the effect of the heat transfer improvement on the flow was more pronounced, while the outlet bulk temperature was affected less. Figure 27 illustrates this behavior. The frequency increase with temperature is also

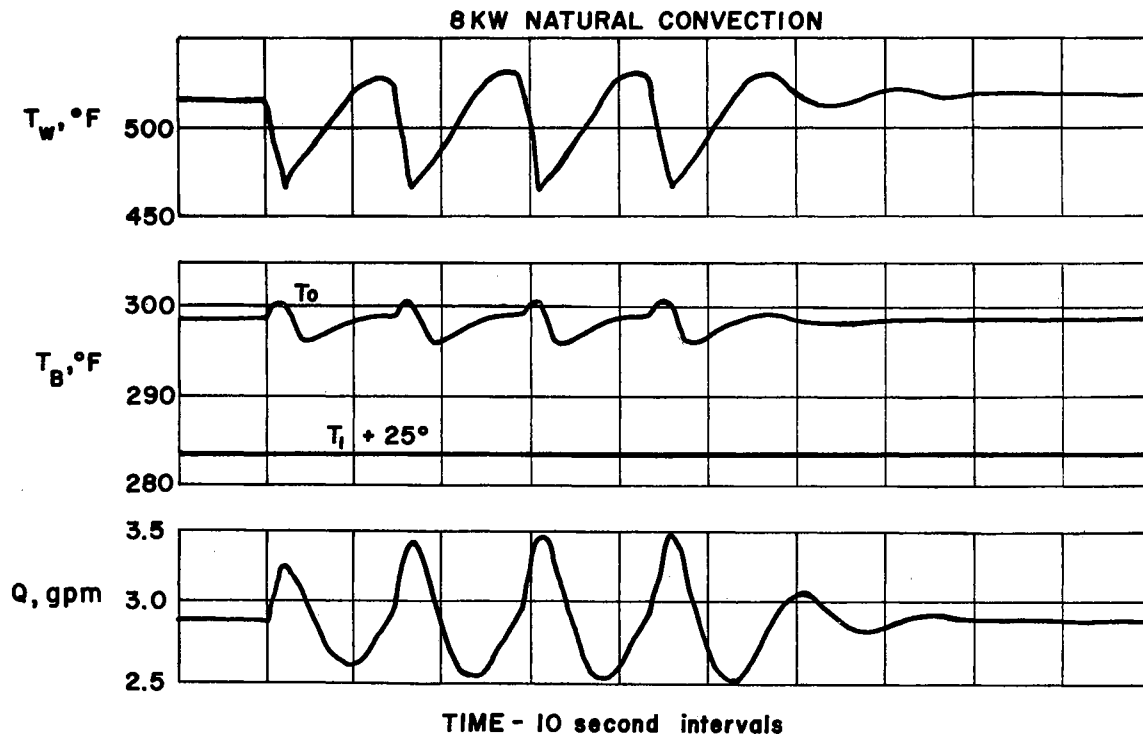


Fig. 27. Calculated Behavior of Slow Oscillations;  
Higher Inlet Temperatures

evident, when compared with Fig. 26.

At lower temperatures, the heat transfer improvement caused a relatively large outlet bulk temperature increase, while the flow rate varied less as shown in Fig. 28. This figure should be compared with Fig. 9. Although the temperature level was less in Fig. 9 and the "boiling-like" behavior was of a more sustained nature, the similarity is apparent.

The simulation of the "boiling-like" behavior by the step changes could be modified so as to make the changes less abrupt, particularly during the "boiling" termination, in order to match the experimental wall temperature behavior more closely. However, the model

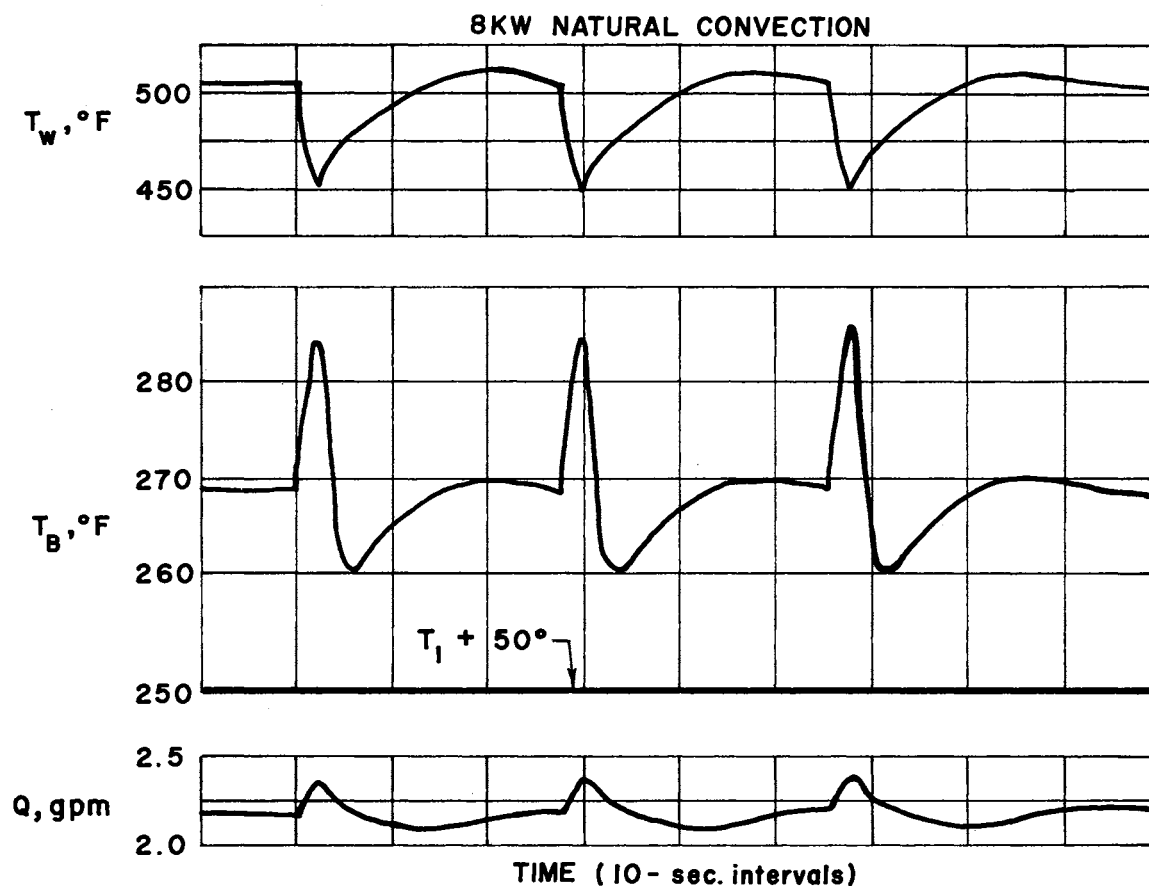


Fig. 28. Calculated Behavior of Slow Oscillations;  
Lower Inlet Temperatures

which was used is sufficient to demonstrate the importance of the wall temperature variation in triggering and maintaining the slow oscillations. Including the effect of the pressure and mass flow variation with time and distance, which would involve considerably more effort, could also result in a better match of the data. The agreement between the calculated and experimental results was judged to be sufficiently close so as to not warrant such an effort in the present investigation.

## CHAPTER VII

### SUMMARY AND CONCLUSIONS

Two distinct types of oscillatory behavior were observed during the tests. Pressure and flow oscillations occurred with bulk temperatures below the pseudocritical and with heater wall temperatures exceeding the pseudocritical. Hence, during the oscillatory behavior, the fluid in the heated boundary layer was at least partly in the pseudovapor state while the bulk of the fluid was in the pseudoliquid state. The fluid temperature equalled the pseudocritical temperature at some point in the heated boundary layer during the oscillations.

The basic cause of both types of oscillatory behavior appears to have originated in the heated boundary layer. An analytical solution to this type of problem is beset with many of the difficulties which have prevented a satisfactory solution of the analogous subcritical boiling instability problem. For one thing, the nebulous behavior of the viscosity and thermal conductivity at the pseudocritical temperature must be considered. Also it is highly likely that nonequilibrium conditions are involved, similar to the "superheat" required to initiate nucleate boiling. This lack of equilibrium may have contributed to the suddenly decreased wall temperatures, which is referred to as a "boiling-like" phenomenon in the thesis. Despite the rather complex nature of the cause of the oscillations, the oscillations

themselves are shown to be special examples of commonly encountered behavior.

The first type of oscillation was of an acoustic nature, exhibiting harmonic pressure and flow oscillations in the frequency range of 5 to 30 cps. The acoustic oscillations are believed to have been initiated by a local disturbance, which resulted in pressure waves being propagated at sonic speed away from the disturbance. In the constant diameter design employed during the present tests, the pressure wave traversed the closed loop, returning to the point of disturbance diminished by the external acoustic damping. If the disturbance had originated in a small diameter heated section, such as has been employed in other tests reported in the literature, the pressure wave would have been reflected at the ends of the small diameter section, returning to the point of disturbance in a relatively shorter time. In order for the oscillation to have been maintained, it is necessary that a mechanism existed such that the acoustic pressure wave was reinforced upon passing a given point in the system. In addition, the acoustic damping could not have been so large so as to have dissipated the pressure wave before it returned to this given point. The introduction of acoustic damping would provide a means for eliminating this type of oscillation.

A mechanism which would cause the acoustic pressure wave to be reinforced is postulated. Since the fluid in the heated boundary layer was in a pseudovapor state, a pressure wave passing the heated surface would have tended to compress the boundary layer, improve the thermal conductivity, and cause an increased heat transfer rate from



the wall to the fluid. A rarefaction wave passing the heated surface would have caused the boundary layer to expand, the thermal conductivity to decrease and resulted in a decreased heat transfer rate to the fluid. This pressure dependent heat transfer rate would have caused a resonant acoustic oscillation to have been maintained.

When the outlet bulk temperature was slightly below the pseudo-critical temperature, a different type of oscillation was observed. This type of oscillation was characterized by a frequency two orders of magnitude slower than the sonic oscillations. The frequency of the acoustic oscillations decreased with temperature while the frequency of the slow type increased with temperature. Occasionally both types of oscillations occurred simultaneously, which further verified that they were of a distinct nature. Instead of acoustic pressure waves traversing the loop, the slow type of oscillation may be described by considering the fluid in the loop as a solid body performing a mechanical vibration about the equilibrium position.

The data indicate that this type of oscillation was initiated and sustained by a sudden improvement of the heat transfer coefficient, which is attributed to the occurrence of a "boiling-like" phenomenon in the supercritical fluid. The heat transfer coefficient improvement resulted in a sudden drop of the wall temperature, less energy stored in the heater wall, and an increased heat transfer rate to the fluid from the wall, even though the electrical heating power remained constant. An approximate numerical solution, which closely matched the experimentally observed results during the slow oscillations, verified the importance of the heat transfer improvement in triggering and

maintaining the oscillations. Varying the heat transfer coefficient so as to approximately duplicate the observed wall temperature behavior resulted in sustained flow oscillations, whose amplitude and frequency closely matched the experimental results.

The assumptions which were made to simplify the numerical solution prevented this model from duplicating the experimentally observed acoustic oscillations. It is estimated that a more general model, theoretically capable of predicting the acoustic oscillations as well as not requiring empirical friction factor or heat transfer coefficient correlations, would have increased the computer time by at least four orders of magnitude. Such a solution would be no better than the property data which is available, and would have to account for the nonequilibrium effects.

Both the acoustic and slow type of oscillation also occur during subcritical boiling heat transfer. Generally, the acoustic type has been considered of secondary interest, but a large amount of attention has been focused on the second type due to its importance in nuclear reactor applications. Despite the large effort, the boiling instability is still not well understood, perhaps because of the lack of a satisfactory physical explanation of the phenomenon. It has been found that the subcritical boiling instability occurs only when the subcooling of the fluid entering the test section is in a definite range. The boiling instability does not occur if the inlet fluid is saturated or only slightly subcooled, which implies that the mechanism by which nucleate boiling is initiated may be an important contributing factor to the boiling instability. The results of the present

supercritical studies contribute an insight into the physical nature of the instabilities which should be applicable for both subcritical and supercritical systems.

NOMENCLATURE

Symbol	Description	Units
A	Area	ft <sup>2</sup>
c <sub>p</sub>	Specific heat	Btu/lb <sub>m</sub> - °F
c	Acoustic velocity	ft/sec
C	Thermal capacitance	Btu/°F
f	Frequency	cps
f	Fanning friction factor	Dimensionless
F	Friction pressure drop	lb <sub>f</sub> /ft <sup>2</sup>
g	Gravitational acceleration	ft/sec <sup>2</sup>
g <sub>c</sub>	Gravitational constant	ft - lb <sub>m</sub> /lb <sub>f</sub> sec <sup>2</sup>
G	Mass flow rate per unit area	lb <sub>m</sub> /sec - ft <sup>2</sup>
h	Specific enthalpy	Btu/lb <sub>m</sub>
H	Heat transfer coefficient	Btu/sec - ft <sup>2</sup> - °F
k	Thermal conductance	Btu/sec - ft - °F
L	Length	ft
p	Pressure	psia
P	Amplitude of pressure oscillations	psia
q	Heat transfer rate	Btu/sec
Q	Volumetric flow rate	gpm
R	Thermal resistance	sec - °F/Btu
s	Specific entropy	Btu/lb <sub>m</sub> - °F

## NOMENCLATURE (Contd.)

Symbol	Description	Units
t	Time	second
T	Temperature	°F
u	Specific internal energy	Btu/lb <sub>m</sub>
v	Specific volume	ft <sup>3</sup> /lb <sub>m</sub>
x	Position coordinate	ft
z	Position coordinate	ft
<u>Greek Letters</u>		
λ	Acoustic wave length	ft
μ	Viscosity	lb <sub>f</sub> - sec/ft <sup>2</sup>
ρ	Density	lb <sub>m</sub> /ft <sup>3</sup>
τ	Shear force per unit length	lb <sub>f</sub> /ft
<u>Sub-Scripts</u>		
b	Bulk	
cr	Critical state	
e	Electrical	
j	Space index, specifies axial position at beginning of <u>j</u> th space segment	
s	Steady-state	
w	Wall	
<u>Super-scripts</u>		
—	Average value	
*	Pseudocritical	
'	Per unit length	
'''	Per unit volume	

## BIBLIOGRAPHY

1. Goldmann, K., "Heat Transfer to Supercritical Water at 5000 psi Flowing at High Mass Flow Rates Through Round Tubes," Proceedings of the 1961 International Heat Transfer Conference, Part III, August, 1961, 561-578.
2. Van Wie, N. H., and R. A. Ebel, "Some Thermodynamic Properties of Freon-114," Report No. K-1430, Vol. I and II, Chemistry-General (T.I.D. - 4500, 14th Ed.) available from the Office of Technical Services, U. S. Dept. of Commerce, 1959.
3. Anderson, N. S., and L. P. Delsasso, "The Propagation of Sound in Carbon Dioxide Near the Critical Point," Journal of the Acoustical Society of America, 23, No. 4, July 1951, 423-429.
4. Stiel, L. I., and G. Thodos, "The Prediction of the Transport Properties of Pure Gaseous and Liquid Substances," Progress in International Research on Thermodynamic and Transport Properties, New York, Academic Press, 1962, 352-365.
5. Simon, H. A., and E. R. G. Eckert, "Laminar Free Convection in Carbon Dioxide Near its Critical Point," Int. J. Heat Mass Transfer, 6, 1963, 681-690.
6. Sengers, J. V., and A. Michels, "The Thermal Conductivity of Carbon Dioxide in the Critical Region," Progress in International Research on Thermodynamic and Transport Properties, New York, Academic Press, 1962, 434-440.
7. Schmidt, E., E. Eckert, and U. Grigull, "Heat Transfer by Liquids Near the Critical State," Air Material Command, AAF Translation No. 527, Wright Field, Dayton, Ohio, 1939.
8. Holman, J. P., and J. H. Boggs, "Heat Transfer to Freon-12 Near the Critical State in A Natural-Circulation Loop," Journal of Heat Transfer, Trans. ASME, Series C, 82, August 1960, 221-226.
9. Van Putte, D. A., and R. J. Grosh, "Heat Transfer to Water in the Near-critical Region," Technical Report No. 4, Purdue University, ANL Subcontract 31-109-38-704 (August 1960).
10. Chalfant, A. I., "Heat Transfer and Fluid Friction Experiments for the Supercritical Water Reactor," PWAC-109, June 1, 1954, unclassified.

## BIBLIOGRAPHY (Contd.)

11. Goldmann, K., "Special Heat Transfer Phenomenon for Supercritical Fluids," NDA-2-31, Nov. 1956, unclassified.
12. Goldmann, K., "Boiling Songs," Nuclear Development Associates, Inc., Report No. NDA 10-68, May 14, 1953.
13. Firstenberg, H., "Boiling Songs and Associated Mechanical Vibrations," Report NDA-2131-12, June 1960.
14. Griffith, J. D., and R. H. Sabersky, "Convection in a Fluid at Supercritical Pressures," ARS Journal, 30 (3), March 1960, 289-291.
15. Graham, R. W., R. C. Hendricks, and R. C. Ehlers, "An Experimental Study of the Pool Heating of Liquid Hydrogen in the Subcritical and Supercritical Pressure Regimes Over a Range of Accelerations," NASA TMX,-52039, August 1964.
16. Dickinson, N. L., and C. P. Welch, "Heat Transfer to Supercritical Water," Trans. ASME, 80, April 1958, 746-752.
17. Doughty, D. L., and R. M. Drake, "Free Convection Heat Transfer from a Horizontal Right Cylinder to Freon-12 near the Critical State," Trans. ASME., 78, 1956, 1843-1850.
18. Bonilla, Charles F. and Leon A. Sigel, "High-Intensity Natural-Convection Heat Transfer near the Critical Point," Chemical Engineering Progress Symposium Series, No. 32, 57, 1960, 87-95.
19. McCarthy, J. R., and H. Wolf, "The Heat Transfer Characteristics of Gaseous Hydrogen and Helium," Rocketdyne Research Report RR-60-12, December 1960.
20. Thurston, R. S., "Pressure Oscillations Induced by Forced Convection Heat Transfer to Two-Phase and Supercritical Hydrogen," Los Alamos Report LAMS-3070, February 1964.
21. Hines, W. S., and H. Wolf, "Pressure Oscillations Associated with Heat Transfer to Hydrocarbon Fluids at Supercritical Pressures and Temperatures," ARS Journal, 32, March 1962, 361-366.
22. Guevara, F. A., B. B. McInteer, and R. M. Potter, "Temperature Flow Stability Experiments," LAMS-2934, July 1963.
23. Powell, W. B., "Heat Transfer to Fluids in the Region of the Critical Temperature," Jet Propulsion, 27, July 1957, 776-783.

## BIBLIOGRAPHY (Contd.)

24. Koppel, L. B., and J. M. Smith, "Turbulent Heat Transfer in the Critical Region," Proceedings of the 1961 International Heat Transfer Conference, Part III, Aug. 1961, 585-590.
25. Wood, R. D., and J. M. Smith, "Heat Transfer in the Critical Region - Temperature and Velocity Profiles in Turbulent Flow," AIChE Journal, 10, No. 2, March 1964, 180-186.
26. Bringer, R. P., and J. M. Smith, "Heat Transfer in the Critical Region," AIChE Journal, 3, 1957, 49-55.
27. Petukhov, B. S., E. A. Krasnoschekov, and V. S. Protopopov, "An Investigation of Heat Transfer to Fluids Flowing in Pipes under Supercritical Conditions," Proceedings of the 1961 International Heat Transfer Conference, Part III, Aug. 1961, 569-578.
28. Harden, D. G., "Transient Behavior of a Natural-Circulation Loop Operating near the Thermodynamic Critical Point," ANL-6710, May 1963.
29. Gouse, S. W., Jr., "An Index to the Two-Phase Gas-Liquid Flow Literature, Part I," MIT Engineering Projects Laboratory Report DSR-8734-1, May 1963.
30. Gouse, S. W., Jr., and C. D. Andrysiak, "Flow Oscillations in a Closed Loop with Transparent Parallel Vertical Heated Channels," MIT Engineering Projects Laboratory Report 8973-2, Mechanical Engineering Department, June 1963.
31. Anderson, R. P., and P. A. Lottes, "Boiling Stability," Progress in Nuclear Energy, Series IV, 4, London: Pergamon Press, 1961, Ch. 1.
32. Beckjord, E. S., "Hydrodynamic Stability in Reactors," Nuclear Safety, 4, Sept. 1962, 1-10.
33. Ledinegg, M., "Instability of Flow During Natural and Forced Circulation," Die Wärme, 61, 1938, 891-898.
34. Chilton, H. A., "A Theoretical Study of Stability in Water Flow through Heated Passages," J. of Nucl. Energy, 5, 1957, 273-284.
35. Pulling, D. J., and J. G. Collier, "Instabilities in Two-Phase Flow - Preliminary Experiments," AERE-M1105, July 1963.
36. Quandt, E. R., "Analysis and Measurements of Flow Oscillations," Chemical Engineering Progress Symposium Series, No. 32, 57, 1961, 111-126.



## BIBLIOGRAPHY (Contd.)

37. Anderson, R. P., L. T. Bryant, J. C. Carter, and J.F. Marchaterre, "Transient Analysis of Two-Phase Natural Circulation Systems," ANL-6653, December 1962.
38. Becker, K. M., S. Jahnberg, I. Haga, P. T. Hanson, and R. P. Mathisen, "Hydrodynamic Instability and Dynamic Burnout in Natural Circulation Two-Phase Flow, An Experimental and Theoretical Study," AE-156, September 1964.
39. Nahavandi, A. N., "A Digital Computer Analysis of Loss of Coolant Accident for a Multicircuit Core Nuclear Power Plant," Nuclear Science and Engineering, 14, 1962, 272-86.
40. Meyer, J. E., "Hydrodynamic Models for the Treatment of Reactor Thermal Transients," Nuclear Science and Engineering, 10, 1961, 269-277.
41. Meyer, J.E. and R. R. Rose, "Application of a Momentum Integral Model to the Study of Parallel Channel Boiling Flow Oscillations," Journal of Heat Transfer, Trans. ASME, 85, Feb. 1963, 1-9.
42. Wallis, G. B., and J. H. Heasley, "Oscillation in Two-Phase Flow Systems," Journal of Heat Transfer, Trans. ASME, Series C, 83, August 1961, 363-369.
43. Wissler, E. H., et al., "Oscillatory Behavior of a Two-phase Natural-circulation Loop," AIChE Journal, 2, June 1956, 157-162.
44. Ulrich, A. J., "Results of Recent Analysis of Borax-II Transient Experiments," ANL-5532, 1956.
45. Gouse, S. W., Jr., "A Survey of the Velocity of Sound in Two-phase Mixtures," ASME Publication 64 WA/FE-35, 1964.
46. Fleck, J. A. Jr., "The Influence of Pressure on Boiling Water Reactor Dynamics Behavior at Atmospheric Pressure," Nuclear Science and Engineering, 9, 1961, 271-280.
47. Christensen, H., "Acoustical Oscillation in Steam Systems," Nukleonik, 5, No. 7, 1963, 279-285.
48. Hoglund, B. M., "The Effect of Small Additions of Methanol on Film Boiling Heat Transfer in Water," Nuclear Technology Laboratory, Report 2, Stanford, California, March 1958, p. 16.
49. Viskanta, R., "Natural Frequency of Oscillation of Armadilla," ANL Internal Memo.

## BIBLIOGRAPHY (Contd.)

50. Levy, S., and E. S. Beckjord, "Hydraulic Instability in a Natural Circulation Loop with Net Steam Generation at 1000 psi," ASME Publication 60-HT-27, 1960.
51. Blumbough, A. L., and E. R. Quandt, "Analysis and Measurement of Flow Oscillations," WAPD-AD-TH-538, November 1960.
52. Research Laboratory, Ramo-Wooldridge Division, Thomson-Ramo-Wooldridge, Inc., Annual Summary Report 1959, "Kinetic Studies of Heterogeneous Water Reactors," RWD-RL-167, February 1960.
53. Lindahl, E. J., "Pulsation and its Effect on Flowmeters," Trans. ASME, 68, November 1946, 883-894.
54. Grey, J., and F. F. Liu, "Methods of Flow Measurement," ARS Journal, May-June 1953, 133-140.
55. Shafer, M. R., "Performance Characteristics of Turbine Flowmeters," Trans. ASME, 84, December 1962, 471-485.
56. Grey, J., "Transient Response of the Turbine Flowmeter," Jet Propulsion, February 1956.
57. Green, S. J., and T. W. Hunt, "Accuracy and Response of Thermocouples for Surface and Fluid Temperature Measurements," Temperature, Its Measurement and Control, Vol. 3, Part 2, Reinhold Publishing Co., 1962, 695-722.
58. Handbook of Chemistry and Physics, Cleveland, Chemical Rubber Publishing Co., 1955.
59. Clark, J. A., Discussion in Trans. ASME, 80, 1958, 1402-1403.
60. Hatch, M. R., and R. B. Jacobs, "Prediction of Pressure Drop in Two-Phase Single-Component Fluid Flow," AIChE Journal, 8, March 1962, 19-25.
61. Sondhauss, Pogg. Ann., 109, pp. 1, 426, (1860).
62. Lord Rayleigh, The Theory of Sound, Vol. II, 2d ed., London, MacMillan 1940, p. 226 ff.
63. McManus, H. N. Jr., and E. E. Soehngen, "Flow Separation and Acoustic Effects," Journal of Heat Transfer, Trans. ASME, Series C, 82, August 1960, pp. 166-169.
64. Merlini, C., private communication, "Natural Circulation Heat Transfer to Supercritical Water," to be published as an ANL report.

## BIBLIOGRAPHY (Contd.)

65. Schlichting, H., Boundary Layer Theory, McGraw Hill, New York, 1955.
66. Bird, R. B., W. E. Stewart, and E. N. Lightfoot, Transport Phenomena, Wiley, New York, 1960.
67. Daily, J.W., and K. C. Deemer, "The Unsteady-Flow Water Tunnel at M.I.T." Trans.ASME, 76, 87, 1954.
68. Alstad, C. D., H. S. Isbin, N. R. Amundson, and J. P. Silvers, "The Transient Behavior of a Single-Phase Natural Circulation Water Loop System," ANL-5409, March 1956.
69. Lydersen, A. T., R. A. Greenkorn, and O. A. Hougen, "Generalized Thermodynamic Properties of Pure Fluids," Univ. Wisconsin Expt. Sta. Report 4, Madison, Wisconsin, October 1955.
70. Richtmyer, R. D., Difference Methods for Initial-value Problems, Interscience, New York (1957).
71. Birkhoff, G., and T. F. Kines, "CHIC Program for Thermal Transients," WAPD-TM-245, February 1962.
72. Garlid, K., N. R. Amundson, and H. S. Isbin, "A Theoretical Study of the Transient Operation and Stability of Two-phase Natural-circulation Loops," ANL-6381 (1961).

## APPENDIX A

### CALCULATING PRESSURE DIFFERENCE BETWEEN TWO PRESSURE TAPS DUE TO THEIR ABSOLUTE PRESSURE PHASE VARIATION DURING ACOUSTIC OSCILLATIONS

Consider a closed loop in which a resonant acoustic oscillation is maintained, such that a traveling pressure wave is traversing the loop at the speed of sound in one direction only. This is the type of behavior observed experimentally during the tests. In order to evaluate the pressure difference between two pressure taps, such as those on a venturi, which is caused by the phase variation of the absolute pressure at these locations, the following analysis is presented.

The pressure distribution due to the traveling pressure wave of amplitude  $P$ , frequency  $f$ , and wave length  $\lambda$ , may be expressed as,

$$p(x,t) = P \sin 2\pi(ft-x/\lambda) \quad , \quad (A.1)$$

where the origin of  $x$  is suitably chosen so as to satisfy the initial condition. The pressure difference between the pressure taps, whose axial positions are  $x_1$  and  $x_2$  is,

$$\begin{aligned} p(x_2,t) - p(x_1,t) &= P [\sin 2\pi(ft-x_2/\lambda) - \sin 2\pi(ft-x_1/\lambda)] \\ &= 2P \sin [\pi(x_1-x_2)/\lambda] \\ &\quad \cos \{\pi[2 ft - (x_1+x_2)/\lambda]\} \quad . \quad (A.2) \end{aligned}$$

Thus, the pressure difference due to the phase variation also exhibits a harmonic oscillation with the same frequency as that of the absolute

pressure, and with an amplitude of:

$$2P \sin [\pi(x_1 - x_2)/\lambda] \quad .$$

When the distance,  $x_2 - x_1$ , between the taps is much less than the wave length, the ratio of the differential pressure to the absolute pressure amplitude is approximately,

$$\Delta p/P = 2\pi(x_2 - x_1)/\lambda \quad . \quad (A.3)$$

Using appropriate experimental values, this ratio for the venturi is calculated to be

$$\frac{(\Delta p)_{\text{venturi}}}{P} = \frac{2\pi(0.208)}{49.1} = 0.027 \quad . \quad (A.4)$$

This low value demonstrates that the relatively severe venturi differential pressure oscillations were partially, but not entirely due to the pressure phase effect. Experimentally determined values of this ratio exceeded the value calculated above by up to a factor of 4 for the present tests and by an order of magnitude in Reference 28.

## APPENDIX B

### UNDAMPED NATURAL FREQUENCY OF A CLOSED HEAT TRANSFER LOOP

It has been noted that the frequency of oscillation during many reported instances of boiling instability was comparable to the undamped natural frequency of the system considered as a vibrating solid body. The comparison was made for systems with free surfaces and flow paths which could be considered analogous to a U-tube manometer. The purpose of the following analysis is to evaluate the undamped natural frequency of a closed flow loop with no free surfaces vibrating as a solid body about an equilibrium position.

Consider the system shown in Fig. 29, in which the heater and

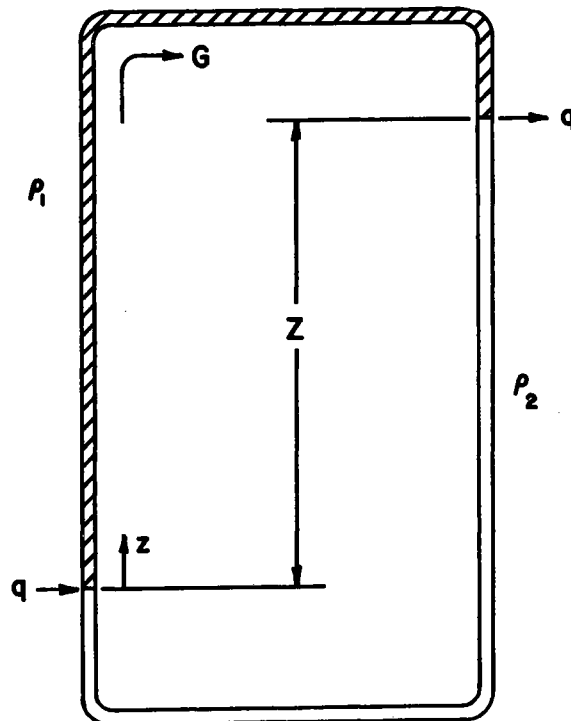


Fig. 29. Idealized Model of Heat Transfer Loop

cooler are represented as point heat sources, and the connecting tubing is filled with a fixed amount of fluid with density  $\rho_1$  and  $\rho_2$ . The loop approaches an equilibrium condition such that the density head  $(\rho_2 - \rho_1) Z$  balances the steady-state frictional head  $F_s$ . If the system is disturbed from this initial equilibrium position by an amount,  $z$ , the fluid may perform a damped oscillation about the equilibrium condition or may approach the equilibrium condition asymptotically, depending upon the loop parameters.

Applying Newton's second law to the idealized system results in the equation,

$$\frac{\rho L}{g_c} \ddot{z} + F(t) + \frac{g}{g_c} (\rho_1 - \rho_2) (Z - 2z) = 0 \quad (B.1)$$

which may also be derived from Eq. (6.6) by letting  $G(t) = G_s + \rho \dot{z}$ . The frictional pressure drop  $F$  may be considered as the sum of a steady-state and a transient component,

$$F(t) = F_s + F' \quad (B.2)$$

Since  $F_s + \frac{g}{g_c} (\rho_1 - \rho_2) Z = 0$ , Eq. (B.1) reduces to

$$\frac{\rho L}{g_c} \ddot{z} + F' + 2 \frac{g}{g_c} (\rho_2 - \rho_1) z = 0 \quad (B.3)$$

Eq. (B.3) is a second order differential equation such as is frequently encountered in mechanical or electrical vibration problems.

The undamped natural frequency of such a system is

$$f = \frac{1}{2\pi} \left( \frac{2(\rho_2 - \rho_1) g}{\rho L} \right)^{1/2} \quad (B.4)$$

The frequency of a physical system is less than the undamped natural frequency due to the effects of the system's damping. The

frequency will also be affected by the enthalpy transport and wall temperature effects. Due to the nonlinear characteristics of the physical problem, these effects are best handled by methods such as those employed in Chapter 6. Nevertheless, Eq. (B.4) gives an order of magnitude estimate of the frequencies which should be expected from this type of oscillation. The experimentally determined frequencies during the slow oscillations were 50 to 70 percent of the value calculated by Eq. (B.4). The difference is believed to be due to the system damping.

The model may be used to estimate the effects of geometry on the frequency of the oscillations. For instance, if the cooler were located in the upper horizontal section, rather than on a vertical leg, the coefficient of  $z$  in Eq. (B.3) would be reduced by  $1/2$  and result in calculating an undamped natural frequency which was reduced by a factor of  $\sqrt{2}$ . The experimental results and values calculated by the method of Chapter 6 tended to show such a decrease.

The loop schematic shown in Fig. 30 represents the geometry of the University of Minnesota flow loop. The experimental results from this loop exhibited periods in the hundreds of seconds, which are at least an order of magnitude greater than results from other loops (43,68,72). It can be shown by an analysis similar to the above that this effect is due to the geometry. The loop shown in Fig. 30 has a horizontal cooler, and a heater with a large cross sectional area  $A$  inclined at an angle  $\theta$  of  $22.5^\circ$  with the horizontal, all of which contribute to a low frequency. The displacement  $z_1$  in the part of the loop with area  $a$  is related to the displacement  $z_2$



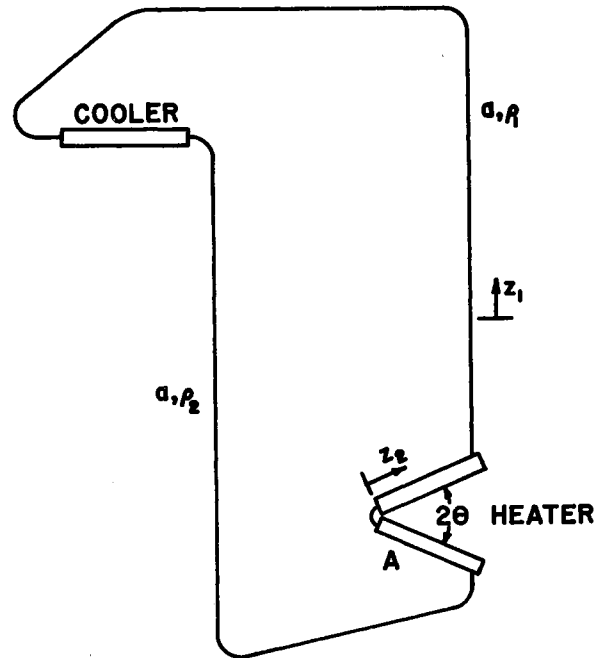


Fig. 30. Schematic of Minnesota Heat Transfer Loop

in the heater by

$$z_2 = \frac{a}{A} z_1 \quad (\text{B.5})$$

Applying Newton's second law to the mass of fluid  $m_2$  in the heater and the mass  $m_1$  in the tubing of area  $a$

$$\frac{m_2}{g_c} \ddot{z}_2 + F' + A \frac{g}{g_c} (\rho_2 - \rho_1) \sin \theta z_2 = - \frac{m_1}{g_c} \ddot{z}_1 \quad (\text{B.6})$$

which simplifies to

$$\frac{1}{g_c} (m_2 + m_1 \frac{A}{a}) \ddot{z}_2 + F' + A \frac{g}{g_c} (\rho_2 - \rho_1) \sin \theta z_2 = 0 \quad , \quad (\text{B.7})$$

for which the undamped natural frequency is,

$$f = \frac{1}{2\pi} \sqrt{\frac{A(\rho_2 - \rho_1) g \sin \theta}{m_2 + m_1 \frac{A}{a}}} \quad (\text{B.8})$$

The calculated undamped natural frequency for the loop, at the conditions described by Alstad, et al., (68) is about 45 percent of the experimentally determined value, which is consistent with the results observed for the present tests. Consequently, the geometry factors which are considered in this analysis can account for the relatively large periods characteristic of this apparatus.

In their numerical analysis of this loop, Garlid, Amundson and Isbin (72) neglected the inclination of the heater element. Their calculated frequencies were larger than the observed frequencies by nearly a factor of two which was attributed to the small number of subdivisions in their mixing-cell model. However, Eq. (B.8) shows that neglecting the inclination would result in a larger frequency by a factor of  $(\sin \theta)^{-1/2} = 1.64$ , which accounts for a large proportion of the reported deviation.

## APPENDIX C

## DIGITAL COMPUTER PROGRAM

```

PROGRAM HTTRLP
C   TRANSIENT HEAT TRANSFER LOOP
    DIMENSION RHO(38),ENT(38),TEMP(38),HTTRCO(38),TFLUID(4,51),
    1FILMCO(4,51),TWALL(2,51),SPA(4),SIZE(4),ITEST(4),DEL(4),
    2DELZ(4),NSPA(4),HB(4,51),H(4,51),HBAR(4,51),HBBAR(4,51),HNU(4,51),
    3RHOBAR(1000),GBAR(1000),P(1000),F(1000),HOUT(1000),TOUT(1000),
    4GMAX(30),GMAXT(30),GMIN(30),GMINT(30),RBAR(4,51),DELP(1000),
    5WALLT(1000),TIME(1000),T(20)
    COMMON RHO,ENT,TEMP,HTTRCO
    CALL TABLE
    1 FORMAT(4I6,1P4E12.5)
    2 FORMAT(6E12.5,E8.4)
    3 FORMAT(2E12.5,I6)
    4 FORMAT(F10.3,1P7E15.4)
    5 FORMAT(3E12.5,I6,E12.5)
    6 FORMAT(I6,8E14.5)
    10 READ INPUT TAPE 7,1,IPROB,IPRES,NTEST1,NTEST2,QBYA,HIN,GBAR(1),
    1EPS1
    IF(EOF,60)105,11
    105 STOP
    11 II=1
    K=1
    IF(NTEST1)12,16,12
    12 HBLAST=0.
    READ INPUT TAPE 7,2,BR1,BR2, BR3, BR4,DM,DN,V
    READ INPUT TAPE 7,2,AFLOW,DIA,RCAWL
    DO15I=1,4
    READ INPUT TAPE 7,3,SPA(I),SIZE(I),ITEST(I)
    DELZ(I)=SIZE(I)/SPA(I)
    NSPA(I)=SPA(I)
    HB(I,1)=HBLAST
    L=NSPA(I)
    DO 14 J=1,L
    HB(I,J+1)=HB(I,J)+DELZ(I)
    14 HBBAR(I,J)=(HB(I,J)+HB(I,J+1))/2.0
    15 HBLAST=HB(I,L+1)
    16 ITER=1
    IF(NTEST2)18,18,17
    17 READ INPUT TAPE 7,2,QCHNG,DELT,TMAX,HTEST,HRATIO
    READ INPUT TAPE 7,5,EL,TCHNG,DELTNU,ITSUP
    READ INPUT TAPE 7,2,(T(I),I=1,7)
    18 H(4,1)=HIN
    L=NSPA(4)
    DO 19 J=1,L
    H(4,J+1)=HIN
    19 HBAR(4,J)=HIN
    195 DO 50 I=1,3
    IF(ITEST(I))40,30,20
    20 DEL(I)=QBYA/SPA(I)/GBAR(1)
    H(1,1)=HIN
    L=NSPA(I)
    DO 25 J=1,L
    H(I,J+1)=H(I,J)+DEL(I)
    25 HBAR(I,J)=(H(I,J)+H(I,J+1))/2.0
    HLAST=H(I,L+1)

```

```

GO TO 50
30 H(I,1)=HLAST
   L=NSPA(I)
   DO 35 J=1,L
     H(I,J+1)=HLAST
35 HBAR(I,J)=HLAST
   GO TO 50
40 DEL(I)=(HLAST-HIN)/SPA(I)
   H(I,1)=HLAST
   L=NSPA(I)
   DO 45 J=1,L
     H(I,J+1)=H(I,J)-DEL(I)
45 HBAR(I,J)=(H(I,J)+H(I,J+1))/2.0
50 CONTINUE
52 NN=4
   GO TO 55
53 NN=3
55 DO 100 I=1,NN
   L=NSPA(I)
60 DO 65 J=1,L
   CALL INTER (HBAR(I,J),RBAR(I,J),TFLUID(I,J),FILMCO(I,J))
63 IF(RBAR(I,J))90,65,65
65 CONTINUE
   GO TO 100
90 WRITE OUTPUT TAPE 6,92,IPROB,I,J,HBAR(I,J)
92 FORMAT(17H1      IN PROBLEM I6,3H H(I2,1H,I2,4H) = 1PE12.5,37H WHIC
1H EXCEEDS THE VALUE OF THE TABLE)
   GO TO (150,340),II
100 CONTINUE
101 RHOBAR(K) =0.
   DELP(K)=0.
   DO 135 I=1,4
     L=NSPA(I)
     PSUM=0.
     RHOSUM=0.
     DO 130 J=1,L
       RHOSUM=RBAR(I,J)+RHOSUM
       IF(HBBAR(I,J)-BR1)115,120,120
115 PSUM=PSUM-RBAR(I,J)
       GO TO 130
120 IF (HBBAR(I,J)-BR2)130,121,121
121 IF (HBBAR(I,J)-BR3)125,122,122
122 IF (HBBAR(I,J)-BR4)130,115,115
125 PSUM=PSUM+RBAR(I,J)
130 CONTINUE
   RHOBAR(K)=RHOSUM*DELZ(I)+RHOBAR(K)
135 DELP(K)=PSUM*DELZ(I)+DELP(K)
   RHOBAR(K)=RHOBAR(K)/EL
   GO TO (139,235),II
139 GBARNU=DN*(RHOBAR(K)*DELP(K))**DM
   IF(ABSF(GBARNU-GBAR(K))-EPS1*GBAR(K))152,152,140
140 GBAR(K)=(GBARNU+GBAR(K))/2.
   ITER=ITER+1
   IF(ITER-26)195,145,145
145 ITER=-25
150 NTEST2=0
152 EM=RHOBAR(K)*V
   GBAR(1)=GBARNU
   CONST=QBYA*AFLOW/3.14159/DIA/SIZE(1)
   L=NSPA(1)
   DO 153 J=1,L
153 TWALL(1,J)=CONST/FILMCO(1,J)/(GBAR(K))**0.8+TFLUID(1,J)

```

```

L=NSPA(2)
DO154 J=1,L
154 TWALL (2,J) = TFLUID(2,J)
156 WRITE OUTPUT TAPE 6,160,IPROB,IPRES,QBYA,QCHNG,DELT,ITER,GBAR(1),
IDELP(1),RHOBAR(1),EM,HLAST,HIN
160 FORMAT(29H1TRANSIENT HEAT TRANSFER LOOP59X8HPROBLEM I6//7X      11H
1PRESSURE = I6,8X6HQ/A = E12.5,8X10HQCHANGE = E12.5,8X10HDELTA T =
2F6.3//9X9HITERATION8X4HGBAR11X7HDELTA P9X6HRHOBAR13X1HM13X5HHOUT
313X5HHIN //I14,E20.5,5E16.5//)
161 WRITE OUTPUT TAPE6, 162
162 FORMAT(6H0      J5X9HHBAR(1,J)3X11HRHOBAR(1,J)4X10HTWALL(1,J)3X
111HTFLUID(1,J)//)
L=NSPA(1)
DO 165 J=1,L
165 WRITE OUTPUT TAPE 6,6,J,HBAR(1,J),RBAR(1,J),TWALL(1,J),
ITFLUID(1,J)
180 IF(NTEST2)200,10,200
200 K=2
KK=2
HOUT(1)=HLAST
IGMAX=1
GMAX(IGMAX)=GBAR(1)
TIME(2)=DELT
GSIGN=1.
210 QBYA=QBYA+QCHNG
211 HNU(1,1)=HIN
IF(TIME(K)-T(1))2110,2113,2113
2110 IF(TIME(K)-T(2))2111,2114,2114
2111 IF(TIME(K)-T(3))2112,2115,2115
2112 IF(TIME(K)-T(7))2117,2117,2118
2113 IF(TIME(K)-T(4))2117,2117,2118
2114 IF(TIME(K)-T(5))2117,2117,2118
2115 IF(TIME(K)-T(6))2117,2117,2118
2117 HINCR=HRATIO
GO TO 2119
2118 HINCR=1.0
2119 CONTINUE
DO 231 I=1,2
IF(ITEST(I))212,215,212
212 QOVERA=QBYA
GO TO 220
215 QOVERA=0.
HINCR =1.0
220 CONST =DELT*QOVERA*AFLOW/RCAWL/SIZE(I)
BETA=3.14159*DIA*DELT/RCAWL*HINCR
L=NSPA(I)
DO 221 J=1,L
221 TWALL(I,J)=CONST+BETA*FILMCO(I,J)*(GBAR(K-1))**.8*(TFLUID(I,J)
1-TWALL(I,J))+TWALL(I,J)
L=NSPA(I)+1
DO 229 J=2,L
ALPHA=GBAR(K-1)*DELT/RBAR(I,J-1)/DELZ(I)
QBYV=3.14159*DIA/AFLOW*FILMCO(I,J-1)*(GBAR(K-1))**.8*(TWALL(I,J-1)
1-TFLUID(I,J-1))*HINCR
2211 IF(ITEST(I))222,223,222
222 HNU(I,J)=H(I,J-1)+(H(I,J)-HNU(I,J-1))*(1.-ALPHA)/(1.+ALPHA)+2.
1*QBYV*DELT/RBAR(I,J-1)/(1.+ALPHA)
GO TO 229
223 HNU(I,J)=(H(I,J)+ALPHA*HNU(I,J-1)+QBYV*DELT/RBAR(I,J-1))/(1.+
1ALPHA)
229 CONTINUE
IF(I-2)230,231,231

```

```

230 L=NSPA(I)
    HNU(I+1,1)=HNU(I,L+1)
231 CONTINUE
    DO 233 I=1,2
        L=NSPA(I)+1
        DO 232 J=1,L
232 H(I,J)=HNU(I,J)
233 CONTINUE
    L=NSPA(2)
    DEL(3)=(H(2,L+1)-HIN)/SPA(3)
    H(3,1)=H(2,L+1)
    L=NSPA(3)
    DO 2335 J=1,L
2335 H(3,J+1)=H(3,J)-DEL(3)
        DO 239 I=1,3
            L=NSPA(I)
            DO 238 J=1,L
238 HBAR(I,J)=(H(I,J)+H(I,J+1))/2.0
239 CONTINUE
    IF(HTEST)236,237,236
236 IF(K-2)2360,2360,2362
2360 WRITE OUTPUT TAPE 6,2361
2361 FORMAT(35HOHEATER WALL AND FLUID TEMPERATURES//
    1                                4HO K6X3HJ=18X1H28X1H38X1H4
    28X1H58X1H68X1H78X1H88X1H97X2H107X2H117X2H12//)
2362 WRITE OUTPUT TAPE 6,2363,K,(TWALL(1,J),J=1,12),(TFLUID(1,J),J=1,
    112)
2363 FORMAT(I5,12F9.1/5X12F9.1/)
237 II=2
    GO TO 53
235 P(K)=TFLUID(2,18)
    N=NSPA(1)+1
    HOUT(K)=H(1,N)
    WALLT(K)=TWALL(1,N-1)
    TOUT(K)=TFLUID(2,1)
    F(K-1)=(GBAR(K-1)/DN)**(1./DM)/RHOBAR(K-1)
    GBAR(K)=GBAR(K-1)+(32.2*DELT/EL)*(DELP(K)-F(K-1))
250 IF(GSIGN)265,255,255
255 IF(GBAR(K)-GBAR(K-1))260,300,300
260 GMAX(IGMAX )=GBAR(K-1)
    GMAXT(IGMAX)=TIME(K)-DELT
    GSIGN=-1.
    GO TO 300
265 IF(GBAR(K-1)-GBAR(K))270,300,300
270 GSIGN=1.
    GMIN(IGMAX)=GBAR(K-1)
    GMINT(IGMAX)=TIME(K)-DELT
272 IGMAX=IGMAX+1
    GO TO 300
282 LL=K-1
277 WRITE OUTPUT TAPE 6,278
278 FORMAT(35HO TRANSIENT ANALYSIS RESULTS//6X4HTIME7X4HGBAR8X
    17HDELTA P9X6HRHOBAR8X12HTFLUID(2,18)6X5HH OUT11X5HT OUT9X5HTWALL/)
    DO 279 L = KK,LL,ITSUP
279 WRITE OUTPUT TAPE 6,4,TIME(L),GBAR(L),DELP(L),RHOBAR(L),P(L),
    1HOUT(L),TOUT(L),WALLT(L)
        WRITE OUTPUT TAPE 6,4,TIME(K),GBAR(K),DELP(K),RHOBAR(K),P(K),
    1HOUT(K),TOUT(K),WALLT(K)
        KK=K+1
    GO TO (304,400),JJ
400 WRITE OUTPUT TAPE 6,401
401 FORMAT(23HO TIME14X4HGMAX15X4HTIME14X4HGMIN//)

```

```
      WRITE OUTPUT TAPE 6,402,(GMAXT(J),GMAX(J),GMINT(J),GMIN(J),J=1,  
XIGMAX)  
402 FORMAT(OPF23.4,1PE21.6,OPF16.4,1PE21.6)  
      GO TO 10  
300 IF(TMAX-TIME(K))3000,3000,301  
3000 JJ=2  
      GO TO 282  
301 IF(TCHNG)305,305,302  
302 IF(TIME(K)-TCHNG)305,303,303  
303 TCHNG=0.  
      JJ=1  
      GO TO 282  
304 DELT=DELTNU  
305 K=K+1  
      TIME(K)=TIME(K-1)+DELT  
      GO TO 211  
340 JJ=2  
      GO TO 282  
      END
```

SUBROUTINETABLE  
 DIMENSIONENT(38),RHO(38),TEMP(38),HTTRCO(38)  
 COMMONENT,RHO,TEMP,HTTRCO

ENT(1)=56.0		
ENT(2)=58.0		
ENT(3)=60.0	RHO(22)=33.90	HTTRCO(3)=0.0013
ENT(4)=62.0	RHO(23)=30.55	HTTRCO(4)=0.0013
ENT(5)=64.0	RHO(24)=27.75	HTTRCO(5)=0.0013
ENT(6)=66.0	RHO(25)=25.25	HTTRCO(6)=0.0013
ENT(7)=68.0	RHO(26)=23.38	HTTRCO(7)=0.0013
ENT(8)=70.0	RHO(27)=21.64	HTTRCO(8)=0.0013
ENT(9)=72.0	RHO(28)=20.22	HTTRCO(9)=0.0013
ENT(10)=74.0	RHO(29)=19.00	HTTRCO(10)=0.0013
ENT(11)=76.0	RHO(30)=18.00	HTTRCO(11)=0.0013
ENT(12)=78.0	RHO(31)=17.13	HTTRCO(12)=0.0013
ENT(13)=80.0	RHO(32)=16.36	HTTRCO(13)=0.0013
ENT(14)=82.0	RHO(33)=15.64	HTTRCO(14)=0.0013
ENT(15)=84.0	RHO(34)=15.10	HTTRCO(15)=0.0013
ENT(16)=86.0	RHO(35)=14.54	HTTRCO(16)=0.0013
ENT(17)=88.0	RHO(36)=14.10	HTTRCO(17)=0.0013
ENT(18)=90.0	RHO(37)=13.65	HTTRCO(18)=0.0013
ENT(19)=92.0	RHO(38)=13.29	HTTRCO(19)=0.0013
ENT(20)=94.0	TEMP(1)=193.2	HTTRCO(20)=0.0013
ENT(21)=96.0	TEMP(2)=200.2	HTTRCO(21)=0.0013
ENT(22)=98.0	TEMP(3)=207.5	HTTRCO(22)=0.0013
ENT(23)=100.0	TEMP(4)=214.6	HTTRCO(23)=0.0013
ENT(24)=102.0	TEMP(5)=221.8	HTTRCO(24)=0.0013
ENT(25)=104.0	TEMP(6)=228.8	HTTRCO(25)=0.0013
ENT(26)=106.0	TEMP(7)=235.8	HTTRCO(26)=0.0013
ENT(27)=108.0	TEMP(8)=242.1	HTTRCO(27)=0.0013
ENT(28)=110.0	TEMP(9)=248.8	HTTRCO(28)=0.0013
ENT(29)=112.0	TEMP(10)=255.3	HTTRCO(29)=0.0013
ENT(30)=114.0	TEMP(11)=261.9	HTTRCO(30)=0.0013
ENT(31)=116.0	TEMP(12)=268.2	HTTRCO(31)=0.0013
ENT(32)=118.0	TEMP(13)=274.4	HTTRCO(32)=0.0013
ENT(33)=120.0	TEMP(14)=280.3	HTTRCO(33)=0.0013
ENT(34)=122.0	TEMP(15)=285.4	HTTRCO(34)=0.0013
ENT(35)=124.0	TEMP(16)=290.0	HTTRCO(35)=0.0013
ENT(36)=126.0	TEMP(17)=293.8	HTTRCO(36)=0.0013
ENT(37)=128.0	TEMP(18)=296.2	HTTRCO(37)=0.0013
ENT(38)=130.0	TEMP(19)=298.0	HTTRCO(38)=0.0013
RHO(1)=78.10	TEMP(20)=299.0	RETURN
RHO(2)=77.05	TEMP(21)=299.9	END
RHO(3)=75.85	TEMP(22)=300.4	
RHO(4)=74.74	TEMP(23)=301.4	
RHO(5)=73.58	TEMP(24)=302.8	
RHO(6)=72.35	TEMP(25)=304.9	
RHO(7)=70.92	TEMP(26)=307.5	
RHO(8)=69.54	TEMP(27)=311.2	
RHO(9)=68.05	TEMP(28)=316.0	
RHO(10)=66.43	TEMP(29)=321.3	
RHO(11)=64.80	TEMP(30)=327.1	
RHO(12)=63.05	TEMP(31)=333.8	
RHO(13)=61.30	TEMP(32)=340.0	
RHO(14)=59.40	TEMP(33)=346.8	
RHO(15)=57.44	TEMP(34)=354.0	
RHO(16)=55.25	TEMP(35)=361.2	
RHO(17)=52.65	TEMP(36)=368.9	
RHO(18)=49.80	TEMP(37)=376.8	
RHO(19)=46.50	TEMP(38)=384.9	
RHO(20)=42.50	HTTRCO(1)=0.0013	
RHO(21)=37.80	HTTRCO(2)=0.0013	



```
SUBROUTINE INTER(HH,R,T,FC)
DIMENSION ENT(38),RHO(38),TEMP(38),HTTRCO(38)
COMMON ENT,RHO,TEMP,HTTRCO
L=1
IF(HH-ENT(1))1115,1130,1105
1105 DO1110LL=2,38
L=LL
IF(HH-ENT(LL))1150,1130,1110
1110 CONTINUE
1115 R=-1
GOTO1160
1130 R=RHO(L)
T=TEMP(L)
FC=HTTRCO(L)
1150 RATIO=(ENT(L)-HH)/(ENT(L)-ENT(L-1))
R=RHO(L)-RATIO*(RHO(L)-RHO(L-1))
T=TEMP(L)-RATIO*(TEMP(L)-TEMP(L-1))
FC=(HTTRCO(L)-RATIO*(HTTRCO(L)-HTTRCO(L-1)))
1160 RETURN
END
SCOPE
```

## Program Nomenclature

<u>Input</u> <u>Variable Name</u>		<u>Example</u> <u>Input Data</u>
IPROB	Problem number	11
IPRES	Pressure	500 psia
NTEST 1	Tests to determine if loop has been divided into space increments	1
NTEST 2	Test to determine whether to perform transient calculations	1
QBYA	Electrical power/cross-sectional flow area	1600.0 Btu/sec ft <sup>2</sup>
HIN	Heater inlet enthalpy	73.0 Btu/lb <sub>m</sub>
GBAR (1)	Initial estimate of mass flow rate	87.0 lb <sub>m</sub> /sec ft <sup>2</sup>
EPS 1	Steady-state mass flow rate convergence criterion	0.005
BR 1	Axial distance from heater inlet to upper corner above heater	15.8333 ft
BR 2	Axial distance from heater inlet to upper corner above cooler	22.8333 ft
BR 3	Axial distance from heater inlet to lower corner below cooler	40.79166 ft
BR 4	Axial distance from heater inlet to lower corner below heater	47.875 ft
DM	Constant derived from Eq. (6.11)	0.629
DN	Constant derived from Eq. (6.11)	0.252
V	Volume of loop	0.236 ft <sup>3</sup>
AFLOW	Cross-sectional flow area	0.00471 ft <sup>2</sup>
DIA	Diameter	0.0775 ft
RCAWL	$(\rho c_p A)_{\text{wall}}$	0.042433 Btu/°F ft

## Program Nomenclature (Contd.)

<u>Input Variable Name</u>		<u>Example Input Data</u>
SPA (1)	Number of space increments in heater	12.0
SIZE (1)	Length of heater	3.0 ft
ITEST (1)	Identifies heater	1
SPA (2)	Number of space increments in riser	19.0
SIZE (2)	Length of riser	22.1667 ft
ITEST (2)	Identifies riser	0
SPA (3)	Number of space increments in cooler	12.0
SIZE (3)	Length of cooler	5.0 ft
ITEST (3)	Identifies cooler	-1
SPA (4)	Number of space increments in downcomer	28.0
SIZE (4)	Length of downcomer	19.8333 ft
ITEST (4)	Identifies downcomer	0
QCHNG	Change of QBYA	0.0 Btu/sec ft <sup>2</sup>
DELT	Time increment	0.1 sec
TMAX	Total problem time	80.0 sec
HTEST	Test to determine whether to print out supplementary data	0.0
HRATIO	Ratio by which $H/G^{0.8}$ is increased to simulate "boiling-like" behavior	1.60
EL	Loop length	50.0 ft
TCHNG	Tests whether time increment is to be changed	0.0 sec
DELTNU	New value of time increment	0.0 sec
ITSUP	Specifies number of time increments between printed output data	1

## Program Nomenclature (Contd.)

<u>Input Variable Name</u>		<u>Example Input Data</u>
T (1)	The program causes $H/G^{0.8}$ to increase	47.5 sec
T (2)	by a factor of HRATIO from 0 to T (7),	31.3 sec
T (3)	T (3) to T (6), T (2) to T (5), and T (1)	15.1 sec
T (4)	to T (4) seconds in order to simulate	49.5 sec
T (5)	4 cycles of the "boiling-like" events.	33.3 sec
T (6)	Setting these values equal to 0.0 bypasses	17.1 sec
T (7)	this feature of the program.	2.0 sec

<u>Output Variable Name</u>		
PROBLEM	IPROB	
PRESSURE	IPRES	psia
Q/A	QBYA	Btu/sec ft <sup>2</sup>
QCHANGE	QCHNG	Btu/sec ft <sup>2</sup>
DELTA T	DELT	sec
ITERATION	Number of steady-state iterations	
GBAR	Mass flow rate per unit area	lb <sub>m</sub> /sec ft <sup>2</sup>
DELTA P	Density head	lb <sub>f</sub> /ft <sup>2</sup>
RHO BAR	Average density of fluid in loop	lb <sub>m</sub> /ft <sup>3</sup>
M	Mass of fluid in loop	lb <sub>m</sub>
HOUT	Heater outlet enthalpy	Btu/lb <sub>m</sub>
HIN	Heater inlet enthalpy	Btu/lb <sub>m</sub>
HBAR (1,J)	Average enthalpy of <u>j</u> th heater increment	Btu/lb <sub>m</sub>

## Program Nomenclature (Contd.)

Output		
<u>Variable Name</u>		
RHO BAR (1,J)	Average density of <u>j</u> th heater increment	lb <sub>m</sub> /ft <sup>3</sup>
TWALL (1,J)	Wall temperature of <u>j</u> th heater increment	°F
TFLUID (1,J)	Bulk temperature of <u>j</u> th heater increment	°F
TIME	Time	sec
TFLUID (2,18)	Bulk temperature of 18th increment in riser	°F
TOUT	Heater outlet bulk temperature	°F
TWALL	Wall temperature at heater exit	°F
GMAX	Maximum value of GBAR	lb <sub>m</sub> /sec ft <sup>2</sup>
GMIN	Minimum value of GBAR	lb <sub>m</sub> /sec ft <sup>2</sup>

## Selected Variable Names which are Used Internally in the Program

ENT	Tabulated values of enthalpy
FILMCO	H/G <sup>0.8</sup>
H	Enthalpy (h) of fluid at end of space increment. (This is only place in thesis where H does not refer to heat transfer coefficient).
HBAR	Enthalpy of fluid at midpoint of space increment.
HNU	Enthalpy of fluid at end of time increment.
HB	Axial distance to end of space increment.
HBBAR	Axial distance to midpoint of space increment.
HTTRCO	Tabulated values of H/G <sup>0.8</sup> .
RHO	Tabulated values of density.
RBAR	Average value of density in space increment.

## Program Nomenclature (Contd.)

TEMP	Tabulated values of temperature.
TFLUID	Bulk temperature of fluid.
TWALL	Wall temperature.

VITA

Archie Junior Cornelius

Candidate for the Degree of

Doctor of Philosophy

Thesis: AN INVESTIGATION OF INSTABILITIES ENCOUNTERED DURING HEAT  
TRANSFER TO A SUPERCRITICAL FLUID

Major Field: Mechanical Engineering

Biographical:

Personal Data: Born at Westmoreland, Kansas, October 16, 1931.

Undergraduate Study: Graduated from Vermillion High School,  
Vermillion, Kansas in May, 1949; after operating father's  
farm for four years, and serving two years in the U.S.  
Army, entered Kansas State University in June, 1955; re-  
ceived the Bachelor of Science degree with high honors in  
May, 1958.

Graduate Study: Attended the evening division of the University  
of Tulsa from 1958-1961; received the Master of Science  
degree from Oklahoma State University in May 1963; com-  
pleted the requirements for the Doctor of Philosophy degree  
from Oklahoma State University in May, 1965.

Professional Experience: Worked during the summer of 1957 as a  
student engineer for Sheffield Steel Corporation, Houston,  
Texas; employed as a research engineer by Jersey Production  
Research Company, Tulsa, Oklahoma since June, 1958;  
employed as a resident student associate by the Argonne  
National Laboratory, Argonne, Illinois while conducting the  
research described in this thesis.

Professional and Honorary Organizations: Member of Pi Tau Sigma,  
Sigma Tau, Phi Kappa Phi, Kansas Engineering Society and  
A.I.M.E.